Diss. ETH N° 18588

Processing strategies in light metal 'Compound Casting'

A dissertation submitted to the
ETH ZÜRICH

for the degree of
DOCTOR OF SCIENCES

presented by
KONRAD JULIUS MAXIMILIAN PAPIS
Dipl.-Ing., ETH Zürich
born on March 14, 1981
citizen of Austria

accepted on the recommendation of
Prof. Dr. Peter J. Uggowitzer, examiner
Prof. Dr. Jörg F. Löffler, co-examiner
PD Dr. habil. Helmut Kaufmann, co-examiner

2009

Diese Arbeit wurde durch das Österreichische Bundesamt für Verkehr, Information und Technologie (BMVIT) im Rahmen der Technologieoffensive ‘Austrian Lightweight Structures’ (ALWS) der Austrian Research Centers (ARCs) finanziell unterstützt.

This work was financially supported by the Austrian ministry for traffic, information and technology within the framework of the technology offensive ‘Austrian Lightweight Structures’ of the Austrian Research Centers.

Contents

Abstract

In lightweight construction, the light metals aluminium and magnesium are employed to an ever increasing extent, as these materials exhibit a low specific gravity of 2.7 and 1.7 g/cm^3, respectively. Their use in vehicles aims at reducing fuel consumption, as less mass has to be propelled. Resources are abundant, but the extraction of the raw metals is energy intensive. For these reasons, efforts are high to work and research on efficient and economical methods to process these materials and thus to reduce the component's dimensions. Whenever a single material does not satisfy the demands of a specific application, compound structures may generate a solution. Especially in lightweight construction, a multi-material-mix can provide ideal specific properties that are suitable for the conditions to which a part is subjected. Typically such combinations of dissimilar materials provide desired properties in various areas of the single part.

Compound casting is a process, which yields such multi-material components: two metal alloys – one in the solid state, the other liquid – are brought into contact with each other in such a manner that a diffusion zone forms at the interface. Inherent difficulties when joining light metals are the natural oxide layer and its thermodynamic stability. If it remains on the solid compound partner, it persists during the compound casting process and prohibits the necessary diffusion reaction. A milestone of this work was the development of a method to avoid that problem by applying a low-melting, reactive metallic zinc coating. The metallic melt, which comes into contact with this layer, supplies enough heat to fuse the outermost regions. The reactivity – and thus wettability – increases drastically, and the coating material is alloyed into the bulk of the compound. The transition between the two compound partners is continuously metallurgic, leading to an area-wide material joint. This method yields, in comparison to conventional approaches such as welding (which is otherwise used in production of such compounds), a connection without a 'weak link'. When it comes to dissimilar materials (Al–Mg) compound casting, a less reactive manganese coating was applied to avoid the formation of undesired low-melting intermetallic phases (IMPs) at the otherwise mechanically deficient interface.

The interfacial areas were investigated in detail: with optical microscopy, metallographically cross-section polished interfaces were examined for continuity and

imperfections. Their graded composition was determined by point-, line- and area-scan energy-dispersive X-ray (EDX) analysis. Microhardness measurements accentuate the mechanical properties of the compound, which are affected by heat input during the wetting experiments.

Diffusion of alloying elements yielded heat-treatable interfacial areas in Al–Al systems, where during tempering precipitation of hardness increasing particles was demonstrated by microhardness measurements. The diffusion processes in the respective transition zones were simulated by thermodynamic calculations using the DICTRA software, going long well with the experimental findings.

In Mg–Mg systems, no imperfections were detectable by optical or electron microscopy. The solidification sequence at the interface determines the possibility of shrinkage cavity formation. Via differential scanning calorimetry and EDX analysis, the compositions of the transition zones were determined experimentally, and the chronology of their solidification, as well as the influence of the coating material, were calculated using the Pandat software.

For investigations on the multilayered interface in the Al–Mg system, mechanical bending tests and EDX analytical methods with high resolution were employed. The latter required the preparation of specimens, which are a fraction of a micron thick, with a focused ion beam. It is hardly possible to obtain a ‘weak-link’-free joint in such systems. Compared to other production methods, the size of the interface was reduced by two orders of magnitude, and a mechanically sound solidification mechanism was realized at the same time.

Zusammenfassung

Mit einem spezifischen Gewicht von ca. 2.7 bzw. 1.7 g/cm^3 gehören die Elemente Aluminium und Magnesium zur Klasse der Leichtmetalle, weswegen diese Materialien in zunehmendem Maße im Leichtbau eingesetzt werden. Dies geschieht hauptsächlich um Kraftstoff beim Antrieb leichterer Maschinen einzusparen. Al- und Mg-Ressourcen sind zwar weit davon entfernt zur Neige zu gehen, der große Nachteil liegt jedoch an der großen Menge Stroms, die zur Gewinnung der reinen Metalle nötig sind. Auch deshalb arbeitet und forscht man an leistungsfähigen und sparsamen Methoden, diese zu verarbeiten und möglichst effizient dimensionieren zu können. Eine Kombination von materialspezifischen Eigenschaften in einem einzigen Verbund-Bauteil zu vereinen ist oft unumgänglich – das Gewichteinsparungspotential ist mit einem Multi-Material-Mix am größten. Diese Dissertation behandelt ein Thema, das die limitierte Anwendbarkeit der beiden Leichtmetalle Aluminium und Magnesium im Bereich der heute verfügbaren Fügeverfahren aufgreift, da diese ausschließlich zu Schwachstellen im Bereich der Naht führen.

Ein Verfahren, das die Vorteile verschiedener Fügepraktiken vereint, ist das Verbundgießen: Hierbei wird unter Entstehung einer großflächigen Diffusions- und Reaktionszone eine Metallschmelze an oder um ein festes (ebenso metallisches) Bauteil gegossen. Durch das Vorhandensein einer natürlichen, thermodynamisch stabilen Oxidschicht an deren Oberfläche gelang es bisher nur unter unbefriedigend hohem ökologischen oder ökonomischen Aufwand von Energie oder Chemikalien, eine metallurgische Reaktion zwischen zwei Teilen aus diesen Materialien zustandezubringen. Ein Meilenstein dieser Arbeit war die Entwicklung eines kombinierten Verfahrens von Vorbehandlungen und Beschichtungen, um die Reaktivität – und dadurch die Benetzbarkeit – der Leichtmetall-Oberflächen gegenüber Metallschmelzen so zu erhöhen, dass Verbundguss einfach zu realisieren ist. Zu diesem Zweck wurden die Legierungen mit einer niedrigschmelzenden Zinkschicht beschichtet, die dadurch hervorragende Benetzungseigenschaften zeigten: Bei ähnlichen Materialien (Al–Al und Mg–Mg) wurde die Oberfläche komplett benetzt und ging eine kontinuierlich metallurgische Bindung mit der erstarrten Schmelze ein. Bei Al–Mg Verbundguss kam eine weniger stark reagierende Mangan-

Beschichtung zum Einsatz, die jedoch eine unerwünschte Entstehung niedrigschmelzender intermetallischer Phasen erfolgreich verhinderte.

Die so entstandenen Grenzflächen wurden eingehend analysiert: Metallographisch präparierte Grenzflächen-Querschliffe konnten im Lichtmikroskop auf Kontinuität und Fehlstellen untersucht werden. Deren gradierte Zusammensetzung wurde mittels energiedispersiver Röntgenanalyse (EDX Analyse) in Punkt-, Linien- und Flächenmessung eruiert. Mikrohärtemessungen zeigten die Auswirkung des während des Benetzungsexperiments verursachten Wärmeeintrags auf die mechanischen Eigenschaften der Verbunde.

In Al–Al Systemen, die durch Diffusion der jeweiligen Legierungselemente wärmebehandelbare Grenzflächenregionen aufweisen, wurde auch die während des Temperns erfolgte Ausscheidung härtesteigernder Partikel mit Mikrohärtemessungen nachgewiesen. Die Diffusionsvorgänge in den jeweiligen Übergangsregionen wurden mittels thermodynamischer Berechnungen simuliert, welche die experimentellen Ergebnisse gut wiedergeben.

Auch in Mg–Mg Systemen waren licht- und elektronenmikroskopisch keine Fehlstellen feststellbar. Die Abfolge der Erstarrungssequenz an der Grenzfläche bestimmt, ob sich Lunker bilden können. Mit Differenzial-Scanning-Kalorimetrie und EDX Analyse wurden die Zusammensetzungen der Übergangszonen experimentell ermittelt, und deren Erstarrungsabfolge sowie die Veränderung durch das Beschichtungsmaterial mittels Pandat berechnet.

Bei der Untersuchung der mehrschichtigen Grenzflächen in Al–Mg Systemen kamen mechanische Biegeversuche und EDX Analysemethoden mit höherer Auflösung zum Einsatz. Für letztere war es nötig, Proben mit einer Dicke von Bruchteilen eines Mikrometers in einer Ionenfeinstrahlanalage herzustellen. Es ist bei diesen Systemen kaum möglich, keine Schwachstelle an der Grenzfläche zu verursachen: Im Vergleich zu anderen Verfahren konnte deren Abmessungen um zwei Größenordnungen reduziert und zugleich ein Entstehungsmechanismus, der aus mechanischen Überlegungen günstig ist, realisiert werden.

Chapter 1

Introduction

1.1 What is ‘compound casting’?

Like every fellow Ph.D. student, I am often asked: ‘What is your thesis for?’ – and as I do not want to answer: ‘Well, it’s complex. Ok, imaginary… ($\{\text{Thesis}\} \notin \{\mathbb{R}\}$ wouldn’t be a good sign, either)’[1], I start to explain what the idea of my project is, and why there is a need for it. Apparently, though, I often fail to find the right words, so some people keep asking: ‘How are your polymers doing?’

Well, at least they remember that I am engaged in the field of materials science! Indeed, I tell my friends that I work on a joining technique for metallic materials, and polymers do play a major role in adhesive bonding. Compound casting itself has nothing to do with gluing, as you can guess from its name, but can be described as a process, which takes the advantages of welding and brazing to form a metallurgic joint.

Welding is a method, where two solid metals are fused at the contact areas, and form a bond when the liquid volume, which is hereby created, solidifies. A welding seam with limited depth and mechanical properties is created, often representing the weakest spot of this compound. Furthermore, light metals such as aluminium are not easily welded, as an oxide layer with a high melting point always surrounds the bulk material. If one does not want to melt the parts that are to be joined, and if the joint needs to cover large areas, one can choose brazing to achieve a glued-like all-metallic compound. However, the surface state is the most important variable, and environmentally questionable, highly corrosive fluxes are needed very often.

[1] Tribute to: ‘Piled Higher and Deeper’ (Ph.D.), the comic strip about life (or the lack thereof) in academia, www.phdcomics.com. $\mathbb{R}$ = set of real numbers.

There are methods to join components without these disadvantages, but then, form and force closure are required to hold the construction together. Compound casting represents an area-wide, continuously metallic, 'weak link'-free joining method, which can be applied to a multitude of metals and alloys. As denoted by its name, one step of this joining technique comprises a casting procedure. Hence, this method joins two components at the same time as one of them is being produced: two metal alloys – one in the solid state, the other liquid – are brought into contact with each other in such a manner, that a metallic interface forms. The bonding relies on the material connection alone – the casting does not have to clasp around the solid structure.

1.2 The history of the process

The general idea of creating a compound is to combine the good properties of two or more materials in one single part. Compound casting has been used to place 'inserts' at locations of castings, where special properties or functionalities are needed.
Mainly iron based or composite materials are employed as wear-, heat- or corrosion-resistant, stiff or low-friction reinforcements. Often, the cast material surrounds these inserts, leading to a combination of form-, force- and material-closure. The insert pre-treatments are often energy and cost intensive as well as difficult to handle. Belov *et al.* [Belov, 2002] describe the process of insert metallization prior to the casting process as follows: *'A more reliable metallurgical contact of the insert with the piston* (i.e. cast) *material is ensured by the so-called 'alfin-process'. This technology combines the prior degreasing and shotblasting of the* (iron) *insert and its subsequent holding in a bath with a molten aluminum alloy at a temperature of 700 - 720 °C. … During a very short period of time when the insert extracted from the aluminizing bath is put in contact with the melt in the cast mould, the aluminizing layer on the insert surface must still be liquid.'* (Fig. 1.1a). The aforementioned 'alfin-process' was established in 1969 [Gürtler, 1969] and seem to be the first process to concur with the definition for 'compound casting': The metallurgical formation of interface zones, where the cast alloy's components diffuse into the solid material partly via the formation of solid solutions, and partly via the formation of reaction phases, is described. This procedure indeed involves several laborious pre-treatment steps,

which show its striking disadvantages to other solutions and prove to be a major handicap for a broad application.

Later, other methods of reinforcing heavily stressed locations were introduced. The process described by Brandt et al. and Dienwiebel et al. [Brandt, 1997; Dienwiebel, 2007] involve short fibre or particle preforms, which are placed into the mould and infiltrated with high pressure during casting. With this technique, the range of cast shapes is very narrow, and its application is thus restricted, too. However, these reinforced structures had one single 'matrix' material, i.e. the aluminium alloy, and therefore, the interface between cast and composite structures is free from intermetallic phases (IMPs) or other defects.

To stay in the area of lightweight engine construction, the company Porsche manufactured a local metal matrix composite cylinder crankcase with the trade name 'LOKASIL' in 1996 (Fig. 1.1b) with infiltrated silicon cylinder liner preforms to improve wear resistance and tribological properties.

In 2004, BMW introduced a compound cast R6 (6 in-line cylinders, Figure 1.1c) engine block [Flierl, 2003] with its then new 630i Coupé and Cabrio, and is currently assembled in the majority of the company's models (for more information visit www.bmw.com). The engine comprised an aluminium-magnesium crankcase, which was manufactured by spray-coating the aluminium insert (an assembly comprising cylinder liners, cooling water ducts and crankshaft bearings) and casting the newly-developed, creep-resistant magnesium alloy AJ62 described by Baril *et al.* [Baril, 2003] around it. Compared to its predecessor, it set a new benchmark for specific power (63 kW/dm^3) and decreased its fuel consumption by 12% at an overall weight of 161 kg (weight reduction of 10 kg), as Klüting *et al.* reported in the engineering journal 'Motortechnische Zeitschrift' [Klüting, 2005].

Again, the construction relies on all three forms of closure, because of the formation of intermetallic phases at the interface of two dissimilar metals (here: Al and Mg; for the 'alfin-process': Fe and Al). However, the construction was accomplished with the help of highly computerized CAD and simulation tools, which kept the interface thin and leak-proof. Micromovements, which could cause compound failure, were avoided thereby.

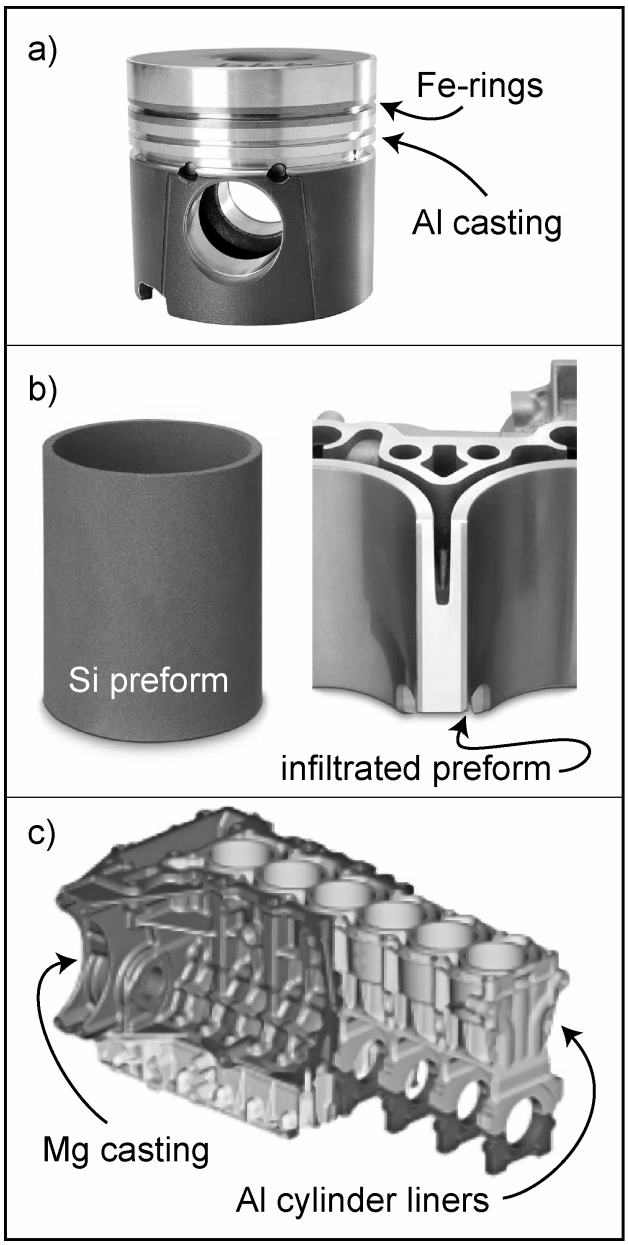

Fig. 1.1, a - c: Fe-Al compound piston, produced with the 'alfin-process (a). Partially reinforced 'LOKASIL' aluminium compound (b). BMW R6 Al-Mg compound cast engine block (c).

With these examples, the development of the compound casting process is outlined. Still, the main idea of a connection with material bonding alone has never been applied – all these constructions rely on force- and form-closure. Even worse (at least for the idea of a material joint), the latter are part of the main construction parameters!

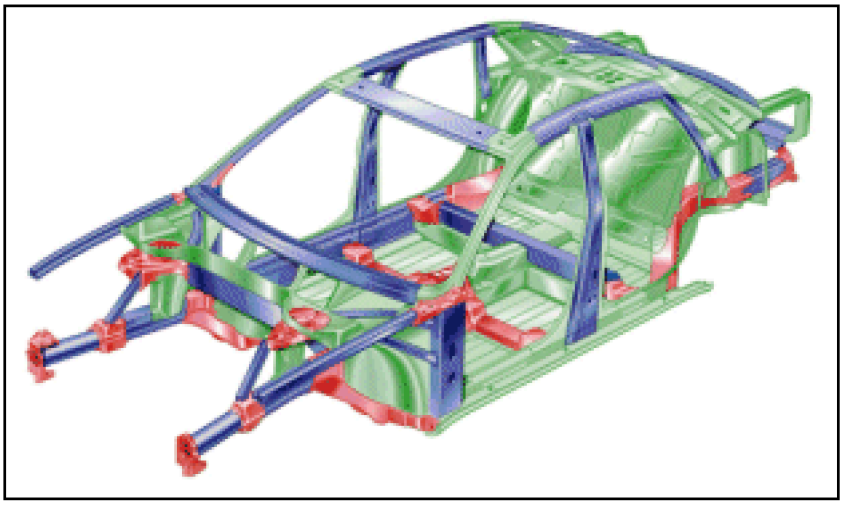

Fig. 1.2: The space frame construction of an aluminium chassis. Sheet material (green) and extrusions (blue) are welded to cast nodes (red). (Resource: Audi AG)

In 2005, the Austrian Research Centers GmbH (ARCs) launched a project entitled Austrian Lightweight Structures (ALWS), founded by the Austrian government's department for traffic, innovation and technology (Bundesministerium für Verkehr, Innovation und Technologie, BMVIT): This technology initiative considered solutions for lightweight constructions in the automotive industry by means of multimaterial mix. The projects comprised twelve partners in industry and academy, and one of eleven sub-projects (Sub C: This PhD thesis at ETH Zurich, with partners LKR[2] and ECHEM[3] had the goal to develop compound casting processes with various metallic substrates and melts.

This thesis is about developing strategies for compound casting with aluminium or magnesium based substrates (the previously mentioned 'inserts') and aluminium or magnesium based melts (i.e., Al–Al, Mg–Mg and Al–Mg).

[2] ARC Leichtmetallkompetenzzentrum Ranshofen GmbH, Postfach 26, 5282 Ranshofen, Austria. www.lkr.at

[3] Kompetenzzentrum für Angewandte Elektrochemie GmbH, Viktor-Kaplan-Str. 2, 2700 Wr. Neustadt, Austria. www.echem.at

1.3 Why light metals?

The main goal of modern automobile development is the reduction of fuel consumption. One possibility to achieve this is to construct vehicles with less mass by the use of light materials or a mixture of such. Predominantly made of heavy iron-based alloys (with a specific weight of ρ_{Fe} = 7.9 g/cm^3), metallic components have constantly been replaced by light metals, such as aluminium (ρ_{Al} = 2.7 g/cm^3) and magnesium (ρ_{Mg} = 1.7 g/cm^3). From 1970 to 1995, the amount of aluminium in an average European car has risen from 30 to 65 [Balleer, 1997] and until now to over 150 kg. With respect to different mechanical properties, a component is up to 40% lighter when made of aluminium instead of iron. With the production of their A8 model beginning in 1994, Audi introduced the Audi Space Frame (ASF, Fig. 1.2) – a car body made of aluminium alloys exclusively, where sheet structures and extruded profiles are welded to complex node castings. Since fusion welding requires specialized operators to ensure good welds, laser welding was applied from 2002. This car comprises aluminium constructions with a total weight of 550 kg, which approximately corresponds to 35% of the total net weight. The space frame technology was also applied to construct the magnesium body of Audi's one-liter-car – a groundbreaking lightweight construction with amazingly low fuel consumption of 0.99 l/km!

All these examples have one thing in common: light metals are used with the aim of weight reduction and bringing down fuel consumption. Compound casting could further improve the mechanical properties of the bonding, and thus give new possibilities to optimize the construction in terms of lower weight and superior functionality.

1.4 Aims and outline

Aims of the thesis

The goal of this thesis is a new approach to facilitate bonding via compound casting, by combining surface treatment processes to significantly increase wetting properties of the substrate material, to avoid the inclusion of oxides and to prevent excessive formation of intermetallic phases.

First, chemical and electrochemical as well as heat treatment procedures were established to generate reactive surfaces on aluminium and magnesium alloys. Second, a non-isothermal device for wetting experiments and compound production was developed, comprising a horizontal furnace, a sample manipulator and a quartz glass tube to handle small amounts of metallic melts. For the Al–Al system, experiments were scaled up close to industrial dimensions, performing compound casting in a squeeze-casting machine at the project partner LKR. Third, the interfaces of the hereby produced compounds were investigated by metallurgical methods, including Optical and Scanning Electron Microscopy (OM and SEM, respectively), Energy Dispersive X-ray (EDX) spectroscopy, Differential Scanning Calorimetry (DSC), Focused Ion Beam (FIB) milling and microhardness measurements. In the end, diffusion processes during compound casting and subsequent annealing treatments were numerically simulated, and compared with experimental findings.

Surface pre-treatment procedures

Pickling solutions containing zinc ions were used to replace the naturally occurring oxide layer of aluminium and magnesium alloys by a metallic zinc coating. The main process is a redox-reaction, which ensures a dense metallic deposit. In section 2.2, aqueous solutions for the varying substrate alloys are listed and the reactions are discussed. Subsequent galvanization procedures are detailed in sections 2.2 and 2.3, where the dissimilar challenges of the three compound systems Al–Al, Mg–Mg and Al–Mg play the major role. Adhesion characteristics and measures to increase these are explained in section 2.4.

Wetting experiments and sample production

Sessile drop wetting tests are usually conducted under isothermal conditions. As the substrate and droplet materials have the same melting points, wetting experiments in this work have to be non-isothermal. Therefore, a setup to control the substrate's temperature by limited heating time was installed in a horizontal furnace and is detailed in section 3.3. By pushing the substrate platelet from ambient conditions into the heated area of the furnace and waiting for a certain time, the temperature of the substrate was different from that of the melt (thus non-isothermal). After the

positioning of the droplet onto the substrate, the compound could be retracted from the heated zone with the same mechanism.

Interface analysis

The hereby-produced samples were analyzed with various methods, focussing on interface integrity, microstructure, composition and mechanical properties. Most investigations were done on cross-sections of the specimens, which had to be cut in halves and metallographically prepared. The influence of heat treatment procedures on the composition, size and mechanical properties of Al–Al interfaces was explored and is described in sections 4.2 and 4.3. In section 5.1, a characterization of the chemical composition in Mg–Mg specimens is detailed. Furthermore, phases at the interface of Al–Mg samples were analyzed by EDX, which involved special ion milling preparation methods for small samples with a thickness of a fraction of a micron (section 6.1).

Calculations on interface composition

Several couple compositions were investigated in this thesis. However, there are a multitude of aluminium and magnesium alloys with a huge variety of alloying elements, which are possible candidates for commercial applications. At the interface, interdiffusion causes a zone of element concentration gradients. This is not only an indication of a successful compound cast bonding, but provides the opportunity to selectively modify this area's mechanical properties, e.g. via artificial ageing of aluminium alloys (discussed in section 4.5).

Some binary alloys have therefore been used as cast material both in experiment and simulation with the aim to verify the possibility of numerical replication of the interface formation processes in real compounds. This assists estimations of interface width and phase formation, and helps to keep experimental efforts to a minimum for assessing future compound systems.

Outline of the thesis

In the following, Chapter 2 describes the methods for coating the aluminium and magnesium alloy substrates and circumventing the problem of natural oxidation via deposition of metallic layers. Furthermore, the challenges of excessive formation of

IMPs at the interface of Al–Mg couples and the solution approaches are detailed in this section. In Chapter 3, results of wetting experiments for Al–Al, Mg–Mg and Al–Mg couples are shown. Interface formation and their properties are discussed for each of these compound compositions in chapters 4 to 6, respectively. Thermodynamic calculations of interdiffusion at the interface are compared to experimental findings and thus assessed for predictions using software tools. Chapter 7 is used to summarize and conclude the thesis.

1.5 Wetting and diffusion

A detailed understanding of the mechanisms, which are involved in bonding formation, is of vital importance to locate potential for improvements or reasons of failure. The intensity of the reactions at the interface between a solid and a liquid determines the joint's properties to a great extent. Also, it dictates the formation of IMPs, which may cause mechanical problems. In the following, an introduction to the basics in wetting reactions from an energy point of view is given, and the connection between these and the measure for wettability, the wetting angle, is explained. At the end of this section, the possibilities to simulate diffusion events at the interface, and thus its composition after the compound casting process, are delineated.

Wetting

The nature of an interfacial interaction to join two materials can be chemical, physical, or simply mechanical. Joining processes resulting in physical or chemical bonding, such as solid-state diffusion, brazing and compound casting, are ruled by the general thermodynamic principle of energy reduction: the elimination of two surfaces to form an interface reduces the total Gibbs free energy G of the system, which Nascimento *et al.* [Nascimento, 2003] expressed as

$$G = G^0 + A\gamma, \tag{1.1}$$

with the Gibbs free energy of the system assuming identical surface and bulk properties G^0, the solid-liquid interfacial area A and interfacial energy γ. The last term in equation 1.1 describes the excess energy due to the presence of an interface.

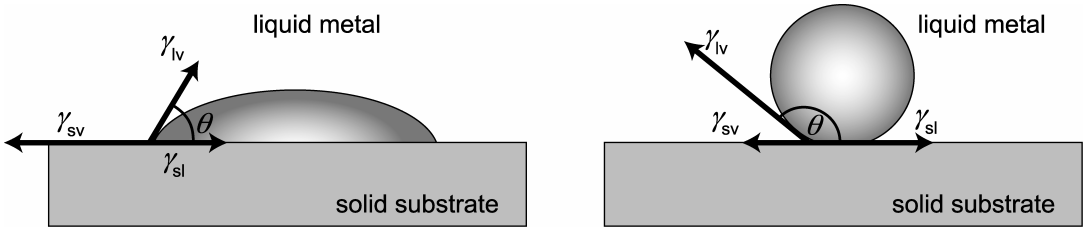

Fig. 1.3: Contact angle θ of a sessile drop on a solid substrate. Good (l) and poor (r) wetting. The interfacial energies are represented as vectors with lengths qualitatively related to the respective energy values.

In thermodynamic balance, the interfacial energies determine good or poor wettability (Fig.1.3). Non-reactive wetting leads to the following expression of the wetting angle θ (Young's equation):

$$\cos(\theta) = (\gamma_{sv} - \gamma_{sl}) / \gamma_{lv}, \tag{1.2}$$

with γ_{sv}, γ_{sl} and γ_{lv} being the solid-vapour, solid-liquid and liquid-vapour interfacial energies, respectively.

The sessile drop method, which was developed by Bashforth and Adams in 1883 [Bashforth, 1883], is an important way to obtain absolute values for surface and interface energies. An angle of 70° is considered to represent the threshold for wetting to take place [Moorhead, 1986].

In our experiments, we assume that the outermost microns of the substrate are fused, and that the wetting event is accompanied by the blending of this layer with the melt droplet. A reaction will therefore influence (and actually facilitate) wetting, which adds a term to the driving force for wetting in the form of a variation of the Gibbs free energy. This term ΔG_r, however, can only be roughly estimated due to unassessed correlations of interfacial reactions to wetting kinetics [Eustathopoulos, 1998]. The various reactions that can take place between solid and liquid have been summarized by Nascimento *et al.* [Nascimento, 2003], who also schematically described various stages of reactive wetting. In our systems, we observe total wetting for Al–Al and Mg–Mg couples, which indicate strong interfacial reactions. In the Al–Mg system, the coating material has only very limited solubility in the melt, which prevents an intense reaction and thus leads to bigger wetting angles. Still, the

reactivity is great enough to ensure a metallurgic bonding between substrate and droplet.

Diffusion and Thermodynamic calculation tools (TC/DICTRA/Pandat)[4]

With the same principle of energy reduction as delineated for wetting reactions, one can calculate diffusion, solidification and phase formation processes in a multitude of systems. Diffusion and mobility data for light metals and alloys are accessible, and several programs to do calculations on them are available, such as TC/DICTRA and Pandat.

To set the parameters for an interface diffusion calculation, some assumptions and simplifications have to be made, partly due to idealizing alloy compositions and wetting kinetics, restrictions in sample handling and lack of process parameter control, and partly due to limitations of the used softwares. Therefore, the sample volume of interest is confined to a sub-millimetre range, where temperature gradients and variations in cooling rates can be neglected.

Calculations on diffusion of alloying elements during sample production have been done with ThermoCalc/DICTRA (Al–Al) and Pandat (Mg–Mg), whereas subsequent heat treatments were simulated and applied experimentally only for Al–Al compounds. A detailed description of calculations and corresponding results is given in sections 4.4 and 5.3 for Al–Al and Mg–Mg couples, respectively.

[4] TC/DICTRA: ThermoCalc Software, www.thermocalc.se.

Pandat: CompuTherm LLC, www.computherm.com.

References

Balleer, H.-L., Bönning, M., Datta, J., Gross, G.H., Kammer, C., von der Osten-Sacken, E., Philp, S., Rösch, F., Schemme, K., Zehnder, J. Aluminium im Verkehrswesen. Aluminium-Taschenbuch. *Aluminium Verlag GmbH,* Düsseldorf (D), p. 545-773 (1997).

Baril, E., Labelle, P., Pekguleryuz, M.O. Elevated temperature Mg-Al-Sr: creep resistance, mechanical properties, and microstructure. *JOM*, 11:34-39 (2003).

Bashforth, F., Adams, J.C. An attempt to test the theory of capillary action. *Cambridge University Press,* Cambridge (UK) (1883).

Belov, N.A., Aksenov, A.A., Eskin, D.G. Iron in aluminum alloys: impurity and alloying element. ed., *CRC Press,* Boca Raton (USA), p. 360 (2002).

Brandt, D., Büchen, W., Güsgen, J., Huppatz, W., Koewius, A., Linn, W., Sedlaceck, G., Wahle, M. Konstruieren mit Aluminium. Aluminium-Taschenbuch. *Aluminium Verlag GmbH,* Düsseldorf, (D), p. 359-543 (1997).

Dienwiebel, M., Pühlmann, K., Scherge, M. Origins of the wear resistance of AlSi cylinder bore surfaces studies by surface analytical tools. *Tribology International*, 10-12:1597 (2007).

Eustathopoulos, N. Dynamics of wetting in reactive metal/ ceramic systems. *Acta Materialia*, 7:2319 (1998).

Flierl, R., Wolf, J., Gibisch, R. Cylinder-crankcase of a liquid cooled internal combustion engine. Patent EP20020700217, 24 (2003).

Gürtler, G. Verbundguss. *DGM,* Düsseldorf (D), p. 368-373 (1969).

Klüting, M., Landerl, C. Der neue R6-Ottomotor von BMW. *MTZ,* 11:(2005).

Moorhead, A.J., Keating, H. Direct Brazing Of Ceramics For Advanced Heavy-Duty Diesels. *Welding Journal*, 10:17-31 (1986).

Nascimento, R.M., Martinelli, A.E., Buschinelli, A.J.A. Review Article: recent advances in metal-ceramic brazing. *Cerâmica*, 178-198 (2003).

Chapter 2

Strategies for developing coating systems

To enable a metallurgical reaction at the surface of light metals and thereby generate good wetting properties towards metallic melts, the natural, ever-present oxide/hydroxide layer has to be overcome and replaced permanently. The following chapter gives an overview of surface treatments and introduces the strategies for developing coating systems for the application in compound casting. The challenges that we met (2.1) lead to specific coating systems for each of the three compound systems Al–Al, Mg–Mg (2.2) and Al–Mg (2.3). The coatings are investigated by analyzing polished cross-sections with optical (OM) and scanning electron microscopy (SEM), and glow discharge optical spectroscopy (GDOS). Heat treatments, used to increase adhesion of the coating on magnesium substrates and spalling tests of coatings are carried out (2.4). A short conclusion of the successive surface modifications summarizes the findings at the end (2.5).

2.1 Challenges

2.1.1 Surfaces of light metals

Neither You nor me have ever touched metallic aluminium. This light metal, as any other of this material class ($\rho \leq 4.7$ g/cm^3), is covered with a few nanometers (naturally) to several hundreds of µm (depending on surface treatments) thick oxide and/or hydroxide layer. If it is removed by mechanical, chemical or electrochemical methods, the underlying aluminium atoms react instantly with oxygen or oxygen containing molecules from the environment to rebuild this coating (i.e. passivation layer). Actually, this can be called a corrosion product, but it is thermodynamically stable, inert, very hard (9 Mohs), and has a very high melting point (2050 °C, compared to the melting point of 660 °C for Al).

Besides the low specific weight, the surface of aluminium is its key success factor. With anodic and thermal modifications, a huge variety of surface structures can be achieved. In nearly every aluminium application, the oxide layer plays a vital role. Methods to increase or decrease the thickness, density, porosity and roughness of the oxide layer all result in a highly specific functionality of the aluminium surface.

None of the methods that modify the oxide layer constantly remove this coating. The deposition of a metallic coating, however, often implies a replacement of the oxide. This is done for applications aiming at increasing resistance towards abrasion, corrosion or heat, increasing electrical conductivity, weldability or hardness, decreasing friction or simply for decorative aspects, as summarized by Huppatz [Huppatz, 1996]. Chemical treatments to deposit metallic layers on light metal surfaces via ion exchange reactions have been developed for electroindustrial applications, for example to improve electrical conductivity at a contact. In section 2.2, the application of such treatments and further tasks to improve these coating systems is demonstrated.

2.1.2 Zinc as alloying element in light metals

Together with a low melting point and other properties explained in this chapter, it would be desirable to use a coating, whose composition plays also a role as alloying element. Zinc (T_m = 419 °C) is used in commercial aluminium and magnesium alloys with equal importance: In aluminium based cast and wrought materials (Zn is the

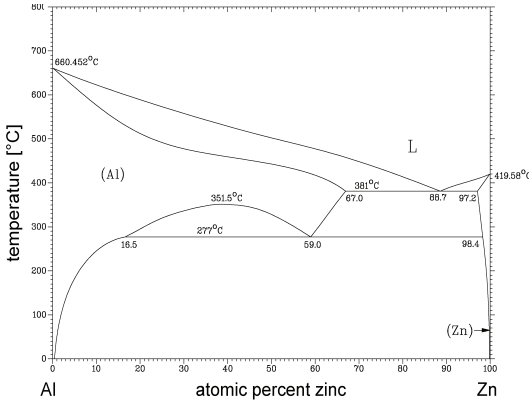

Fig. 2.1: The aluminium-zinc phase diagram. Zn is the element with the highest solubility (up to 70 at-%) in Al.

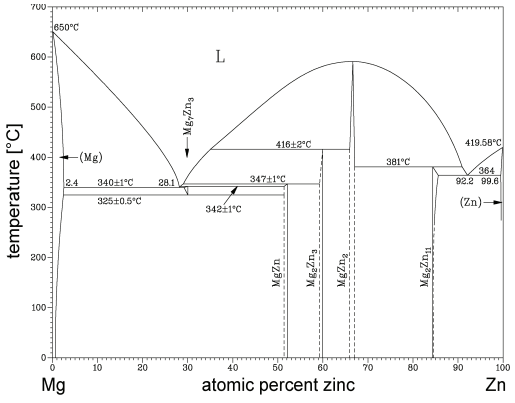

Fig. 2.2: The magnesium-zinc phase diagram. Note the low eutectic temperature.

main alloying element in cast 7xx.x and wrought 7xxx series). Zinc has the best solubility in aluminium (Fig. 2.1) of all elements, making it a valuable component in cast and wrought alloys. It gives the possibility of natural and artificial ageing (precipitation hardening) in combination with magnesium. The strength is substantially improved by the formation of $MgZn_2$ precipitates. Furthermore, it increases the solution potential for use in protective cladding and sacrificial anodes [ASM, 1993].

Natural ageing (e.g. in the 7075 alloy) refers to spontaneous formation of a Guinier-Preston (GP) zone structure at room temperature, which result from clustering or segregation of solute atoms to selected atomic planes, depending on the alloy system [Polmear, 1995]. These GP zones resist dislocation movement through the lattice better than alloy atoms in solution, making the material stronger. However, as under these conditions the alloy would practically never become stable (in contrast to copper containing alloys of the 2xxx series), it is rarely used in the naturally aged temper, but rather artificially aged [ASM, 1993].

When exposing the alloy to elevated temperatures, metastable coherent (i.e. with the same crystal structure as the solvent phase) transitional precipitates form and contribute to precipitation strengthening. Further heating increases their size and converts them to the equilibrium phases, which generally are not coherent, and thus soften the material again. In any case, a solution heat treatment at high temperatures to maximize solubility followed by a quench to obtain a supersaturated solid solution is performed prior to ageing.

In magnesium alloys, zinc (designated with the letter 'Z' in ASTM alloy definitions, e.g. AZ91 stands for Mg–9Al–1Zn, ZK31 for Mg–3Zn–1Zr) has beneficial influence on castability, strength, and other mechanical properties at room temperature. The newest high-purity (HP) generation of the alloy ZK60 exhibits, apart from major strengthening effects, excellent casting properties even for most complex and thin-walled components, which is partly the consequence of the formation of a eutectic at 340 °C in the binary Mg–Zn system (Fig. 2.2). However, microporosity and susceptibility to hot cracking are disadvantages when alloying this element. In wrought alloys, zinc is the second most important component after aluminium [Kainer, 2000].

2.1.3 Zinc as coating material

If zinc is applied as a coating, it is usually done to protect the underlying material – most often steel – from cathodic corrosion: If the surface is penetrated by a scratch, it self-heals without the need of maintenance. About 50% of the worldwide zinc consumption is for corrosion protection, and over 90% of these layers are deposited via hot-dip galvanization, where a structure is immersed in a bath of liquid zinc. Today, the boilers for this process measure up to 20 meters and may contain 700 tonnes of zinc. This method is most suitable for coating large quantities of sheet or wire [Johnen, 1981].

Other techniques to deposit a metallic zinc layer exist; the most important being galvanization, flame spraying and powder plating. These are suitable for coating small areas or piece numbers, which is most interesting for this project. As the shape of the specimens for this thesis is very simple (platelets of 2 mm x 20 mm x 100 mm for the coating process), galvanizing is a straightforward approach and easy to realize. Acidic and alkaline cyanide-free electrolytes are commercially available. In Figure 2.3, the Pourbaix-diagrams of aluminium and magnesium are shown. These indicate regions of immunity, passivation and corrosion in aqueous solutions. The region of passivation for aluminium, an amphoteric material, lies between pH values of 4 and 8.5, whereas the surface of magnesium passivates above pH 10 only. Therefore, different electrolytes have to be used for these materials to avoid the evolution of gas (which usually occurs when metal corrodes) during plating and thus poor adhesion or even complete delamination.

From mild acidic solutions, zinc can only be deposited with a very high excess voltage. As the metal is at hand in simple, heavily dissociate salts, plating is effected with nearly one hundred percent of current yield. No or only marginal amounts of hydrogen is co-precipitated. Apart from zinc salts other components for uniform deposition such as conduction salts, complexing agents for glossy appearance and additives for improved anode dissolubility have to be added. These baths are generally easy to handle and to maintain, deposits are smooth and dense, and show only little danger of hydrogen embrittling the substrate material.

Alkaline electrolytes may contain cyanides, which would require special equipment and precautions due to the toxicity of these components. Therefore, cyanide-free solutions were used here. The current density is relatively low, and the purity of the initial ingredients is crucial to achieve good plating results. Nevertheless, the advantage of leaving out wastewater cleaning is superior to the disadvantage of unstable bath conditions, as despite this, dense and homogeneous zinc layers were obtained with these baths. Compositions of the plating electrolytes, which were products of the company SurTec[1], and the process parameters are given in Table 2.1.

In combination with the processes to replace the oxide layer with a metallic zinc deposit, which are described in section 2.2, zinc plating via galvanization gives us a strong tool to improve reactivity and thus wettability of light metals.

Table 2.1: Compositions of zinc galvanizing electrolytes and parameters

on aluminium (SurTec757)	on magnesium (SurTec704)
85 g/l $ZnCl_2 \cdot 1.5\ H_2O$	120 g/l NaOH
210 g/l KCl	12.5 g/l ZnO
22.4 g/l H_3BO_4	50 g/l Na_2CO_3
50 ml/l *SurTec757 I*	10 ml/l *SurTec704 I*
4 ml/l *SurTec757 II*	10 ml/l *SurTec704 R*
400 s, 25 °C (i.e. room temperature, RT)	1 ml/l *SurTec704 II*
pH = 5 - 6	500 s, RT
$S = 6$ A/dm^2	pH = 13
	$S = 2$ A/dm^2

[1] Surface Technology GmbH, Surtec-Str. 2, 64673 Zwingenberg, Germany. www.surtec.de

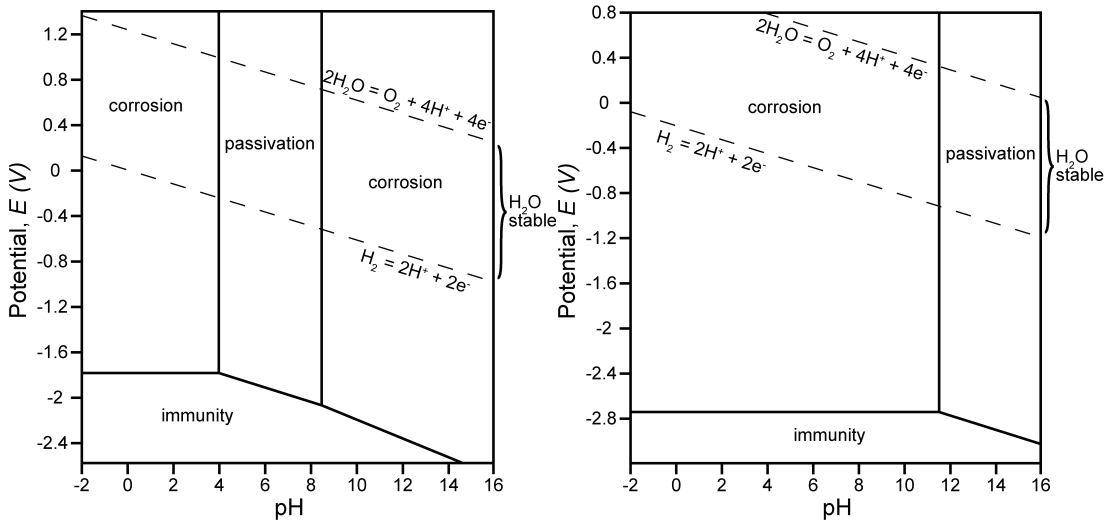

Fig. 2.3: Pourbaix (or Potential/pH) diagrams of Al (l) and Mg (r) in water at 25 °C. Aluminium is amphoteric, whereas magnesium passivates only at high pH values.

2.1.4 Specific prerequisites for compound casting dissimilar materials

Bringing the surface into contact with a metallic melt generates further challenges. Tight bonding is a function of wettability, and thus reactivity. The formation of undesired products at the interface needs to be prohibited by precautious choosing the right, or a particular combination of several, coating elements. This becomes especially important if the joined materials are dissimilar, e.g. iron and aluminium [Fragner, 2006; Dybkov, 1990; Mehrer, 1997; Eggersmann, 2000; Yajiang, 2005; Choe, 2008] or aluminium and magnesium [Schubert, 2001; Klüting, 2005; Borrisutthekul, 2005; Mahendran, 2008; Paramsothy, 2008], where the interface is composed of several IMPs, which usually exhibit poor mechanical properties. There, the coating is assigned another function: instead of purely enhancing the reactivity, it has to protect the underlying substrate from excessively blending with the melt. This has to come about without cutting too much on wettability, which severely narrows the prospects of finding a mechanically acceptable candidate. An approach towards such a coating is described in section 2.3.

2.2 Strategies for surface modifications to join similar materials

For this project, processes that constantly remove the oxide layer by replacement with metallic depositions are of great importance. If a metallic melt is cast onto a light metal substrate, the oxide would persist due to its thermal stability and thus prevents a metallurgic connection needed for material closure (see section 1.2). Novel combinations of coating techniques together with heat treatments (in the case of Mg–Mg couples) were the key factors to successfully facilitate a wetting reaction on light metal surfaces.

In the following, the development of tailor-made surface modifications for the application of compound casting is described.

2.2.1 Aluminium alloys[2]

Oxide layer

A method widely applied – the so-called 'zincate process' – is described by various authors [Saito, 2005; Qi, 2002a; Tang, 2001; Robertson, 1995]. The use of this process has been reported for Ni plating of aluminium surfaces in electrical applications [Chen, 2006; Monteiro, 1991] and for pre-treatments prior to electroplating [Pearson, 1997; Qi, 2002b; Armyanov, 1982]. It replaces the Al_2O_3-layer of aluminium alloys with a metallic Zn film, via two parallel chemical reactions. The first is an etching procedure, which removes the aluminium oxide layer; the second is a redox reaction, where metallic Al oxidizes and dissolves (see eq. 2.1) and zincate anions dissociate and are reduced and deposited as a dense metallic layer (eqs. 2.3 and 2.4, respectively) [Zipperian, 1987]. This process was carried out here with a single solution containing NaOH and Zn anions with the trade name 'SurTec652' (Table 2.2). When working with zincate(II)-anions, enough OH^- ions have to be present, as otherwise, the tetrahydro-complex $[Zn(OH)_4]^{2-}$ prevails. This is achieved by working at a pH of 12 or more. In addition to the process' simplicity, this treatment

[2] K.J.M. Papis, B. Hallstedt, J.F. Löffler and P.J. Uggowitzer. Interface formation in aluminium-aluminium compound casting. Acta Mater. 13 (2008), 3036-3043.

does not require the special atmospheres, which are otherwise used to avoid aluminium oxide formation [Polmear, 1995].

Oxidation (anodic reaction):

$$Al_{(s)} + 4OH^- \rightarrow [Al(OH)_4]^- + 3e^- \quad (2.1)$$

$$[Al(OH)_4]^- \rightarrow AlO_2^- + 2H_2O \quad (2.2)$$

Reduction:

$$Zn(OH)_4^{2-} \rightarrow Zn^{2+} + 4OH^- \quad (2.3)$$

$$Zn^{2+} + 2e^- \rightarrow Zn_{(s)} \quad (2.4)$$

Sum (cathodic reaction):

$$[Zn(OH)_4]^{2-} + 2e^- \rightarrow Zn_{(s)} + 4OH^- \quad (2.5)$$

Total reaction:

$$2Al_{(s)} + 3[Zn(OH)_4]^{2-} \Leftrightarrow 3Zn_{(s)} \downarrow + 2[Al(OH)_4]^- + 4OH^- \quad (2.6)$$

Anodic side reaction for H_2-production:

$$Al + 3OH^- \rightarrow AlO_2^- + H_2O + \tfrac{1}{2}H_2 \uparrow + 2e^- \quad (2.7)$$

The plating reaction is kinetically controlled via local nucleation, and continues as long as the solution containing zincate ions has direct contact to aluminium oxide. It thus leaves a dense metallic Zn layer with a thickness of about 200 - 300 nm on top of the bulk metallic aluminium. On some substrate alloys, however, the reaction lasts longer, as the deposits do not form a dense layer. This leads to a thicker coating with coarser zinc crystallites (Fig. 2.7).

This method can be applied to various substrate alloys. For reasons of availability, alloying elements and commercial use as sheet or extruded material, AlMg1[3] was mainly used for wetting experiments and sample production. Some successful coating and casting experiments (investigations on the influence of component size on the diffusion at the interface, see section 4.6) were done with the wrought alloy AlMg3[4] and the foundry alloy AlSi7Mg[5], without substantially altering the solution compositions.

Important surface condition

The treatment works well only if one starts with thin oxide layers. Sheet aluminium is produced via rolling, which always leaves behind irregular layers of oxides, lubricant remainders and other inclusions with a thickness of several microns. It is therefore necessary to remove this 'rolling layer', either mechanically or chemically, and clean the surface thoroughly prior to immersion in a zincate solution. This was done here with a mild pickling solution at 55 °C, applying ultrasound for 15 minutes to remove lubricant contaminations. Subsequently, the rolling layer was etched away in a strong alkaline NaOH solution (100 g/l, pH > 13) for 1 minute at 55 °C. The pickling layer, which builds up during this process, was removed by etching in 35% nitric acid at room temperature for 30 s. Between each of these important cleaning steps the samples were rinsed in deionized water for 1 minute. Compositions of solutions and parameters are given in Table 2.2 on page 28. After these pre-treatments, the platelets showed a surface with smooth etching pits (Fig. 2.4), ready to be zinc-coated by the zincate process described above. Figures 2.5, 2.6 and 2.7 show the zincate treated surfaces of the alloys AlMg1, AlMg3 and AlSi7Mg, respectively.

[3] AlMg1, i.e. Al-alloy (AA) 5005, is composed of: 1.0 Mg, 0.4 Fe, 0.25 Si, 0.15 Mn, (balance Al) – all in mass-%

[4] AlMg3 (AA5754) is composed of: 3.1 Mg, 0.4 Fe, 0.4 Si, 0.5 Mn, (balance Al) – all in mass-%

[5] AlSi7Mg (AA357) is composed of: 7.0 Si, 0.5 Mg, 0.15 Ti, (balance Al) – all in mass-%

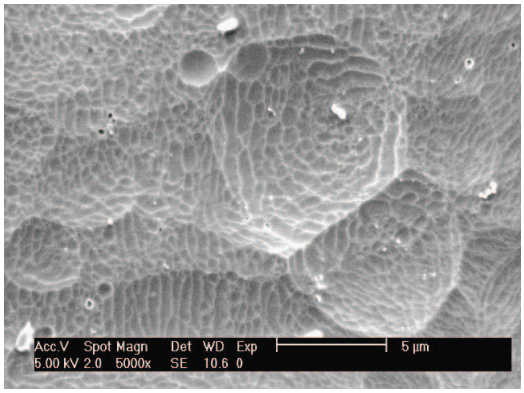

Fig. 2.4: After pickling and cleaning the substrate, its surface structure appears evenly etched.

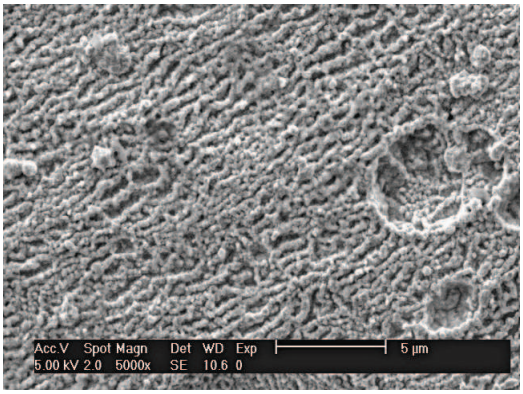

Fig. 2.5: The zincate treatment replaces the aluminium oxide layer with a poly-crystalline, metallic zinc film of 200 - 300 nm thickness, here on AlMg1.

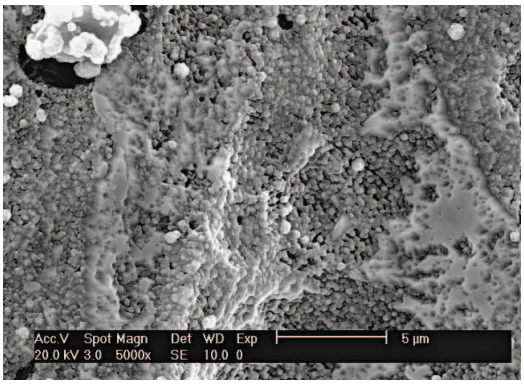

Fig. 2.6: Zincate treated surface of alloy AlMg3. The Zn layer appears fine-grained and dense.

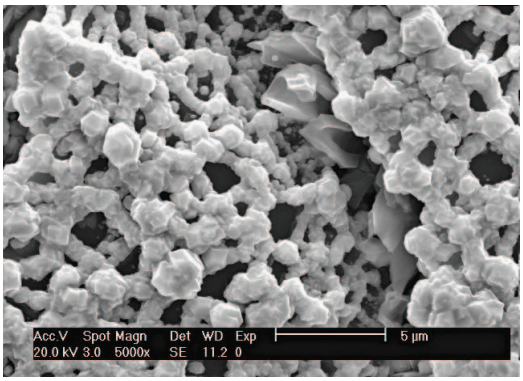

Fig. 2.7: Zincate treated surface of alloy AlSi7Mg. The layer's porous structure leads to coarser crystallites and a thicker 'primer'.

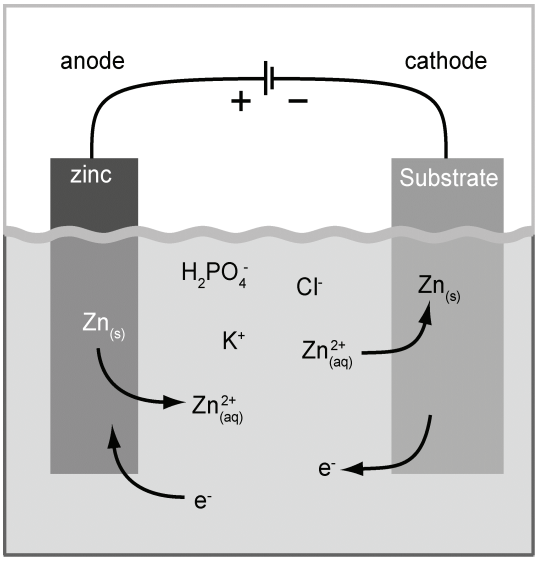

Fig. 2.8: A single chamber electrolytic cell with a schematic illustration of chemical reactions and charge transfer paths.

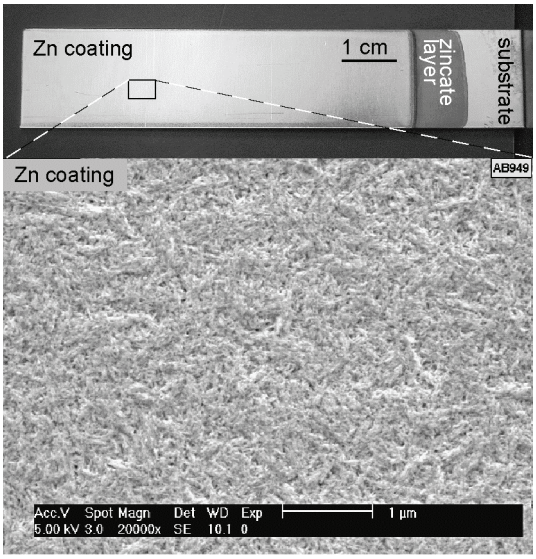

Fig. 2.9: The final glossy and smooth zinc deposit on an AlMg1 substrate.

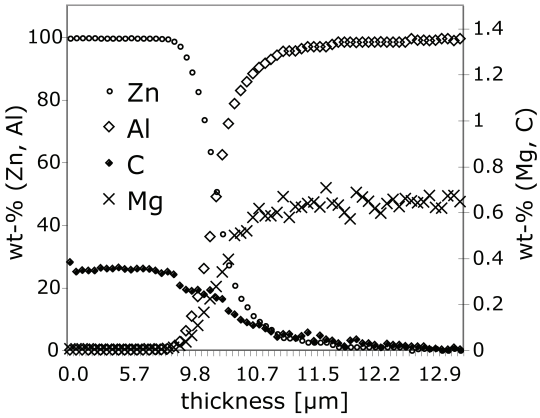

Fig. 2.10: GDO spectrogram of a zinc galvanized AlMg1 specimen with a 10 µm thick zinc layer.

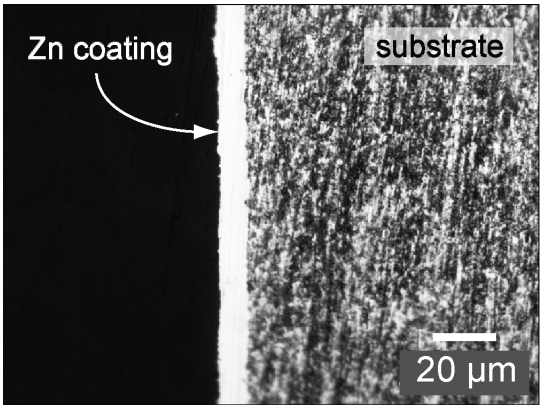

Fig. 2.11: Cross-section of a zinc galvanized AlMg1 specimen substrate.

Layer thickness and melting point

For the application in compound casting, the reactive surface layer has to persist until the metallic melt is touching. In a die casting mould, temperatures of around 250 °C prevail, which would cause the thin Zn layer obtained by the zincate process to be alloyed into the substrate. As zinc has a very high solubility in aluminium (Fig. 2.1), reoxidation of the Al-substrate can occur if it completely diffuses into the bulk substrate at these elevated temperatures.

The coating thickness was therefore increased to 5 - 10 µm. Johnen [Johnen, 1981] described several techniques to do this, ranging from hot-dip galvanizing to flame spraying, powder deposition techniques and galvanization methods. We chose zinc galvanizing to be the most straightforward method to uniformly cover the flat surface of the sheet material used as substrate in this project. This technique is most suitable to coat small areas of flat specimens, and is applicable with rather simple devices in a laboratory, whereas other methods would require massive and more expensive tools.

To galvanize a conductive substrate, a simple electrolytic cell can be used. Its setup is very simple if working in a single chamber device (Fig. 2.8). With temperature, current, bath movement and plating area, there are some parameters, which need to be adjusted according to the electrolyte's specifications.

A commercial zinc electrolyte was used for optimum coating appearance and density (SurTec757, Table 2.1). The Zn deposits originating from the zincate process represent an ideal surface for good adhesion of the galvanizing layer – a 'primer', so to speak. The resulting layer thickness was adjusted according to the current density, checked by glow discharge optical spectroscopy (GDOS, Fig. 2.10) and optical microscopy (Fig. 2.11), and determined to be ideally around 10 µm (current density $S = 600$ A/m^2, $t = 400$ s, $T = 25$ °C). Small amounts of carbon (up to 0.4%) were present in the coating: a result of the electrolyte's composition, which did not affect the coating's function. The obtained coating appeared glossy, dense and fine-grained (Fig. 2.9).

Another important factor when choosing the appropriate element as coating material is its melting temperature. If, during the compound casting process, the melt touches the substrate's surface, it is crucial to liquefy the outermost microns to enhance blending. With 419 °C (Fig. 2.1), the melting point of zinc is about 300 °C

lower than the processing temperature of aluminium based melts (700 - 750 °C), and therefore beneficial for reacting with these.

2.2.2 Magnesium alloys[6]

Oxide layer

Similar procedures to replace the oxide/hydroxide layer are described by Chen *et al.*, Zhu *et al.*, Taylor and Jelinek [Chen, 2006; Zhu, 2006; Taylor, 2001; Jelinek, 2005] for magnesium alloys. An immersion solution containing zincsulphate anions, buffering agents and emulsifiers was prepared for carrying out the ion exchange reaction, much the same means to replace the oxide/hydroxide layer with a metallic one as applied for aluminium. Similarly, a pickling process occurs parallel to the redox-reaction forming the zinc coating.

Commercially available AZ31[7] and ZK31[8] wrought magnesium alloys in extruded state were used as a substrate for experiments. With magnesium alloys, the pre-treatments are much more sensitive to alloy composition than when working on varying aluminium alloys. Two very different sets of solutions, listed in Tables 2.3 and 2.4, were applied to achieve similar results. These are either commonly applied solutions or partially adapted from the works of Jelinek, Chen *et al.* and Zhu *et al.* [Jelinek, 2005; Chen, 2006; Zhu, 2006].

Micrographs of immersed samples are shown in Figures 2.12 and 2.13. On ZK31, uncoated areas can be seen. These are locations of secondary phases, which are revealed by the activation treatment. The immersion process affects only primary Mg solid solution. To optimize the adhesion of subsequently deposited material, the total area of uncoated surface should be kept to a minimum. However, complete coverage can only be achieved with single-phased alloys, and good adhesion can even be achieved with some uncovered spots if the subsequent plating is done meticulously. In combination with a heat treatment, the adhesion can be further increased (Fig. 2.14).

[6] K.J.M. Papis, J.F. Löffler, P.J. Uggowitzer. ‚Interface formation between liquid and solid Mg alloys – An approach to continuously metallurgic joining of magnesium parts'. Materials Science and Engineering: A, 527 (2010) 2274-2279.

[7] The alloy AZ31 is composed of: 3.0 Al, 1.0 Zn, (balance Mg) – all in mass-%

[8] The alloy ZK31 is composed of: 3.0 Zn, 0.6 Zr, (balance Mg) – all in mass-%

Table 2.2: Compositions of solutions and parameters for surface treatments of aluminium alloys

Cleaning	Pickling	Activation	Zincate treatment
Gardoclean 854/5 (Chemetall GmbH, Germany) pH ~10 15 min 55 °C Ultrasound	100 g/l NaOH pH > 13 60 s 55 °C	35% nitric acid pH < 1 30 s RT	a) 50 g/l ZnO 230 g/l NaOH [Saito, 2005] *or* b) 200 ml/l *SurTec 652* pH > 12 60 s RT

Table 2.3: Compositions of solutions and parameters for AZ31 surface treatments

Pickling [Jelinek, 2005]	Activation [Chen, 2006]	Immersion [Zhu, 2006]
200 ml/l glacial acetic acid 50 g/l $NaNO_3$ 30 s RT	65 g/l $K_4P_2O_7$ 7 g/l KF 15 g/l Na_2CO_3 120 s 75 °C	30 g/l $ZnSO_4$ 120 g/l $K_4P_2O_7$ 7 g/l NaF 5 g/l Na_2CO_3 180 s 80 °C

Table 2.4: Compositions of solutions and parameters for ZK31 surface treatments

Pickling	Activation	Immersion
90 ml phosphoric acid 10 ml H_2O dist. 30 s RT	1.5% H_2SO_4 pH = 0.79 20 s RT	28 g/l $ZnSO_4$ 97 g/l $K_4P_2O_7$ 3 g/l LiF 5 g/l Na_2CO_3 30 s 65 °C

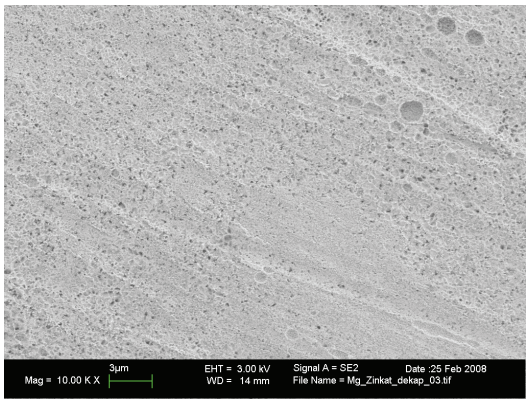

Fig. 2.12: Immersed AZ31 surface. The treatment replaces the magnesium oxide layer with a polycrystalline metallic zinc film of several hundred nm.

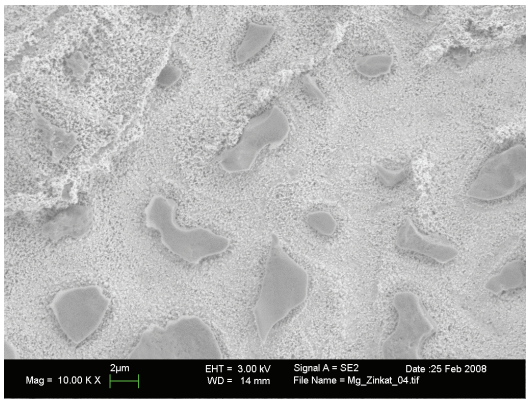

Fig. 2.13: Immersed ZK31 surface. Second phase areas are exempted from being coated.

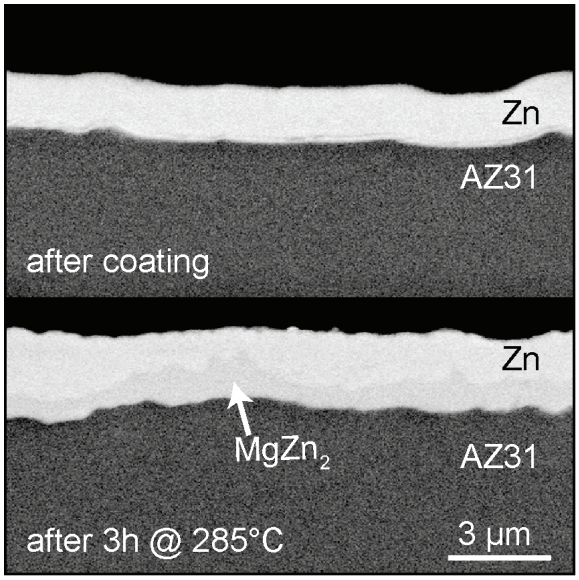

Fig. 2.14: SEM images in BSE mode. Building up an intermetallic interlayer via heat treatments increases the adhesion of the zinc coating.

Oxidation, reduction, and the total reaction at the substrate's surface are summarized as follows:

Oxidation:

$$Mg_{(s)} + 2OH^- \rightarrow Mg(OH)_2 + 2e^- \quad (2.8)$$

Dissociation of zinc sulphate:

$$ZnSO_4 + H_2O \rightarrow Zn^{2+} + HSO_4^- + OH^- \quad (2.9)$$

Reduction:

$$Zn^{2+} + 2e^- \rightarrow Zn_{(s)} \quad (2.10)$$

Sum:

$$ZnSO_4 + H_2O + 2e^- \rightarrow Zn_{(s)} + HSO_4^- + OH^- \quad (2.11)$$

Total reaction:

$$Mg_{(s)} + ZnSO_4 + H_2O + OH^- \Leftrightarrow Zn_{(s)} \downarrow + Mg(OH)_2 + HSO_4^- \quad (2.12)$$

These reactions continue to run as long as some primary magnesium is in direct contact with the solution, much the same as during the zincate processing of aluminium. Again, the layer that is obtained by this procedure is about 200 - 300 nm thick. The basic concept of this redox-reaction applies to both substrates used herein, ZK31 and AZ31, as the immersion solutions were only slightly different (in contrast to the cleaning and activation steps).

Layer thickness

The immersed magnesium alloys were zinc galvanized – analogue to aluminium beforehand – to increase the zinc layer's thickness after immersion. A different mechanism of oxide layer formation on a magnesium surface prevails: In acidic and neutral solutions, corrosion occurs instead of passivation. The latter starts only above

a pH value of 11.5, as depicted in the Pourbaix-diagram (Fig. 2.3). Therefore, electrodeposition with the previously used electrolyte would result in a poorly adhering coating. A commercially available alkaline galvanizing solution was used for plating magnesium alloys (SurTec704) to a thickness of 2 - 5 µm (Fig. 2.14). For composition and process parameters see Table 2.1 in section 2.1.3. Subsequently, a heat treatment was applied to the substrate to increase the adhesion of the coating (see section 2.4).

2.3 Strategy for surface modifications to join dissimilar materials Al and Mg[9,10]

2.3.1 Introduction

In addition to the basic challenge of constantly removing the oxide layer, another important issue has to be dealt with when joining dissimilar metals: the formation of 'unfavourable' intermetallic compounds at the newly created interface. As described in section 1.2, there have been attempts to compound cast magnesium alloys to aluminium inserts. These lead to products that excellently comply with guidelines for lightweight construction, but not necessarily with our definition of a sound compound cast component.

Other techniques aiming at joining aluminium to magnesium parts comprise friction stir lap joining [Chen, 2008], laser beam welding [Schubert, 2001; Borrisutthekul, 2005], diffusion bonding [Mahendran, 2008] or even hot coextrusion [Paramsothy, 2008]. All of these report the formation of IMPs, as predicted from the Al–Mg phase diagram in Figure 2.15, to a greater or lesser extent. Although the stoichiometry of Al_3Mg_2 suggests a simple structure of this phase, and thus the possibility of more or less ductile fracture behaviour, the unit cell is reported to count 1168 atoms by Urban *et al.* [Urban, 2004] amongst others. The mechanical properties are very poor, and fracture occurs extremely brittle. Even worse, the melting point is more than 200 °C lower than those of the pure elements ($T_{m(Al)} = 660$ °C,

[9] K.J.M Papis, J.F. Löffler and P.J. Uggowitzer. Light metal compound casting. Sci. China Ser. E Technol. Sci. 52 (2009), 46-51.

[10] K.J.M Papis, J.F. Löffler and P.J. Uggowitzer. Interface formation in Al-Mg compound cast couples. (in preparation).

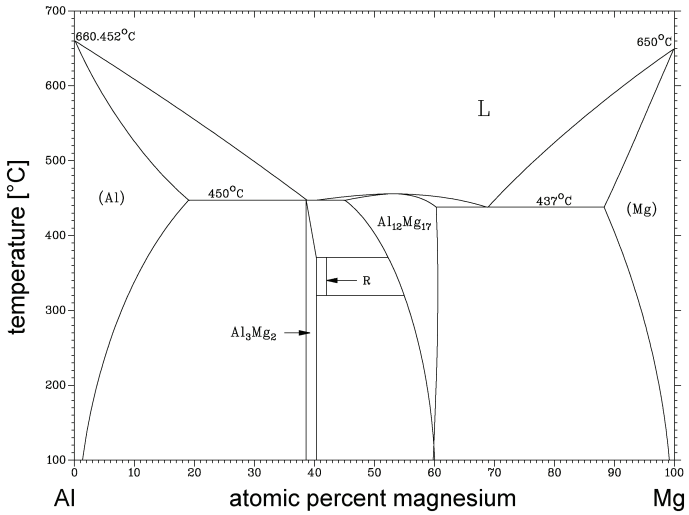

Fig. 2.15: The aluminium-magnesium phase diagram. Note the low liquidus temperatures of the IMPs.

$T_{m(Mg)} = 650$ °C, $T_{m(IMP)} \geq 437$ °C). This contributes substantially to the creep susceptibility of cast magnesium alloys containing aluminium, where Al–Mg IMPs form at the grain boundaries and soften considerably above 110 - 120 °C [Spigarelli, 2001] – a useful temperature range for an engine block cast, as mentioned by Pekguleryuz *et al.* [Pekguleryuz, 2003], lies around 150 - 200 °C. Thus facilitating grain boundary sliding, the product fails even at reduced loadings.

Creep resistant, Al containing cast Mg alloys have been developed by Noranda (Noranda Aluminium, Inc.) for the Al–Mg compound cast BMW engine block (see section 1.2). Baril et al. [Baril, 2003] reported an impeding effect of some elements on the formation of low-melting Al–Mg IMPs by selectively bonding the aluminium, which is inherently used for casting technology reasons, to another component – strontium or calcium – under the formation of hard, lamellar, grain boundary pinning intermetallics.

This approach is successful for bulk alloys, but can it help to avoid the formation of undesired phases when compound casting magnesium to aluminium? Would a strontium coating be a solution to protect the substrate effectively enough to prevent interface failure? An attempt to circumvent these problems and to facilitate Al–Mg compound casting without excessively forming IMPs from the liquid phase is described in the following.

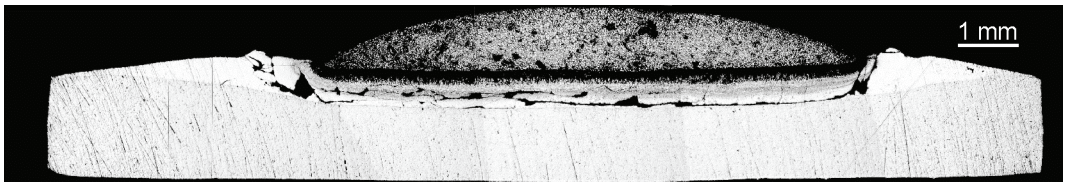

Fig. 2.16: A magnesium alloy droplet on AlMg1 substrate. Catastrophic failure due to pronounced formation of IMPs from the liquid phase.

Fig. 2.17: Close-up on the layered structure of the intermetallic interface between aluminium substrate and magnesium droplet.

2.3.2 Prerequisites for a protective layer

Besides the necessity to permanently replace the Al_2O_3 layer on aluminium surfaces by a dense metallic coating, which can effectively be achieved via the zincate process described in section 2.2.1, there are several additional prerequisites when working with dissimilar materials. To illustrate the severity of the issue, unsuccessful results from wetting experiments without taking precautions are briefly delineated:

The previously described Zn coating on AlMg1 substrate increases wettability tremendously, both for aluminium and magnesium melts. However, when one looks at the interface of Al–Mg couples produced with this coating, a thick interfacial layer, consisting of intermetallic phases, jumps into one's eye. The attempt to decrease the size of this layer by controlling the process parameters is not sufficiently successful: The width of the IMPs is decreased from 800 to 300 µm at best.

Furthermore, the interface shows very poor mechanical properties, as illustrated in Figures 2.16 and 2.17. There, one can see multiple cracks, which form during sample production already. The Mg melt liquefies the Al substrate excessively, by reason of a 220 °C lower melting point of the IMPs hence formed (Al–Mg phase diagram, Fig. 2.15). Therefore, the interfacial material solidified last, and, due to solidification shrinkage, high tensile stresses build up after crystallization. These lead to immediate failure of the interfacial IMPs.

These drawbacks are created by the excellent reactivity of the applied zinc layer and the fact, that aluminium and magnesium form IMPs with low melting points. An effort had thus to be made to modify the intermetallic compounds at the interface, and to prevent the substrate material from being liquefied by the magnesium melt. Binary phase diagrams of metal-magnesium were analyzed for various points. In the following, the prerequisites for such a coating system are listed:

- The coating material has to exhibit a higher melting point than the processing temperature of magnesium.
- The liquidus temperature should not be lowered by adding magnesium (i.e. no eutectic system).
- There has to be some solubility at elevated temperatures to ensure wetting.
- No IMPs form in this system.
- The material has to be applicable as a coating.

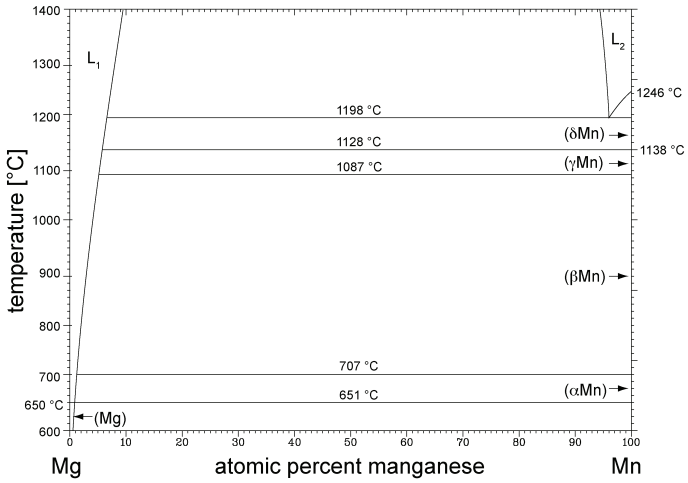

Fig. 2.18: The magnesium-manganese phase diagram, which shows no formation of IMPs.

The only element that complies with these prerequisites is manganese. The magnesium-manganese phase diagram is shown in Figure 2.18.

2.3.3 Electroplating of manganese from aqueous solutions

After deposition of the 200 - 300 nm thick zinc coating by means of the zincate process, a 3 - 4 µm thick Mn layer was applied electrochemically. The electrolyte's composition and the process parameters are listed in Table 2.5. These are partly adapted from the works of Gong *et al.* and Boshkov [Gong, 2001; Boshkov, 2003].

With these settings, current efficiencies of up to 70% were reported by Gonsalves *et al.*, Mendonza de Araujo *et al.* and Boshkov [Gonsalves, 1990; Mendonca de Araujo, 2006; Boshkov, 2003]. This efficiency is hard to achieve, as manganese is the element with the lowest standard hydrogen electrode (SHE) potential of -1.18 V depositable from aqueous solutions (compared to -1.66 V for Al) [Vanysek, 2009]. The electrolytic cell that was used here comprised a single chamber. Therefore, much more hydrogen was generated, and the efficiency dropped to 25%. The time to deposit a certain layer thickness was thus increased, but the result was a dense layer, nevertheless.

Various current densities S have been evaluated, with 600 A/m^2 yielding the best results (Fig. 2.19). Inappropriate process parameters (too low pH value, too high/low current density) result in unfavourable coatings. As Gong *et al.* [Gong, 2003] reported, certain additives have beneficial effects on metal deposition due to their

activity as complexing agents. For applying manganese as a coating, EDTA[11] improved the mechanical properties and homogeneity of the deposits but didn't have any influence on current efficiency or coating appearance in our experiments. Therefore, manganese galvanizing was performed without additives.

The intention was to keep the coating's thickness at a minimum, as mechanical properties of manganese are comparably poor. With a 3 - 4 µm thin coating (see Figure 2.20), its protective qualities already come into effect.

Table 2.5: Composition of electrolyte and parameters for Mn electrodeposition

Manganese electrolyte	Coating parameters
0.6 M $MnSO_4$	$S = 600$ Am^{-2}
1 M $(NH_4)_2SO_4$	pH 2.5 - 6
(0.05 M additive EDTA)	800 s
	RT

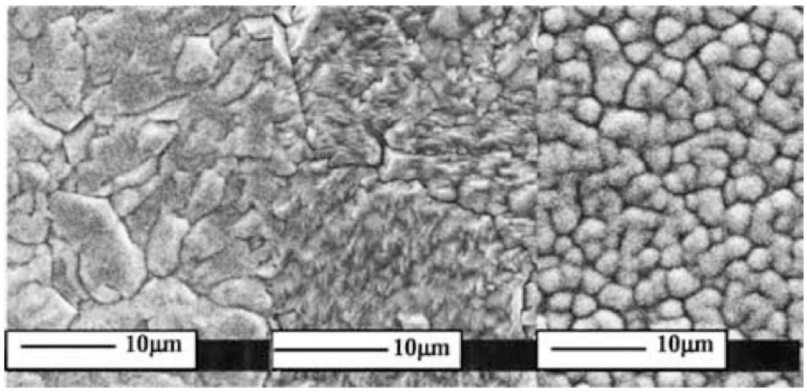

Fig. 2.19: Mn coating morphologies at different conditions: (left) current density $S = 650$ A/m^2, pH = 6.4 (silvery, polycrystalline, matte: good result); (middle) $S = 650$ A/m^2, pH = 2.1 (shiny, domain-like micro-structure: bad result); (right) $S = 3300$ A/m^2, pH = 6.4 (black, cellular, glossy: bad result).

[11] EDTA stands for ethylenediaminetetraacidic acid, $[CH_2N(CH_2CO_2H)_2]_2$

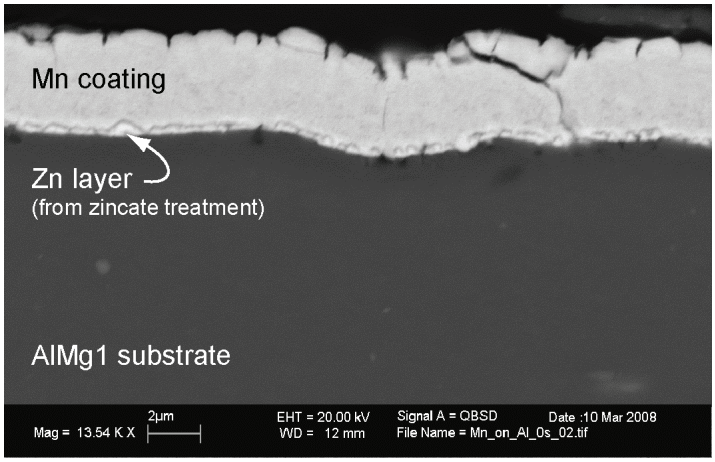

Fig. 2.20: The thickness of the protective manganese coating is around 3 - 4 µm.

2.4 Mechanical properties of platings

With the aim to develop a combination of light metal pre-treatments for application in compound casting, coating systems that tailor the surface properties of the substrates were applied to aluminium and magnesium alloys. These coatings are of stable and durable nature, which is a benefit for transportation or storage of treated components. Important aspects for handling these are robustness and adhesion.

Zinc on aluminium

In section 2.2.1, the layered structure of zinc coatings was described. The first, thin metallic coating originating from the zincate treatment, acts as a priming layer towards further depositions, much the same as when painting a surface that needs a pre-treatment to avoid peeling of the paint. Figure 2.5 shows the fine-grained crystalline structure of this layer, which covers the entire surface. The final zinc coating is shown in Figure 2.11. No spallation could be seen when the substrate was bent (Fig. 2.21a). The observed excellent adhesion of the galvanized coating could be a result of the roughness and sometimes slightly porous nature of the first layer, which can be observed on AlSi7Mg substrate in Figure 2.7.

Fig. 2.21, a - c: Coated samples after bending. Zinc on aluminium (a), zinc on magnesium (b) and manganese on aluminium (c). None of these coatings start to peel off the substrate.

Zinc on magnesium

The function as a 'primer', as mentioned for coating of aluminium substrates, was less pronounced for magnesium substrates, which implicates a treatment to increase adhesion. A heat treatment procedure was applied to the coated substrate, heating it for three hours to 285 °C. An intermetallic Mg–Zn interlayer (predominantly $MgZn_2$, measured by Energy-Dispersive X-ray Spectroscopy (EDX)), which was formed during this procedure via diffusion reaction, creates a firm chemical bond between coating and substrate (Fig. 2.14). Adhesion was improved, and bending tests show, that the substrate material breaks before the coating starts to chip (Fig. 2.21b).

Manganese on aluminium

Manganese is a brittle material: one cannot expect the coating to deform in a uniform way as the substrate. With bad adhesion, this would result in large areas of coating detachment, and thus to compound failure if such a component would be deformed. Similarly to galvanic zinc layers on zincate treated aluminium substrates, the adhesion is very good (Fig. 2.21c). The bending results in microcracks in the layer, but not in a loss of contact to the substrate.

2.5 Conclusions

Strongly adherent, dense and smooth metallic layers have been deposited electrochemically onto pre-treated, oxide-free light metal surfaces. Reoxidation is prevented permanently, and combined with an increased reactivity towards metallic melts by facilitating (partial) fusion of the coating/substrate, the surface of the aluminium and magnesium alloys that are used in this work are prepared for the purpose of compound casting.

The success of applying a firmly adhering metallic coating is strongly dependent on pre-treatments, involving cleaning, etching and ion exchange reactions. These create an effective support for subsequent galvanizing layers. If needed, adhesion can further be increased via simple heat treatments at moderate temperatures, as applied to magnesium substrates.

When it comes to joining dissimilar metals, the formation of low-melting intermetallic compounds at the interface needs to be suppressed to avoid compound failure already at low stress levels. This has to be done without cutting down too much on reactivity and thus wetting properties. A protective manganese coating was applied electrochemically. This element was chosen after assessing several of the binary Mg–Mn system's characteristics, such as solubility, melting temperature, formation of IMPs and deposition potential. With this coating system, Al–Mg compound casting displaying a very thin interface is feasible. The melt will thus solidify without forming brittle intermetallic components.

References

Armyanov, S., Vangelova, T., Stoyanchev, R. Pretreatment of Al-Mg alloys for electrodeposition by immersion zinc and electroless nickel. *Surface Technology*, 2:89-100 (1982).

ASM Speciality Handbook: Aluminum and Aluminum Alloys. In: Davis, J.R. (ed.), *ASM International,* Materials Park (USA), p. 784 (1993).

Baril, E., Labelle, P., Pekguleryuz, M.O. Elevated temperature Mg-Al-Sr: creep resistance, mechanical properties, and microstructure. *JOM*, 11:34-39 (2003).

Borrisutthekul, R., Miyashita, Y., Mutoh, Y. Dissimilar material laser welding between magnesium alloy AZ31B and aluminum alloy A5052-O. *Science and Technology of Advanced Materials*, 2:199-204 (2005).

Boshkov, N. Galvanic Zn-Mn alloys--electrodeposition, phase composition, corrosion behaviour and protective ability. *Surface and Coatings Technology*, 2-3:217 (2003).

Chen, J., Yu, G., Hu, B., Liu, Z., Ye, L., Wang, Z. A zinc transition layer in electroless nickel plating. *Surface and Coatings Technology*, 201:686-690 (2006).

Chen, Y.C., Nakata, K. Friction stir lap joining aluminum and magnesium alloys. *Scripta Materialia*, 6:433 (2008).

Choe, K., Park, K., Kang, B., Cho, G., Kim, K., Lee, K., Kim, M., Ikenaga, A., Koroyasu, S. Study of the interface between steel insert and aluminum casting in EPC. *Journal Of Materials Science & Technology*, 1:60-64 (2008).

Dybkov, V.I. Interaction of 18Cr-10Ni stainless steel with liquid aluminium. *Journal of Materials Science*, 3615-3633 (1990).

Eggersmann, M., Mehrer, H. Diffusion in intermetallic phases of the Fe-Al system. *Philosophical Magazine A-Physics Of Condensed Matter Structure; Defects And Mechanical Properties*, 5:1219-1244 (2000).

Fragner, W., Zberg, B., Sonnleitner, R., Uggowitzer, P.J., Loeffler, J.F. Interface reactions of Al and binary Al-alloys on mild steel substrates in controlled atmosphere. In: Mai, Y.W., Murch, G.E., Wohlbier, F.H. (eds.), Materials Science Forum. *Trans Tech Publications Ltd.,* Zürich (CH), p. 1157-1162 (2006).

Gong, J., Zana, I., Zangari, G. Electrochemical synthesis of crystalline and amorphous manganese coatings. *Journal Of Materials Science Letters*, 21:1921-1923 (2001).

Gonsalves, M., Pletcher, D. A study of the electrodeposition of manganese from aqueous chloride electrolytes. *Journal of Electroanalytical Chemistry*, 1-2:185 (1990).

Huppatz, W., Paul, M., Friedrich, S. Oberflächenbehandlung von Aluminium. In: Lehnert, W., Drossel, G., Liesenberg, O., Huppatz, W., Paul, M., Friedrich, S., Kammer, C. (eds.), Aluminium-Taschenbuch Band 2: Umformen, Gießen, Oberflächenbehandlung, Recykling und Ökologie. 15th ed. *Aluminium-Verlag GmbH*, Düsseldorf (D), p.437-551 (1996).

Jelinek, T.W. Vor- und Zwischenbehandlung der Ware. In: Jelinek, T.W. (ed.), Praktische Galvanotechnik. *Eugen G. Leuze Verlag,* Bad Saulgau (D), p. 147-210 (2005).

Johnen, H.J. Zink. First ed., *Metall-Verlag GmbH,* Berlin (D), p. 347 (1981).

Kainer, K.-U. von Buch, F. Stand der Technik und Entwicklungspotenziale für Magnesiumtechnik. In: Kainer, K.-U. (ed.), Magnesium - Eigenschaften, Anwendungen, Potenziale. *DGM/Wiley-VCH,* Weinheim (D), p. 1-24 (2000).

Klüting, M., Landerl, C. Der neue R6-Ottomotor von BMW. *Motortechnische Zeitschrift*, 11:(2005).

Mahendran, G., Balasubramanian, V., Senthilvelan, T. Developing diffusion bonding windows for joining AZ31B magnesium - AA2024 aluminium alloys. *Materials & Design*, 4:1240-1244 (2008).

Mehrer, H., Eggersmann, M., Gude, A., Salamon, M., Sepiol, B. Diffusion in intermetallic phases of the Fe-Al and Fe-Si systems. *Materials Science and Engineering A*, 889 (1997).

Mendonca de Araujo, J.A., Reis de Castro, M.M., Cunha Lins, V.F. Reuse of furnace fines of ferro alloy in the electrolytic manganese production. *Hydrometallurgy*, 3-4:204 (2006).

Monteiro, F.J., Barbosa, M.A., Ross, D.H., Gabe, D.R. Pretreatments To Improve The Adhesion Of Electrodeposits On Aluminum. *Surface And Interface Analysis*, 7:519-528 (1991).

Paramsothy, M., Srikanth, N., Gupta, M. Solidification processed Mg/Al bimetal macrocomposite: Microstructure and mechanical properties. *Journal of Alloys and Compounds*, 1-2:200-208 (2008).

Pearson, T., Wake, S.J. Improvements in the pretreatment of aluminium as a substrate for electrodeposition. *Transactions Of The Institute Of Metal Finishing*, 93-97 (1997).

Pekguleryuz, M.O., Labelle, P., Vermette, P. Magnesium-based casting alloys having improved elevated temperature performance, oxydation-resistant magnesium alloy melts, magnesium-based alloy castings prepared therefrom and methods for preparing same. Patent AU2002349224, 34 (2003).

Polmear, I.J. Light Alloys - Metallurgy of the light metals. Third ed., *Arnold,* London (UK), p. 362 (1995).

Qi, G., Chen, X., Shao, Z. Influence of bath chemistry on zincate morphology on aluminum bond pad. *Thin Solid Films*, 1-2:204-209 (2002a).

Qi, G., Fokkink, L.G.J., Chew, K.H. Zincating morphology of aluminum bond pad: its influence on quality of electroless nickel bumping. *Thin Solid Films*, 1-2:219-223 (2002b).

Robertson, S.G., Ritchie, I.M., Druskovich, D.M. A Kinetic And Electrochemical Study Of The Zincate Immersion Process For Aluminum. *Journal Of Applied Electrochemistry*, 7:659-666 (1995).

Saito, M., Maegawa, T., Homma, T. Electrochemical analysis of zincate treatments for Al and Al alloy films. *Electrochimica Acta*, 5:1017 (2005).

Schubert, E., Klassen, M., Zerner, I., Walz, C., Sepold, G. Light-weight structures produced by laser beam joining for future applications in automobile and aerospace industry. *Journal of Materials Processing Technology*, 1:2 (2001).

Spigarelli, S., Regev, M., Evangelista, E., Rosen, A. Review of creep behaviour of AZ91 magnesium alloy, produced by different technologies. *Materials Science and Technology*, 6:627-638 (2001).

Tang, Y.C., Davenport, A.J. The effect of heat treatment and surface roughness on the zincate treatment of aluminium alloy 6082. *Transactions Of The Institute Of Metal Finishing*, 85-89 (2001).

Taylor, S.R. Coatings for Corrosion Protection: Metallic. Encyclopedia of Materials: Science and Technology. *Elsevier Science Ltd,* Oxford (UK), p. 1269-1274 (2001).

Urban, K., Feuerbacher, M. Structurally complex alloy phases. *Journal of Non-Crystalline Solids*, 143 (2004).

Vanysek, P. Electrochemical Series. In: Lide, D.R. (ed.), CRC Handbook of Chemistry and Physics. *CRC Press/Taylor,* Boca Raton (USA), p. 8-22 (2009).

Yajiang, L. Diffusivity of Al and Fe near the diffusion bonding interface of Fe3Al with low carbon steel. *Bulletin of Materials Science*, 1:69-74 (2005).

Zhu, L., Li, W., Shan, D. Effects of low temperature thermal treatment on zinc and/or tin plated coatings of AZ91D magnesium alloy. *Surface and Coatings Technology*, 6:2768-2775 (2006).

Zipperian, D.C., Raghavan, S., Pritzker, M.D. Physical And Chemical Characteristics Of The Zincate Immersion Process For Aluminum And Aluminum-Alloys. *Journal Of The Electrochemical Society*, 8B:C437-C438 (1987).

Chapter 3

Wetting properties of modified light metal surfaces

The profound insight into the procedures to modify surface properties towards increased reactivity and thus wettability given in chapter 2 is the basis for understanding the subsequent Al–Al, Mg–Mg and Al–Mg compound casting process. This chapter covers materials selection in section 3.2, and wetting experiments in section 3.3, focussing on the experimental setup, process parameters and assessments of the wettability of the various modified substrate surfaces. The end of this chapter comprises an overview of investigation methods on the couples' bonding characteristics (3.4), and short conclusions on the experimental findings (3.5).

3.1 Introduction

In order to evaluate the performance of the previously applied coating systems, i.e. their influence on reactivity between substrate and melt, wetting experiments were performed. In the following, the strategies towards significant conclusions by efficient materials selection and process parameters are detailed. The different compound compositions imply individual solutions for these variables, which leads to unequal aims for each of them.

Joining methods for all-aluminium constructions have not experienced major changes lately – although there are well-refined processes indeed, optimized for particular applications – which set the objective of this work comparably high. Compound casting has to improve the transition between the two compound partners significantly. Therefore, the investigations on Al–Al couples focus on understanding the formation of the interface systematically and thoroughly, as well as modifying its properties via targeted selection of alloying elements and subsequent tempering procedures, including simulations of these incidents. The comparison of experimental findings and calculations on the diffusion processes occurring during couple production and heat treatments allows for predictions on interface microstructure and composition if new alloys were to be used. This will help to significantly cut down on experimental extensiveness. The present work was done mostly with binary alloys to keep the number of variables low and the effects of the varying composition attributable.

Magnesium joints are less well understood, and the materials are usually more susceptible to process imprecision. It is of great importance to facilitate compound casting, with the aim to understand the characteristics of bond formation and the influence of various alloying elements on the interface structure. In the majority of cases, commercially available alloys were thus used for Mg–Mg experiments.

A completely different view on joining is brought up when dealing with dissimilar materials. The predominant issue is to prevent the formation of low melting IMPs at the interface. This work aims at creating a tight bond between substrate and melt in Al–Mg compound cast couples, by protecting the substrate efficiently with a sufficiently reactive, and thus wettable, manganese coating. The focus lies on

investigating the interface's integrity and composition, and on determining the location of the 'weak link'.

3.2 Selection of materials

A multitude of cast and wrought aluminium and magnesium alloys exist. The individual alloying elements (and even more importantly their combinations) strongly affect the material properties. The combinations of elements for this work are chosen for several reasons. First, general differences in composition between wrought and cast products prevail: Wrought alloys generally exhibit superior workability and plastic deformation properties, whereas it is most important for foundry alloys to have high castability and a reduced affinity for hot tearing. Therefore (and due to economical issues), wrought products are generally less alloyed than cast products.

Second, the higher amount of alloying elements also has a reductive effect on the melting temperatures of the latter. This impacts process temperatures (and thus increase the devices' wear-lifespan) and the time of a cast product to solidify, which is vitally important for both ecological and economical reasons.

Third, compound casting creates a zone where alloying elements are blended. With highly variable melt consistencies, as effectuated for aluminium alloys in this work, the interface composition is adjusted in such a manner, that its mechanical properties can be selectively and systematically manipulated, most effectively via heat treatment procedures. This could be a major advantage over other joining processes, where the presence of an interface is of no benefit or even undesirable.

3.2.1 Aluminium alloys

With magnesium as the main alloying component in the 5xxx and 5xx.x series (wrought and cast products, respectively), this material has markedly increased strength without unduly decreasing the ductility. In combination with some other elements (e.g. Si, Zn, Cu), magnesium creates the possibility of precipitation hardening, which is the main reason why experiments in this work are primarily done with the commercial alloy AlMg1 (or AA5005, see section 2.2.1).

Together with copper (2xxx and 2xx.x series), magnesium forms precipitations in the aluminium matrix (S-phase Al_2CuMg). However, alloys containing exclusively 4 -

10% copper were the first to be widely used, as this element alone allows for precipitation hardening (Al_2Cu pre-precipitation) and improves strength and hardness in as-cast and tempered conditions [ASM, 1993]. Castability of aluminium alloys is reduced by the addition of copper, while resistance to hot tearing is increased.

The effect of zinc on magnesium containing aluminium alloys (7xxx and 7xx.x series) was explained in section 2.1.2. Zinc is thus an interesting component for the melt in wetting experiments. Phase diagrams of aluminium and magnesium with zinc are shown in section 2.1, Figures 2.1 and 2.2.

Silicon is the most effective element in improving casting characteristics. Fluidity and hot tear resistance are greatly enhanced, which makes aluminium-silicon compositions (4xxx and 4xx.x designation for the binary alloys, 6xxx and 3xx.x for Al–Si alloys containing also other elements) the most prominently used in all casting processes. This is why: At a concentration of 12.2 at-%, the Al–Si phase diagram (Fig. 3.1) shows a eutectic with a temperature of 577 °C, which is substantially lower than the solidus of pure or low-alloyed aluminium (660 - 630 °C). Cast alloys cover the hypo- and hypereutectic silicon range up to 25%. The relationship between cooling rates and fluidity determine the range of Si content for the various casting processes. Another benefit of alloying silicon is the reduction of specific weight and coefficient of thermal expansion (CTE).

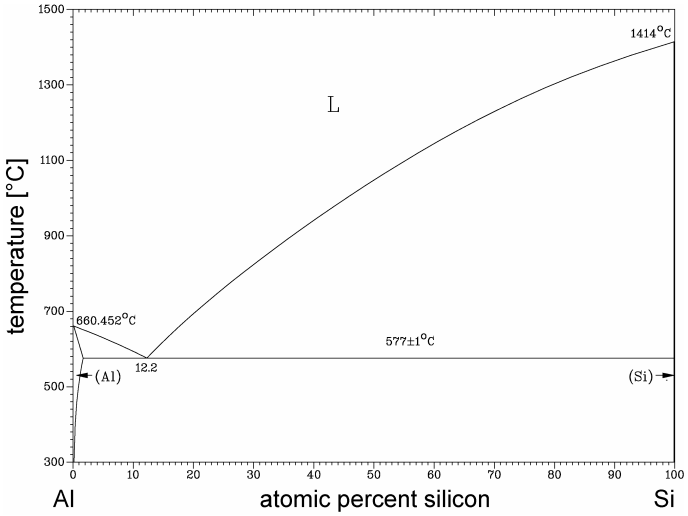

Fig. 3.1: The Al–Si phase diagram shows a eutectic at 12.2 at-% Si and 577 °C.

The melts used in this work were pure 99.98%-aluminium (Al) for reference, and aluminium alloys with 7 mass-% Si (AlSi7), 7 mass-% Cu (AlCu7) and 7 mass-% Zn (AlZn7), respectively. The different solidus temperatures of these alloys, as well as the diffusion characteristics of the individual elements are expected to have varying effects on the interfaces' microstructures and dimensions.

3.2.2 Magnesium alloys

Again, the effect of the coating material zinc (designated with the letter 'Z') on magnesium alloys has been explained in section 2.1.2. It is a common element in cast and wrought products, as it improves castability, tensile and fatigue strength [Kainer, 2000].

The most important and widely used alloying element for magnesium products is aluminium. Its increasing effect on strength was discovered as early as in the 1920s, and these alloys were distributed under the well-known name 'Elektron'. The raised hardness is attributed partly to solid solution hardening and partly to the formation of the IMP $Al_{12}Mg_{17}$ (Al–Mg phase diagram, Fig. 2.15). The melting temperature is reduced significantly, which leads to pronounced improvement of castability, but lowers the alloys' creep resistance, because of the reduced strength of these IMPs above 120 °C [Spigarelli, 2001]. Luo *et al.* suggested introducing precipitates with a higher thermal stability (increased melting or decomposition temperature), via alloying of e.g. Th, Ca, Ce and Y, for automotive and aerospace applications at elevated temperatures [Luo, 1994].

This issue was recently attended with lively interest, as described in section 2.3.1, with the development of a new family of creep-resistant alloys, containing strontium or calcium to restrain the formation of Al–Mg IMPs. Investigations on phase equilibria in the Mg–Al–Sr(–Ca) system started in the early 1980s by Makhmudov *et al.* [Makhmudov, 1981 and 1982], but it was only from the year 2000 on, when studies of the AJ and AX series (A = Al, J = Sr, X = Ca) intensified by an increasing number of researchers [Grobner, 2003; Baril, 2003; Pekguleryuz, 2003; Sato, 2005; Parvez, 2005; Jing, 2006; Aljarrah, 2007; Trojanova, 2007; Medraj, 2007]. Baril *et al.* and Pekguleryuz *et al.* focussed on determining the influence of the Al/Sr ratio on formation of the binary Al_4Sr compound and a ternary, not yet thoroughly identified Mg–Al–Sr phase, and their effect on creep properties of various Mg–Al–Sr alloys.

Amongst others, Jing *et al.* described the grain boundary pinning effect of these thermally stable precipitates, whereas Sato *et al.*, Grobner *et al.* and Parvez and co-workers focussed on determining the (still not precisely characterized) ternary compound, suggesting considerable terminal solubility of Al in the binary $Mg_{17}Sr_2$ phase.

The alloy AJ62 was chosen for this work due to its technical relevance, and with respect to its solidus temperature T_S^{AJ62} of about 530 °C, which is below that of the substrate's ($T_S^{AZ31} \approx 560$ °C, $T_S^{ZK31} \approx 555$ °C); 99.98% pure magnesium was used as a reference and because of its melting temperature of 649 °C, which is higher than the liquidus temperatures T_L of the substrates. Successful experiments with binary cast alloys were done as well, but interface properties were mainly investigated in AZ31/Mg and AZ31/AJ62 couples.

3.3 The wetting experiment[1,2,3]

A sessile droplet wetting experiment is usually done under isothermal conditions. Obviously, as stated in section 1.4 'Aims of the thesis', this is not possible here, as we deal with similar materials as both the substrate and the droplet. The experiment has to be carried out non-isothermally. Furthermore, the melt solidifies almost immediately after being placed onto the solid substrate. These issues implicate an assessment of the wettability only at a terminal stage, i.e. after the sample has left the heated area of the furnace and cooled down. It turns out, that for similar material compounds (Al–Al and Mg–Mg), the wettability is either excellent (complete and spontaneous wetting, $\theta < 10°$) or nearly non-existent (no reaction with the substrate at all, $\theta > 135°$, see Figure 1.3). Therefore, wettability of these compounds can only be classified as 'complete' if a reaction takes place, indicating a significant reduction of free energy upon contact.

[1] K.J.M. Papis, B. Hallstedt, J.F. Löffler and P.J. Uggowitzer. Interface formation in aluminium-aluminium compound casting. Acta Mater. 13 (2008), 3036-3043.

[2] K.J.M. Papis, J.F. Löffler, P.J. Uggowitzer. ‚Interface formation between liquid and solid Mg alloys – An approach to continuously metallurgic joining of magnesium parts'. Materials Science and Engineering: A, 527 (2010) 2274-2279.

[3] K.J.M Papis, J.F. Löffler and P.J. Uggowitzer. Interface formation in Al-Mg compound cast couples. (in preparation).

3.3.1 Installation of a non-isothermal setup with a horizontal furnace

A tool to drop small amounts of metallic melts onto a substrate did not exist before this project started, and an instrument that allows for sessile droplet testing at high temperatures was developed and assembled. The setup for wetting experiments comprises a horizontal furnace with a device designed both to drop metallic melts onto a substrate and to break and shear the oxide hull off the molten metal. For this purpose, a quartz glass tube with a diameter of 6 mm was narrowed at one end. As shown in Figure 3.2, the alloys were melted inside this syringe-like tube, and pushed out using a boron nitride (BN) plunger. If the melt was magnesium-based, the inside of this quartz tube had to be coated with a BN spray to prevent a reaction between the alloy and the tube wall. An overview of the whole apparatus is shown in Figure 3.3.

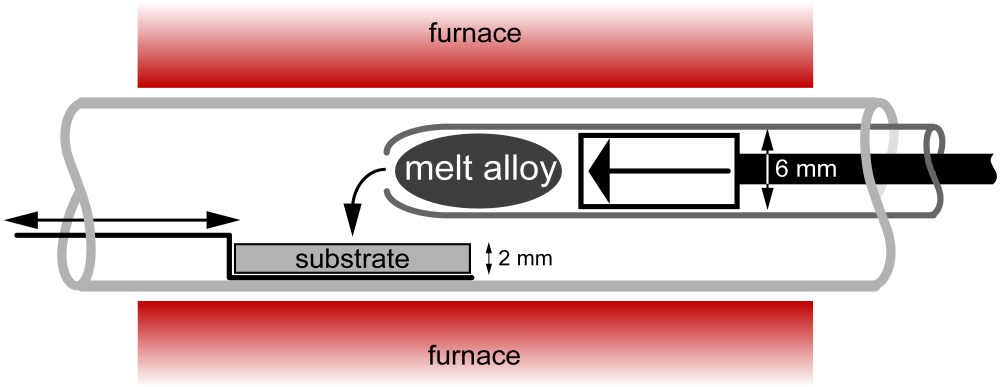

Fig. 3.2: Setup of the horizontal furnace for wetting experiments. The heated area is illustrated, where a plunger pushes the melt through the narrowed tip of a quartz glass tube. The droplet has a clean surface when it touches the substrate.

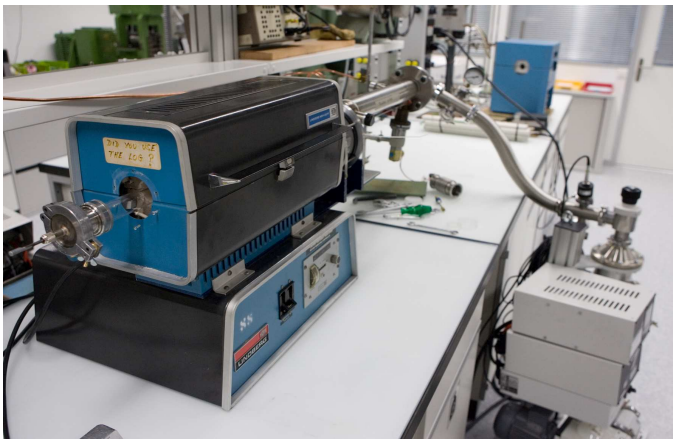

Fig. 3.3: The furnace with quartz tube, manipulators and turbo pump.

Upon dropping onto the substrate's surface, none of the oxide layer debris from the melt is present at the interface. Atmosphere composition and temperatures of melt and substrate can be adjusted, and this setup can be used for all the materials described here.

3.3.2 Parameters for compound production

Wetting tests were carried out with platelets of $20 \times 10 \times 2$ mm^3 as substrate, zincate- or zincsulphate-treated (Al and Mg based substrates, respectively) and electrochemically zinc- or manganese-coated (for similar or dissimilar material compound casting, respectively), as described in sections 2.2 and 2.3.

At a furnace temperature of 700 °C (Al) to 750 °C (Mg) and an inert argon atmosphere (99.998% Ar, 1.2 bar) due to the possibility of melt oxidation with previous evacuation to at least 5 x 10^{-5} mbar, the cast alloys were melted and dropped onto the substrate platelets (droplet weight: 1.0 ± 0.1 g (Al), 0.7 ± 0.1 g (Mg), i.e. approximately of same volume than the substrate), which were previously pushed into the furnace and heated for 30 s (Mg) to 60 s (Al) to temperatures between 250 °C and 400 °C. These parameters were determined to be most suitable for sample production and close to realistic values, as in industry casting moulds are usually pre-heated to a temperature range of 250 - 300 °C, and lower temperatures led to droplet solidification prior to the wetting event.

After the wetting incident, the specimens were pulled out of the heated zone to cool down. The process to retract the specimens from the heated zone took about three to five seconds. Depending on melt composition, and thus liquidus temperature, the droplets started to solidify not earlier than after an additional two seconds.

3.3.3 Light metal couples

Compounds of similar materials

The zinc coating significantly enhanced the wetting properties of the aluminium and magnesium substrates. The wetting angles of all investigated couples reached values of below 10° after the Zn coating (see Figures 3.4 and 3.5), indicating strong interfacial reactions and complete or perfect wetting.

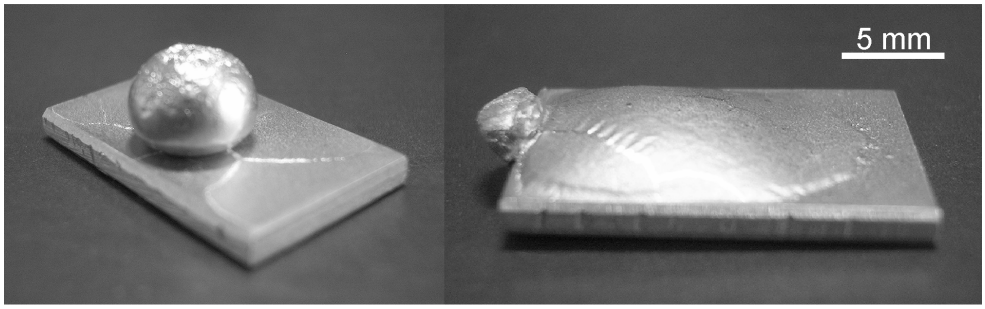

Fig. 3.4: Poor wettability of the untreated AlMg1 substrate with oxide layer (left); excellent wettability of the Zn-coated substrate (right).

Al–Al couples with excellent wetting properties were achieved with the following compositions of substrate/droplet: AlMg1/Al, AlMg1/AlCu7, AlMg1/AlSi7, AlMg1/AlSi12, AlMg1/AlSi17, AlMg1/AlZn7. The first four were investigated in depth.

Complete wetting of the substrate was achieved with the following Mg–Mg couples: AZ31/Mg, AZ31/MgAl7, AZ31/MgZn7, AZ31/AJ62, ZK31/Mg, ZK31/MgAl7, ZK31/MgZn7. Investigations focussed on the compound with commercial alloys, AZ31/AJ62, and on AZ31/Mg reference couples.

Compounds of dissimilar materials

With the protective manganese coating, the wettability is not as good as with the zinc coating, which purely aims at increasing the surface's reactivity. However, the wetting angles were still very low microscopically (Fig. 3.6). This indicates an in

Fig. 3.5: Poor wettability of the untreated AZ31 substrate with oxide layer (right); excellent wettability of the Zn-coated and heat-treated substrate (left).

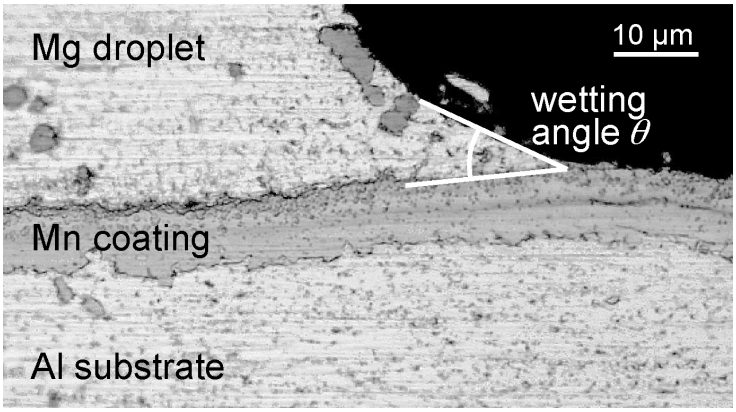

Fig. 3.6: The Mn coated AlMg1 substrate is wetted by the MgAl7 melt. A low wetting angle at microscale is observed in this optical micrograph.

comparison to Al–Al and Mg–Mg experiments reduced, but moderate reaction of magnesium with manganese, as expected from the limited solubility and from the lack of intermetallic compounds in the binary system (see Figure 2.18 in section 2.3.2). This trade-off in wetting properties is presumably a good compromise between high reactivity and low material blending.

Good results, meaning satisfactory wetting properties, were obtained with couples of AlMg1/Mg, AlMg1/MgAl7 and AlMg1/MgZn7.

3.4 Interface microstructure and composition

The samples were cut in halves perpendicular to the interface for further investigations. After polishing, they were analyzed in a Scanning Electron Microscope (SEM, Camscan Series 4) with Energy Dispersive X-ray (EDX) analysis, and microhardness (HV0.05) was measured across the interface. Hereby, the interface's chemical composition and its integrity, i.e. the existence of undesired phases, residues of the coating and other imperfections, were determined.

In general, the microstructure of the interfacial region is directly connected to its composition. As this is commonly known for the used alloys, and the compound casting process affects the composition and microstructure of the interfacial region

only, the focus lies on determining the effect of the zinc coating on the development of the interface together with the concentration gradient of alloying elements.

Investigations on interface composition comprise analyses via EDX in point-, area- and linescan, as well as element mapping modes. These give averaged information on phase compositions with a resolution and penetration depth of several µm (depending on acceleration voltage) in up to two dimensions. Detailed information of this method can be found elsewhere [Goodhew, 2001].

Additionally, the findings from EDX measurements were collected and compared to microhardness data, in respect to the lateral spreading of alloying elements from the compounds' interface.

3.5 Conclusions

Aluminium and magnesium alloys were chosen with the aim to yield significant results in terms of investigating diffusion effects, therefore comprising the most important elements such as copper, magnesium, silicon and zinc (for Al alloys), and aluminium, strontium, zinc and zirconium (for Mg alloys). With a device for non-isothermal wetting experiments that was developed for this thesis, excellent results were obtained in the Al–Al and Mg–Mg systems. With optimal process parameters, wetting angles of 10° and less were achieved.

In the Al–Mg system, the Mn coating was applied with the aim to protect the Al substrate from being liquefied by the Mg melt, and thus inhibit the formation of a thick interface consisting of brittle low-melting IMPs. This was achieved with a 3 to 4 µm thick Mn coating, which proved to be enough for effectively protecting the substrate without completely sacrificing good wettability. Thereby, Al–Mg compounds were successfully fabricated at a laboratory scale.

References

Aljarrah, M., Parvez, M.A., Li, J., Essadiqi, E., Medraj, M. Microstructural characterization of Mg-Al-Sr alloys. *Science and Technology of Advanced Materials*, 4:237 (2007).

ASM Speciality Handbook: Aluminum and Aluminum Alloys. In: Davis, J.R. (ed.), *ASM International*, Materials Park (USA), p. 784 (1993).

Baril, E., Labelle, P., Pekguleryuz, M.O. Elevated temperature Mg-Al-Sr: creep resistance, mechanical properties, and microstructure. *JOM*, 11:34-39 (2003).

Goodhew, P.J., Humphreys, J., Beanland, R. Electron Microscopy and Analysis. Third ed., *Taylor & Francis*, London (UK), p. 251 (2001).

Grobner, J., Kevorkov, D., Chumak, I., Schmid-Fetzer, R. Experimental investigation and thermodynamic calculation of ternary Al-Ca-Mg phase equilibria. *Zeitschrift für Metallkunde*, 9:976-982 (2003).

Jing, B., Yangshan, S., Shan, X., Feng, X., Tianbai, Z. Microstructure and tensile creep behavior of Mg-4Al based magnesium alloys with alkaline-earth elements Sr and Ca additions. *Materials Science and Engineering: A*, 1-2:181 (2006).

Kainer, K.-U., von Buch, F. Stand der Technik und Entwicklungspotenziale für Magnesiumtechnik. In: Kainer, K.-U. (ed.), Magnesium - Eigenschaften, Anwendungen, Potenziale. *DGM/Wiley-VCH*, Weinheim (D), p. 1-24 (2000).

Luo, A., Pekguleryuz, M.O. Review: Cast magnesium alloys for elevated temperature applications. *JOM*, 5259-5271 (1994).

Makhmudov, M.M., Bodak, O.I., Vakhobov, A.V., Dzhurayev, T.D. Phase-Equilibria In The Mg-Al-Sr System. *Russian Metallurgy*, 6:209-212 (1981).

Makhmudov, M.M., Vakhobov, A.V., Dzhurayev, T.D. Examination Of Quasibinary Sections Of The Mg-Al-Sr System. *Russian Metallurgy*, 1:122-124 (1982).

Medraj, M., Parvez, M.A., Essadiqi, E., Li, J. New phases in the Mg-Al-Sr system. *THERMEC 2006*, 1-5:1620-1625 (2007).

Parvez, M.A., Medraj, M., Essadiqi, E., Muntasar, A., Dénès, G. Experimental study of the ternary magnesium-aluminium-strontium system. *Journal of Alloys and Compounds*, 1-2:170 (2005).

Pekguleryuz, M.O., Labelle, P., Vermette, P. Magnesium-based casting alloys having improved elevated temperature performance, oxydation-resistant magnesium alloy melts, magnesium-based alloy castings prepared therefrom and methods for preparing same. Patent AU2002349224, 34 (2003).

Sato, T., Mordike, B.L., Nie, J.F., Kral, M.V. An electron microscope study of intermetallic phases in AZ91 alloy variants. *Magnesium Technology 2005*, 435-440 (2005).

Spigarelli, S., Regev, M., Evangelista, E., Rosen, A. Review of creep behaviour of AZ91 magnesium alloy, produced by different technologies. *Materials Science and Technology*, 6:627-638 (2001).

Trojanova, Z., Kral, R., Chatey, A. Deformation behaviour of an AJ50 magnesium alloy at elevated temperatures. *Materials Science and Engineering: A*, 1-2:202 (2007).

Chapter 4

Aluminium-aluminium compound casting

By applying the surface treatments described in chapter 2, Al–Al compounds were successfully produced using various alloying elements in the melt and the substrate. The first section 4.1 of this chapter outlines the interfacial microstructure and composition of all-aluminium couples. After undergoing heat-treatment procedures (solution annealing and artificial ageing, section 4.2), the interfacial regions, where diffusion of the main alloying elements occurred, exhibit significant changes in their mechanical properties (section 4.3). The casting and heat-treatment procedures were simulated by means of diffusion kinetics calculations (section 4.4), and the results are discussed in section 4.5. Thereafter follows a description of scale-up experiments, performed at the project partner LKR (4.6), and short conclusions (4.7).

4.1 Microstructure and composition of Al–Al compounds[1,2,3]

After compound casting in the horizontal furnace, which was set up for non-isothermal wetting experiments, the interfacial areas of the various Al–Al couples were analyzed in detail. The process of casting a melt onto a metallic substrate has major impact on the microstructures and compositions of both parts, mainly in proximity of the interface. These in turn determine the mechanical properties of the compound. The focus lies therefore on investigations regarding variations of grain structures and the transition of alloying elements from substrate to droplet. A fine grasp of the interfacial area's properties is established by optical and scanning electron microscopy in combination with EDX analysis and thermodynamic simulation of the diffusion processes at the joint.

4.1.1 Microstructure

Micrographs of the samples show that the interface is free of oxide inclusions, pores and other undesired defects after the compound casting process (Figs. 4.1, a - h). For the AlMg1/AlCu7 and AlMg1/AlSi7 couples a continuous transition from the single-phase substrate to the partially eutectic droplets can be observed (Figs. 4.1, a - d). For the AlMg1/AlZn7 couple only slight formation of second phase is visible directly at the interface (Figs. 4.1, e and f), while for the AlMg1/Al reference pair a reaction zone about 150 µm wide with little eutectic fraction is clearly distingushable between substrate and droplet (Figs. 4.1, g and h).

[1] K.J.M. Papis, B. Hallstedt, J.F. Löffler and P.J. Uggowitzer. Interface formation in aluminium-aluminium compound casting. Acta Mater. 13 (2008), 3036-3043.

[2] K.J.M. Papis, J.F. Loeffler, P.J. Uggowitzer, W. Fragner, H. Kaufmann. Production of composite casting part for motor vehicles, comprises removing aluminium oxide from joining zone of solid body, treating the zone with zinc solution, depositing metallic layer on the layer, and contacting the body with melt. Patent application, AT504923-A1 (published 15.09.2008).

[3] H. Kaufmann, K.J.M. Papis, J.F. Löffler, P.J. Uggowitzer, W. Fragner. Verbundgussteil. Utility patent, AT010478-U1 (published 15.04.2009).

Summing up, the compounds' interfacial structure can be described as one single matrix material with two areas of composition (substrate and droplet) and state (wrought and cast), with an uninterrupted, graded transition inbetween. The location of this zone can be easily distinguished in the micrographs shown in Figure 4.1 if the microstructures of the compound partners vary significantly (e.g. AlMg1/AlCu7 or AlMg1/AlSi7).

4.1.2 Composition of the interfacial area

A typical EDX mapping of an AlMg1/AlSi7 couple's interface in the as-cast state is illustrated in Figure 4.2. Zinc from the coating could hardly be detected by EDX analysis, indicating little to no negative influence of the surface treatments on the quality of the joints. If any, traces of Zn were detected in the primary Al phase at the droplet's side of the interface, which can be attributed to the high solubility of this element in aluminium. From a microstructural perspective, the transition from single-phased substrate to the eutectic structure of the droplet is around 50 µm, and hardness measurements of the non-solution annealed T5 state (see section 4.3.2) are expected to have approximately the same outcome.

4.2 Heat treatments of aluminium couples

Similarly to commercial alloys, heat treatments were applied to Al–Al compounds. As in the diffusion reaction zone around the interface, the alloying elements of the compound partners blend, the possibility of precipitation hardening is explored via bringing the compounds to the temper states T5 and T6, and quantified by microhardness measurements. These experiments are the subject of the following sections.

To determine diffusion zone dimensions and the degree of interdiffusion of alloying elements experimentally, Al–Al couples (AlMg1/Al, AlMg1/AlSi7, AlMg1/AlCu7 and AlMg1/AlZn7) were heat treated and the interface's mechanical properties were investigated. According to industry heat treatments, T5 and T6 states (without and with solution annealing before artificial ageing, respectively) were established for the interface compositions, where heat treatable compositions formed after sample production.

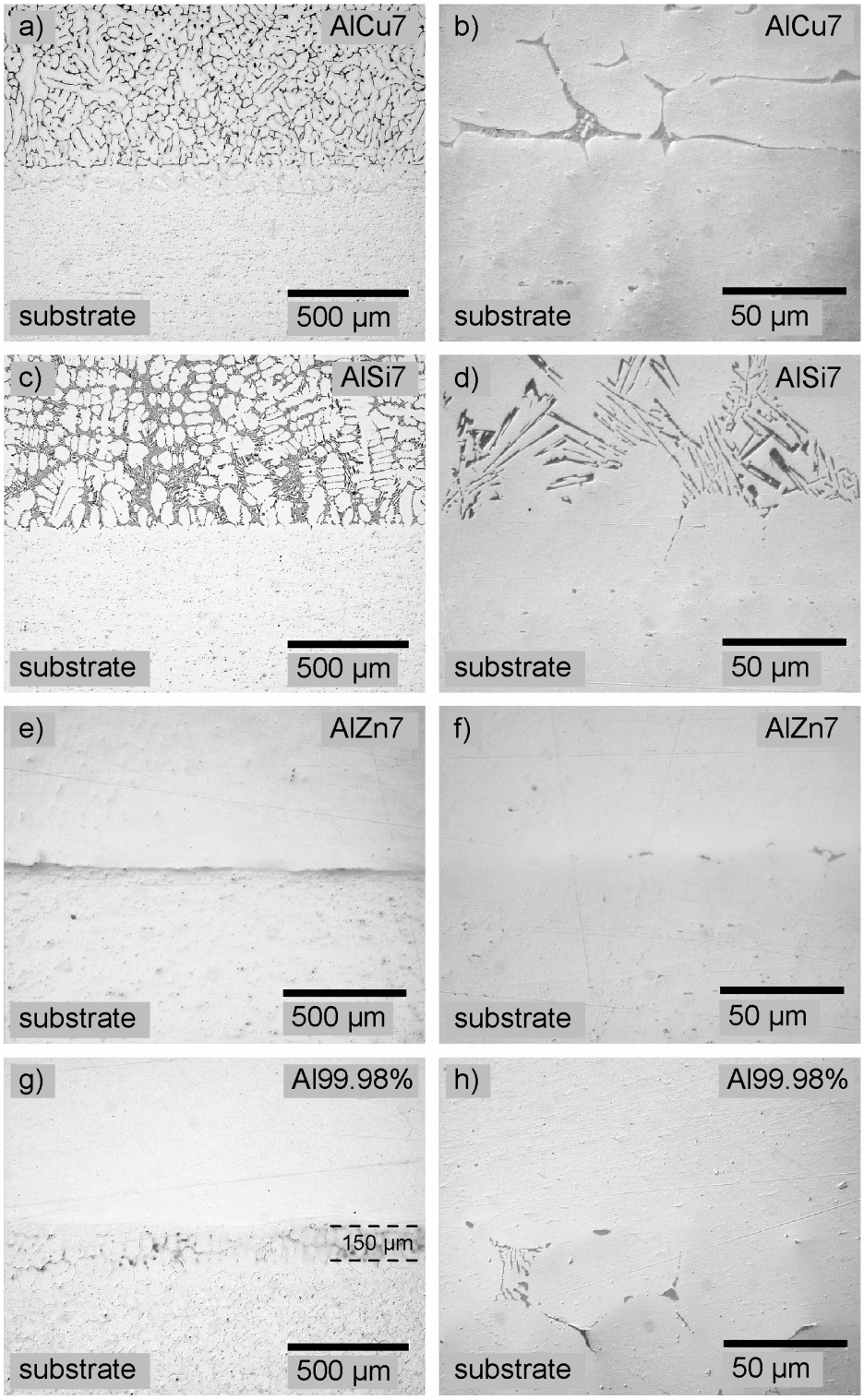

Figs. 4.1, a - h: Optical micrographs of compound cast samples: AlMg1 substrate and Al cast alloys with 7% Cu (a, b); 7% Si (c, d); 7% Zn (e, f); and pure Al (g, h). The images of higher magnification on the right give a detailed view of the various interfaces.

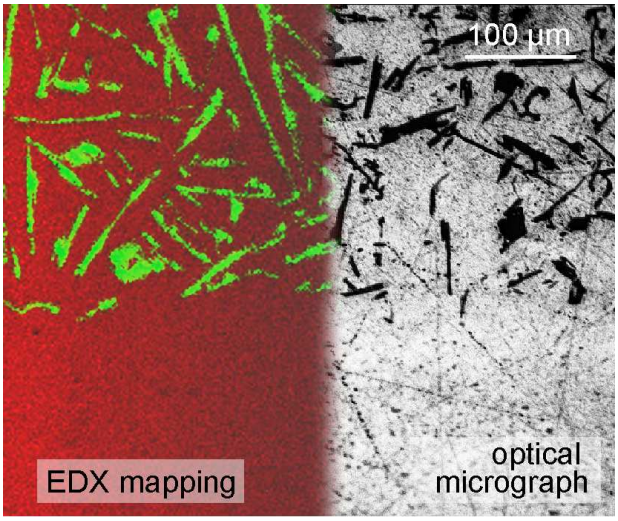

Fig. 4.2: EDX mapping and optical micrograph of Al (red) and Si (green) on an AlMg1/AlSi7 sample. Zn is not detected.

Table 4.1: Parameters for sample production and heat-treatment procedures.

cast alloy	solution annealing (T6 only)	ageing temp. [°C]	ageing steps [h]	ageing time [h] for T5 and T6
AlCu7	500 °C 0.5 h air	190	3, 6, 9, 12, 15	9
AlSi7		170	3, 6, 9, 12, 15	9
AlZn7		120	8, 16, 24, 32, 40	24
Al[4]		170	3, 6, 9, 12, 15	9

In a furnace, the samples were solution-annealed at 500 °C, whereas age-hardening treatments were performed in an oil bath at temperatures commonly used for heat-treatment procedures. In Table 4.1, these heat treatments are listed. The ageing temperatures and times varied for each couple composition according to treatments for commercial alloys with similar compositions and with Si, Cu and Zn as primary alloying elements [ASM, 1993].

Microhardness (HV 0.05) was measured at various distances from the interface before and after solution annealing, and in the course of the age-hardening treatments.

[4] The numbers for pure Al as were taken to be comparable to at least one of the other specimens.

4.3 Microhardness around the interfacial area[5]

4.3.1 T6 temper

Figure 4.3, representative for all compound variations, shows the hardness variation during age hardening of the AlMg1/AlSi7 couple after solution annealing. The lower data points indicate the hardness values of the bulk substrate. As expected for the non-age-hardening AlMg1 alloy the hardness stays nearly constant, this is in fact the case for all couples and hardening procedures. The upper data points reflect the substrate's hardening condition at a position about 50 µm from the interface. A significant hardness increase can be observed, which is similar to that expected in age-hardening AlSiMg alloys (a hardness increase towards T6 condition, followed by a hardness decrease due to over-ageing). Obviously, the hardness increase near the interface is caused by diffusion of Si from the droplet into the substrate.

The substrate of all couples was affected by diffusion of Si, Cu and Zn, respectively, from the droplet into a region less than 200 µm from the interface. For the as-cast and solution-annealed conditions no significant difference in microhardness was recorded along the whole cross-section of the substrate platelet. However, with ageing treatments a significant hardness increase was initiated close to the interface. This effect is less pronounced if no solution annealing was performed prior to artificial ageing, i.e. in the T5 state. Such hardness increase in the vicinity of the interface was not only observed for the substrate but also for the droplet, meaning that Mg also diffuses from the substrate into the droplet. Figures 4.4, a and b, illustrate the hardness profiles perpendicular to the interface for both T6 and T5 temper states. The hardness increase at the interfacial regions and the width of diffusion zones become apparent when hardness values along the samples' cross-sections are compared.

The hardening effect is highest for the AlMg1/AlCu7 and AlMg1/AlSi7 samples, and less pronounced for AlMg1/AlZn7 and AlMg1/Al. It can be assumed that Si, Cu and Zn form precipitates with Mg (and Al), for example β' (Mg_2Si), S' (Al_2CuMg)

[5] K.J.M. Papis, B. Hallstedt, J.F. Löffler and P.J. Uggowitzer. Interface formation in aluminium-aluminium compound casting. Acta Mater. 13 (2008), 3036-3043.

and η' (Zn_2Mg) [Polmear, 1995] as the hardening phases in AlSiMg, AlZnMg and AlCuMg alloys, respectively.

It is worth noting that the positions of the hardness peaks vary slightly. In AlMg1/AlCu7 the peak lies 50 µm off the initial interface position towards the droplet, and in pure Al towards the substrate. For AlMg1/AlSi7 the hardness peak is also slightly shifted towards the substrate, while for Zn-containing samples it lies directly at the interface.

4.3.2 T5 temper[6]

At the T5 state of Al–Al couples, the hardness profiles are displayed in a region of 150 µm to both sides of the interface, the substrate and the droplet material (Fig. 4.4b). The Cu containing samples are the hardest both in the substrate (due to a higher ageing temperature compared to the other couples) and in the droplet. AlMg1/AlSi7 compounds show a little peak directly at the interface, as do Zn containing samples.

A very different image can be drawn for the samples with pure aluminium. The substrate was once again partially melted to a depth of about 150 µm upon contact with the droplet, causing this commercial alloy to solidify with a certain amount of eutectic phase. There, the hardness reaches a high maximum (86 HV) compared to the substrate and droplet values of 50 HV and 21 HV, respectively.

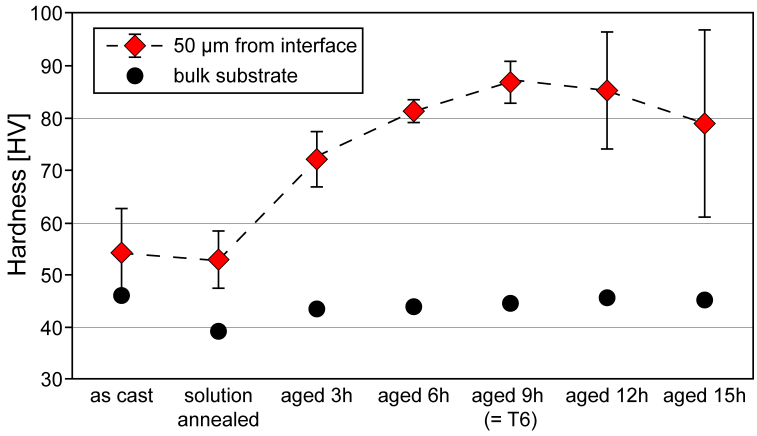

Fig. 4.3: Vickers hardness (HV0.05) plot of AlMg1/AlSi7 samples, measured 50 µm from the interface and in bulk substrate.

[6] K.J.M Papis, J.F. Löffler and P.J. Uggowitzer. Light metal compound casting. Sci. China Ser. E Technol. Sci. 52 (2009), 46-51.

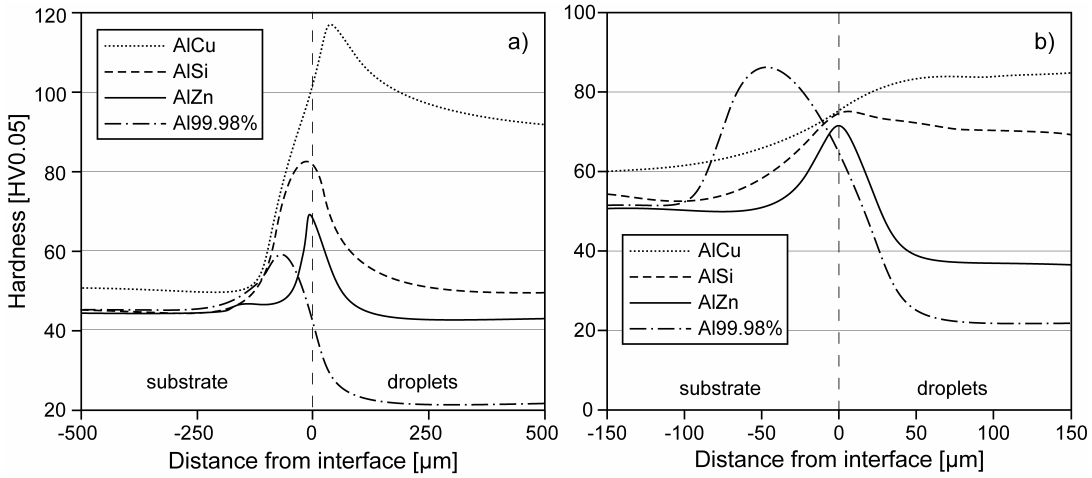

Figs. 4.4, a and b: Hardness profiles T6 (a) and T5 (b), measured across the interface (former substrate surface at position 0) of all sample compositions.

Analogue to the T6 temper, it is very interesting to observe how the substrate is affected by the droplet's alloying elements close to the interface. In Figures 4.5, a - c, hardness measurements in the bulk and 50 µm from the interface in the substrate are plotted versus advancing artificial ageing. The same ageing temperatures as for the T6 temper were taken. The missing solution annealing has a major impact on scattering of the values on the one hand, and on the magnitude of the ageing effect on the other hand.

Samples containing copper show a slight hardening effect after the hardness dropped significantly going from the as cast state to the first annealing step. Silicon also has a hardening effect, which peaks around the T5 condition and decreases subsequently, much the same as for the T6 temper, but less pronounced. Zinc has the same effect on the substrate as copper, with much more distinct scattering. As for couples with a pure aluminium droplet, the interface-near area of the substrate was liquefied down to 150 µm, as shown in Figures 4.1, g and h. Therefore, this region exhibits higher hardness than the remainder of the compound, which is plotted in Figure 4.4b.

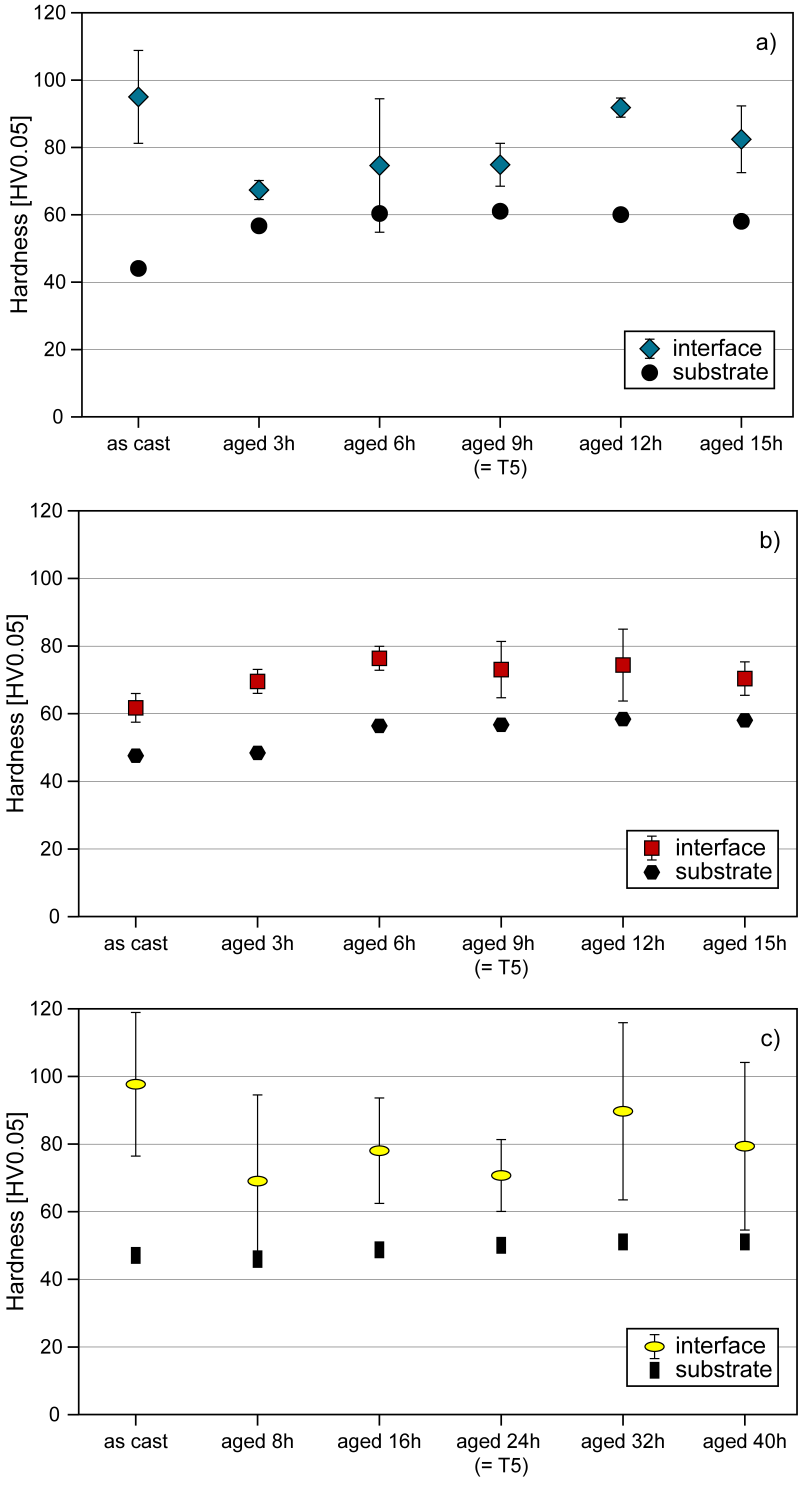

Figs. 4.5, a - c: Hardness plots with values during T5 heat treatment for the bulk substrate and for a position 50 µm from the interface. AlMg1/AlCu7 (a), AlMg1/AlSi7 (b) and AlMg1/AlZn7 (c) samples.

4.4 Calculations on diffusion processes during wetting experiments and heat treatments[7]

The casting and heat-treatment procedures of Al–Al compounds were simulated by means of diffusion kinetics calculations. The solidification of Cu, Si and Zn containing droplets and the blending of alloying elements at the interface was investigated, along with the widening of the diffusion zone during solution annealing.

4.4.1 DICTRA calculations on diffusion processes in Al–Al couples

To verify diffusion zone extensions and thus the area of expected hardness increase, one-dimensional diffusion simulations were performed using DICTRA software [Andersson, 2002]. The thermodynamic data were taken from the COST II database for light-metal alloys [Ansara, 1998], and the diffusion data from the mobility database for aluminium alloys developed in a thesis by Prikhodovsky [Prikhodovsky, 2000]. Both the solidification and solution annealing processes were calculated to illustrate the distribution of the alloying elements at the compounds' interface during sample production and heat-treatment procedures. The diffusion cell was set up as shown in Figure 4.6.

The starting temperature for diffusion simulations during solidification (i.e. the casting process) was chosen to lie below the solidus of the substrate and slightly above the liquidus of the melts (Table 4.2). Changing the start temperature within this range had no significant influence on the simulation results. The liquidus of AlZn7 overlaps with the solidus of AlMg1, and thus the start temperature was chosen within this narrow gap. The liquidus of pure Al obviously lies higher than the substrate's solidus. Therefore it was not possible to perform solidification simulations with the Al 99.98% material.

[7] K.J.M. Papis, B. Hallstedt, J.F. Löffler and P.J. Uggowitzer. Interface formation in aluminium-aluminium compound casting. Acta Mater. 13 (2008), 3036-3043.

Table 4.2: Liquidus and solidus temperatures of the alloys used, and starting temperature for DICTRA simulations.

Alloy	Liquidus [°C]	Solidus [°C]	DICTRA start [°C]
AlMg1	655	645	-
AlCu7	642	548	643
AlSi7	617	577	621
AlZn7	649	633	647

For the simulation, the following simplifying assumptions were made: (i) the solidification front is reasonably planar; (ii) there is no major influence of convection; and (iii) only the fcc and liquid phases are present. Although the cooling rate varies during solidification, a fixed cooling rate has to be chosen for DICTRA simulations. A value of 1 K/s was taken for all casting simulations, which is a rough appraisal of the cooling rates occurring in the experiments.

Because of all the simplifying assumptions the simulation of the solidification needs to be regarded as semi-quantitative. It may also be necessary to consider a temperature gradient within the diffusion cell. This is, however, not possible using the DICTRA software. Subsequent simulations of the solution annealing were performed at 500 °C for 30 minutes using the element distribution profiles arising from solidification simulations.

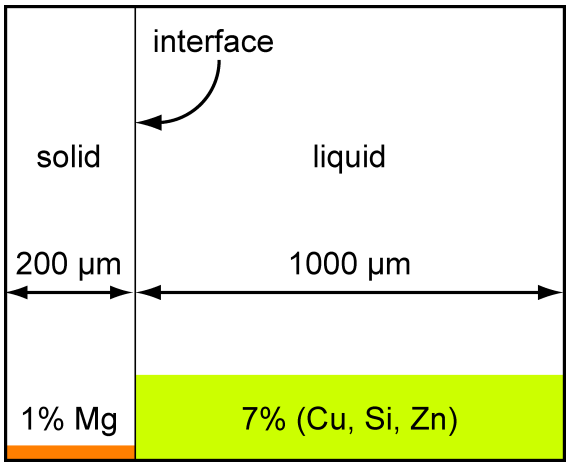

Fig. 4.6: Setup for the DICTRA cell; 200 µm of solid to the left of the interface, and 1000 µm of liquid to the right.

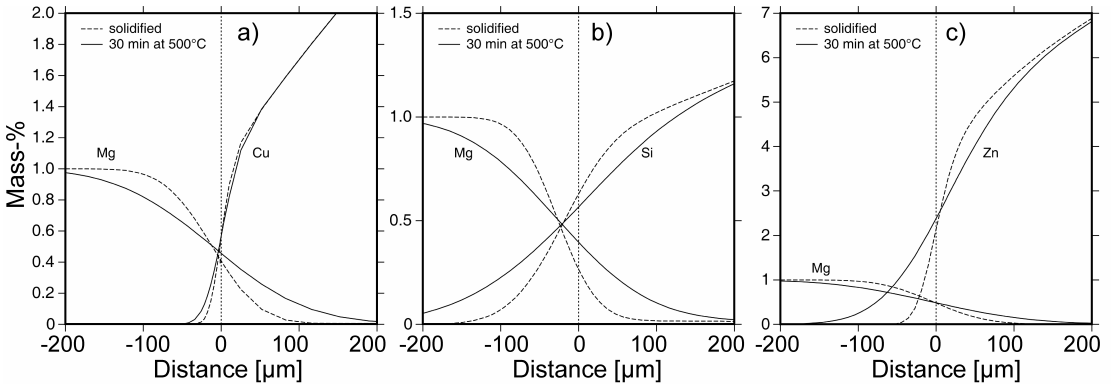

Fig. 4.7, a - c: Concentration profiles after solidification (dashed lines) and after solution annealing (solid lines). The substrate is to the left of the interface; the droplets are on the right; a) AlCu7, b) AlSi7, c) AlZn7.

4.4.2 Zones of diffusing alloying elements

The results of the DICTRA calculations are plotted in Figure 4.7, a - c. The dashed curves show the composition profiles in the as-cast state, and the solid curves after solution annealing. Considerable diffusion of alloying elements from the droplet into the substrate and vice versa occurs in the vicinity of the interface. Diffusion zones form during solidification to an extent between 30 µm (Cu, Zn) and 100 µm (Si) into the substrate and 100 µm (Mg) into the droplet. Solution annealing increased the diffusion zones to 50 - 200 µm into the substrate and 200 µm into the former melt.

4.5 Discussion

At the elevated temperatures during couple production and solution annealing, an exchange of alloying elements occurs through the continuous metallic interface. On the one hand, Cu, Si and Zn from the droplet diffuse into the substrate; on the other, Mg from the substrate diffuses into the droplet. Therefore concentrations gradually change over the interface, creating an area of age-hardenable compositions. The width of these areas was determined by hardness measurements. It depends on the diffusion distances, which were verified for each alloying element by simulations using DICTRA software.

4.5.1 Microstructure

It is generally observed that during solidification and solution annealing, Mg and Si diffuse faster than Zn and Cu [Prikhodovsky, 2000; Polmear, 1995]. This becomes evident if we examine the DICTRA results in Figure 4.7. The AlMg1/AlSi7 couple exhibits the widest diffusion zone, and the AlMg1/AlCu7 couple the smallest. The microstructures shown in Figures 4.1, a - d reflect the concentration gradients at the interfacial region of the AlMg1/AlCu7 and AlMg1/AlSi7 couples by the continuous transition from the single-phase substrate to the partially-eutectic droplets. The eutectic phase formation in the interface region can be examined in more detail by means of Scheil-Gulliver[8] simulations using the Pandat software (see section 5.3). An Al alloy with 0.5 mass-% Cu and 0.5 mass-% Mg, which is the composition of copper-containing samples exactly at the interface, solidifies with 1 mol-% of eutectic Al_2Cu (θ). The bulk AlCu7 forms about 2 mol-% of this eutectic intermetallic phase. Thus the copper gradient is discernible by the content variation of the eutectic phase in Figures 4.1, a and b. For AlMg1/AlSi7 samples the calculated interface composition is about AlSi0.5Mg0.5. Upon solidification, little (≈ 2.5 mol-%) eutectic is formed, but its fraction increases rapidly with Si content; at 2 mass-% Si the eutectic fraction is already 6%. Thus the transition zone of AlMg1/AlSi7 samples appears relatively thin in the micrograph, as the eutectic is already highly visible at low Si content.

Very little second phase can be detected in AlMg1/AlZn7 samples (Figs. 4.1, e and f). Directly at the interface there is about 2.5 mass-% Zn and 0.5 mass-% Mg. According to Pandat calculations about 0.25 mol-% of $(Al,Zn)_2Mg$ will form, but only directly at the interface. In the bulk droplet no intermetallics will precipitate, as the concentration of Mg is too low.

For the pure Al melt the latent heat during solidification is released at 660 °C, causing a holding period at this high temperature and thus an increased heat transfer into the substrate, which obviously results in partial melting of the substrate's surface. As shown in Figures 4.1, g and h, a region of about 150 µm features eutectic intermetallics, which were identified as containing Fe/Si or Mg/Si (EDX measurements). Scheil-Gulliver calculations for the AA5005 substrate confirm the

[8] The Scheil-Gulliver equation describes solute redistribution during solidification by assuming a local equilibrium at the solid/liquid interface. It gives a good approximation to the non-equilibrium reality.

formation of about 0.7 mol-% pre-eutectic $Al_{13}Fe_4$ phase and 0.5 mol-% eutectic Mg_2Si.

4.5.2 Hardening behaviour at the interface region

It is reasonable to assume that a minimum element concentration is required for the formation of effective hardening precipitates, β' (Mg_2Si), S' (Al_2CuMg) and η' (Zn_2Mg), in the substrate and the droplets. If the lower concentration limits of alloying elements for commercial age-hardening Al-alloys are considered (Table 4.3) and applied to the concentration profiles in Figure 4.7, a - c, a hardness increase can be predicted for the regions adjacent to the interface. This can be done for both tempers, T6 and T5 (with and without solution annealing at 500 °C, respectively, prior to artificial ageing).

T6 temper

In T6 condition, the width of these regions from the interface into the substrate is about 30 µm for AlCu7 and 120 µm for AlSi7, and 100 µm (AlCu7) and 70 µm (AlSi7) into the droplet. This lies within the same range as the results from microhardness measurements, where a significant hardness increase is observed at distances of less than 200 µm from the interface into the substrate and into the former melt (Fig. 4.4a).

The lower concentration limit of Mg in heat-treatable 7xxx alloys, however, is higher than the amount of Mg in the substrate used here, AlMg1. Thus not enough magnesium was provided from the substrate to form a significant amount of η' (Zn_2Mg) precipitates (Fig. 4.7c). Because of this, only a slight hardness increase is observed in a narrow region around the interface.

The hardness profile for the AlMg1/AlCu7 couple is shifted towards the droplet side, and for the AlMg1/AlSi7 couple slightly towards the substrate. In the following this phenomenon is discussed in more detail. Cu-containing aluminium alloys are heat treatable even without magnesium. The hardening phase of type θ' (Al_2Cu) forms in the droplet area of the samples. Due to the presence of Mg the S' phase (Al_2CuMg) appears close to the substrate, where the hardness increase is more pronounced. Copper does not diffuse far into the substrate (Fig. 4.7a), and therefore the highest HV values can be detected at the droplet's side of the interface.

Table 4.3: Lower and upper concentration limits of alloying elements in commercial aluminium alloys.

wrought and cast Al-alloy series	mass-% Cu, Si, Zn	mass-% Mg
2xxx/2xx.x	0.1 - >7 Cu	0.1 - 1.8
6xxx/3xx.x	0.2 - >7 Si	0.2 - 1.5
7xxx/7xx.x	0.8 - >7 Zn	1.5 - 4.0

The presence of magnesium is especially important for ageing of 3xx and 6xxx alloys. This is obvious when examining the mechanical properties of conventional AlSi7Mg alloys with varying Mg content, which lies between 0.35 wt.-% (A356) and 0.55 wt.-% (A357). The strength increases by nearly one-third, going from the lower to the higher Mg concentration [Kaufmann, 2007]. Because the precipitation phase in AlMg1/AlSi7 is β' (Mg_2Si), from Figure 4.7b, one would expect the hardness peak to lie at the substrate's side of the interface. This is, however, not the case (Fig. 4.4a), which can be explained by the fact that the optimal ratio of magnesium to silicon in the incoherent β'' precipitations at hand is not 2:1, but rather 1:1 [Murayama, 1999]. Therefore the highest HV values are detected directly at the interface, with a slight shift towards the substrate.

Although the reference couples (AlMg1/Al) showed the expected properties in the bulk areas, i.e. low hardness in the droplet and constant hardness in the substrate, the hardness close to interface was slightly higher than in the bulk. This indicates the presence of a hardening phase in the vicinity of the interface. In contrast to the other couples, the hardness increase was located in the substrate only, whereas the hardness values in the droplet rapidly decreased to the bulk value. This can be explained by the above mentioned structural modification of the near-surface region of the substrate induced by local melting during solidification of the liquid droplet (Fig. 4.1, g and h).

T5 temper

Simulations of the diffusion of alloying elements during the compound casting process without solution annealing are illustrated in Figures 4.7, a - c, plotted with dashed lines. In the as cast condition, from which artificial ageing is performed to get to the T5 temper, the regions of continuous transition of alloying element concentration are narrower than in the solution annealed condition. This is reflected in

narrower areas of less pronounced hardness increase for Cu and Si containing samples, which is illustrated in Figure 4.4b.

Similarly to T6 condition, not enough magnesium was provided from the substrate to form a significant amount of η' (Zn_2Mg) precipitates in AlMg1/AlZn7 couples, which leads to a small hardness increase only at the interface. The fact that copper containing samples exhibit the highest hardness is due to the formation of AlCu species, as described for T6 condition. There, the droplet even reached a higher hardness. A gradual change in hardness from substrate to the droplet was measured, with the interface hardness lying in between these values (75 HV), indicating that no significant blending of the alloying elements had taken place (compared to T6, where there is a distinct peak of hardness at the interface).

The same mechanisms of hardness increase take effect as observed for these couples in the T6 condition. With the lack of enough Mg to significantly add to hardening in the droplet, mainly the phase θ' (Al_2Cu) is believed to cause the droplet's above-average hardness. Similarly to observations at the T6 samples, Si containing couples show a hardness peak directly at the interface. This is effected by the equal distance of Si and Mg diffusion already after the casting process, and indicates a small amount of interdiffusion, forming Mg–Si precipitates as described above.

The same is true for Zn containing couples, which exhibit the peak hardness at the interface. The distinctive hardness peak at the AlMg1/AlZn7 couples' interface even without solution annealing confirms the presence of little second phase already after sample production. This is supported by the optical micrograph in Figure 4.1f, where this specimen's interface is shown in the as cast condition.

The substrate is generally slightly harder than after solution annealing, which effectively softens the material. During ageing at 190 °C, it hardens apparently more than if aged at lower temperatures, which is backed by the hardness values displayed by the copper containing samples.

4.6 Upscale Al–Al compound casting

After the successful wetting experiments and samples production/characterization with Al-Al couples, experiments at a scale close to industry were performed together with the project partner LKR, a specialist in casting and shaping light metals, using a UBE350 HVSC squeeze casting machine. The scope, parameters and results of these experiments are described shortly.

4.6.1 Aims and parameters

Compounds with the following compositions were produced: AlMg3/Al, AlMg3/AlCu7, AlMg3/AlSi7, AlMg3/AlSi12, AlMg3/AlSi17, AlMg3/AlSi7Mg (all squeeze-cast) and AlSi7Mg/AlSi7 (permanent mould casting). The AlMg3 substrate (here: insert) shape was designed to comprise three different wall thicknesses (i.e. insert sizes): 3, 6 and 12 mm (Fig. 4.8).

Solidification of the melt is substantially faster, when it is cast into a mould rather than onto a flat surface. Therefore, the amount of time, during which metallurgic bonding in a compound cast structure can form, is less, and the influence of the substrate's temperature on the formation of the joint is greater for the former process. Various insert pre-heating temperatures were thus evaluated. Furthermore, the melt is cooled upon contact with the mould and the insert, both of which are heated up simultaneously. The bigger the volume of the insert, the less the temperature in this volume (and, more importantly, its surface) will rise. It was assumed, that there exists a critical wall thickness of the insert (this depends mainly on pre-heating of the insert and the melt temperature), above which good bonding will no longer occur in a compound casting sense.

The aims of these tests was to investigate the influence of different quantities of heat capacity, which is controlled by varying the insert's wall thickness, on interface formation and bonding quality.

The inserts were pre-treated in the same way as the platelets for laboratory-scale Al–Al experiments: they were cleaned, pickled, zincate-treated and zinc-electroplated (see section 2.2.1). Table 4.4 gives an overview on insert, melt and casting parameters.

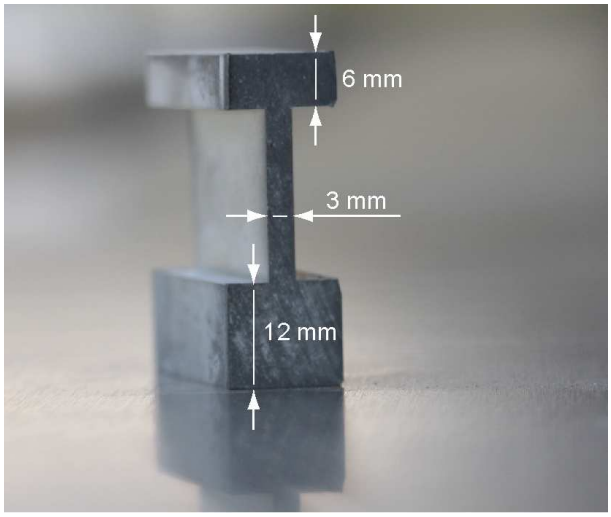

Fig. 4.8: the shape of the AlMg3 inserts comprises three different wall thicknesses: 3, 6 and 12 mm, at a length of 40 mm.

Table 4.4: Parameters for industrial scale experiments with AlMg3 inserts.

cast alloys	AlCu7, AlSi7/12/17, AlZn7, AlSi7Mg, Al
insert pre-heating	None, 100 °C, 300 °C
cast alloy temp.	700 °C, 750 °C
pressure	890 bar (after complete filling, prior to solidification)
filling velocity	0.11 m/s (initial), 0.08 m/s (final)

4.6.2 Interface at varying insert size

The influence of varying insert thickness and thus varying heat capacity on interdiffusion depths, which determine the bonding quality, was investigated on specimens prepared by the squeeze-casting machine. The final shape of the cast compound part is illustrated in Figure 4.9. The best results concerning connection of melt material to the insert were obtained with insert temperatures of 100 °C and 300 °C, and a melt temperature of both 700 °C and 750 °C. Castings produced with insert temperatures of 25 °C (RT, i.e. no pre-heating) sometimes fell apart without significant stress application.

The zinc layer was (partly) sheared off during the casting process no matter the insert temperature. This can be seen on the backside of the specimens, where a bright shadow appears around each insert (Fig. 4.9). One can take this as proof that the melt

was hot enough to liquefy the outermost layer of the inserts, which is a prerequisite to obtain good bonding.

In Figure 4.10, micrographs of the interface in different parts of an AlMg3/AlSi7 compound are shown. The varying width of altered microstructure gives an idea about diffusion zone width and thus blending of alloying elements. Results from laboratory experiments concerning the individual diffusion zones of the different couples agree with the findings of the upscale experiments.

The smaller the wall thickness is, the deeper the melt's alloying elements diffuse into the substrate. This impacts the bonding quality: at the insert's 12 mm thick areas, the solid insert's surface cannot reach sufficient temperatures to guarantee a tight connection, whereas at the thinner areas, a continuous transition is observed in all investigated compound compositions.

Fig. 4.9: The compound cast component with an insert featuring various thicknesses. The Zn coating partially shears off when liquefied by the melt.

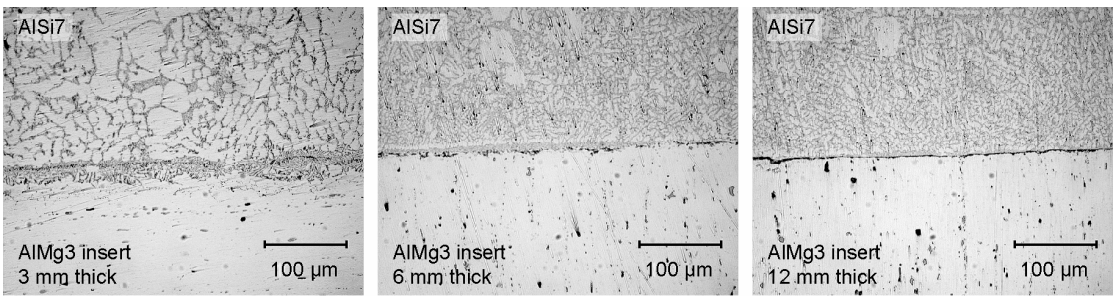

Fig. 4.10: Micrographs of the interfacial areas in AlSi7 castings with varying AlMg3 insert thickness. The thinner the substrate, the better the bonding properties.

The composition of the former melt is altered to some extent, as a fraction of the alloying elements diffuses into the substrate. The better the bonding is (e.g. with a thin insert), the stronger this effect is observed. This is demonstrated by the microstructure of the AlSi7 melt at the interface in 3 mm thick inserts. There, the substrate is heated more by the melt, which in turn solidifies less rapidly. Therefore, a coarser structure of grains and eutectic is observed, and together with the slightly altered composition, the appearance of the interfacial area is quite different.

4.6.3 Interface formation in squeeze-cast compounds

Upscale Al–Al compound casting experiments prove the feasibility of an industry-sized process. With classical alloys for inserts (AlMg3) and melt (Al + 7, 12 and 17% Si), the best results regarding bonding quality are achieved. Nevertheless, tight bonding is also realized with the other alloys, which is a consequence of the substantially improved reactivity of the insert's surface due to the combination of pre-treatments and surface modifications.

Already during laboratory-scale Al–Al compound casting experiments, it became obvious, that only a sufficiently high substrate temperature allows for complete wetting. Squeeze casting aims at reducing production time via fast filling velocities, and a short interval of solidification is beneficial. This means, though, that the time, where the solid insert is in contact with the liquid cast alloy is low, providing enough heat to fuse the coating of thin inserts only. As a consequence, the bonding is best with 3 mm thick inserts, as illustrated in Figure 4.10.

There are several possibilities to deal with this issue. If the inserts are heated to a higher temperature prior to compound casting, the heat of the melt could be enough to liquefy the coating. As pre-heating is economically and practically feasible only to certain temperatures, this is not the optimal option. By alloying other elements, such as tin, the coating's melting temperature can be lowered, thus reducing the amount of heat that is required to fuse it upon contact with the melt. Other issues would arise, though, such as the formation of new phases.

4.7 Conclusions

With a combination of pre-treatments – comprising pickling and activation processes, a redox-reaction to replace the naturally occurring oxide layer with a dense metallic zinc deposit, and a zinc galvanizing procedure – complete wetting was achieved both at laboratory and close to industrial scales (in a non-isothermal wetting experiment and using a squeeze-casting machine, respectively). Together with the project partner LKR, a patent application was filed to protect the intellectual property of these findings.

Investigations on cross-sections of the interfaces showed quickly, that the interfaces were free from imperfections (most importantly oxide layer residues and shrinkage cavities) and showed a continuously metallurgic transition from substrate to melt alloy. The compositions and mechanical properties of the various compound's interfaces were studied in detail. It was found, that a 50 - 200 µm thick transition zone forms upon compound casting and subsequent heat treatment procedures, depending on the alloying elements' diffusivities. Within this zone, the mechanical properties may vary significantly from the surrounding bulk volumes, as the alloying elements from either compound partner blend, which may ultimately lead to particle precipitation at elevated temperatures, and thus hardening. Diffusion zone widths were simulated for many of the produced compound couples using DICTRA. These results go along well with experimental findings on the interface's composition. Therefore, in combination with the process parameters, this calculation method is most suitable to predict diffusion zone widths in aluminium alloy combinations of future Al–Al compound casting examinations.

It has been shown, that the outermost microns of the substrate need to be fused in order to obtain a sufficiently strong reaction. This was achieved for all couples at laboratory scale. When compound casting is applied using a squeeze-casting machine, the volume of the insert is critical for an effective bonding reaction to occur, as the amount of heat, which is necessary to fuse the zinc layer of the substrate, depends on its absolute heat capacity, and thus thickness.

References

Andersson, J.O., Helander, T., Hoglund, L., Shi, P., Sundman, B. Thermo-Calc & DICTRA, computational tools for materials science. *Calphad*, 2:273 (2002).

Ansara, I., Dinsdale, A.T., Rand, M.H. Thermochemical Database for Light Metal Alloys. Luxembourg (LUX) (1998).

ASM Speciality Handbook: Aluminum and Aluminum Alloys. In: Davis, J.R. (ed.), *ASM International,* Materials Park (USA), p. 784 (1993).

Kaufmann, H., Uggowitzer, P.J. Metallurgy and Processing of High-Integrity Light Metal Pressure Castings. *Fachverlag Schiele & Schön GmbH*, Berlin (D), p. 274 (2007).

Murayama, M., Hono, K. Pre-precipitate clusters and precipitation processes in Al-Mg-Si alloys. *Acta Materialia*, 5:1537-1548 (1999).

Polmear, I.J. Light Alloys - Metallurgy of the light metals. Third ed., *Arnold*, London (UK), p. 362 (1995).

Prikhodovsky, A. Thesis. RWTH Aachen University, Aachen (D) (2000).

Chapter 5

Magnesium-magnesium compound casting

With the surface pre-treatments from section 2.2.2, magnesium-magnesium compound casting was facilitated, as described in chapter 3. In the following, the investigations on composition and microstructure of these couples are detailed (5.1). Microhardness measurements of the transition between substrate and melt are shown in section 5.2. Thermodynamic calculations on the enthalpy of the system at the wetting incident are characterized in section 5.3. These focus on the solidification sequence of the composite's interface after casting, and help to determine the area, which is last to solidify. The results are summed up and discussed (5.4), followed by a short conclusion at the end of this chapter (5.5)

5.1 Composition and microstructure of the interfacial area[1]

With the compound cast Mg–Mg couples (as described in chapter 3), investigations on interface structure and composition were performed. Figures 5.1, a - f, show optical micrographs of the interfacial areas that are free from oxide inclusions, cavities or other undesired imperfections. The transition between substrate and droplet can be easily distinguished in couples with different microstructures on either side of the interface: The ZK31 and AZ31 alloys show very little visible structure. MgZn7 and AJ62 are eutectic systems, whereas the microstructure of the pure Mg droplet in Figures 5.1, e and f, appears without contrast. It is especially difficult to make out the interface in these AZ31/'Mg' samples.

With EDX spectroscopy and microhardness measurements, an overview on the compounds' composition and properties was obtained. In ZK31/MgZn7 couples, the information that the elemental analysis yields is not more than what can be seen in optical micrographs. Hardness measurements also show similar results as discussed for other couples. Therefore, only the samples with AZ31 as the substrate material (AJ62 and pure Mg as the melt) are discussed more closely.

EDX mappings of AZ31/Mg and AZ31/AJ62 couples are shown in Figures 5.2 and 5.3. In AZ31/AJ62 couples, the transition from the single-phase substrate to the former droplet, which has a hypo-eutectic microstructure, is well-defined and can be distinguished easily (Fig. 5.2). No undesired phases or shrinkage cavities were detected, and the former Zn/$MgZn_2$-coating seems to have vanished.

[1] K.J.M. Papis, J.F. Löffler, P.J. Uggowitzer. ‚Interface formation between liquid and solid Mg alloys – An approach to continuously metallurgic joining of magnesium parts'. Materials Science and Engineering: A, 527 (2010) 2274-2279.

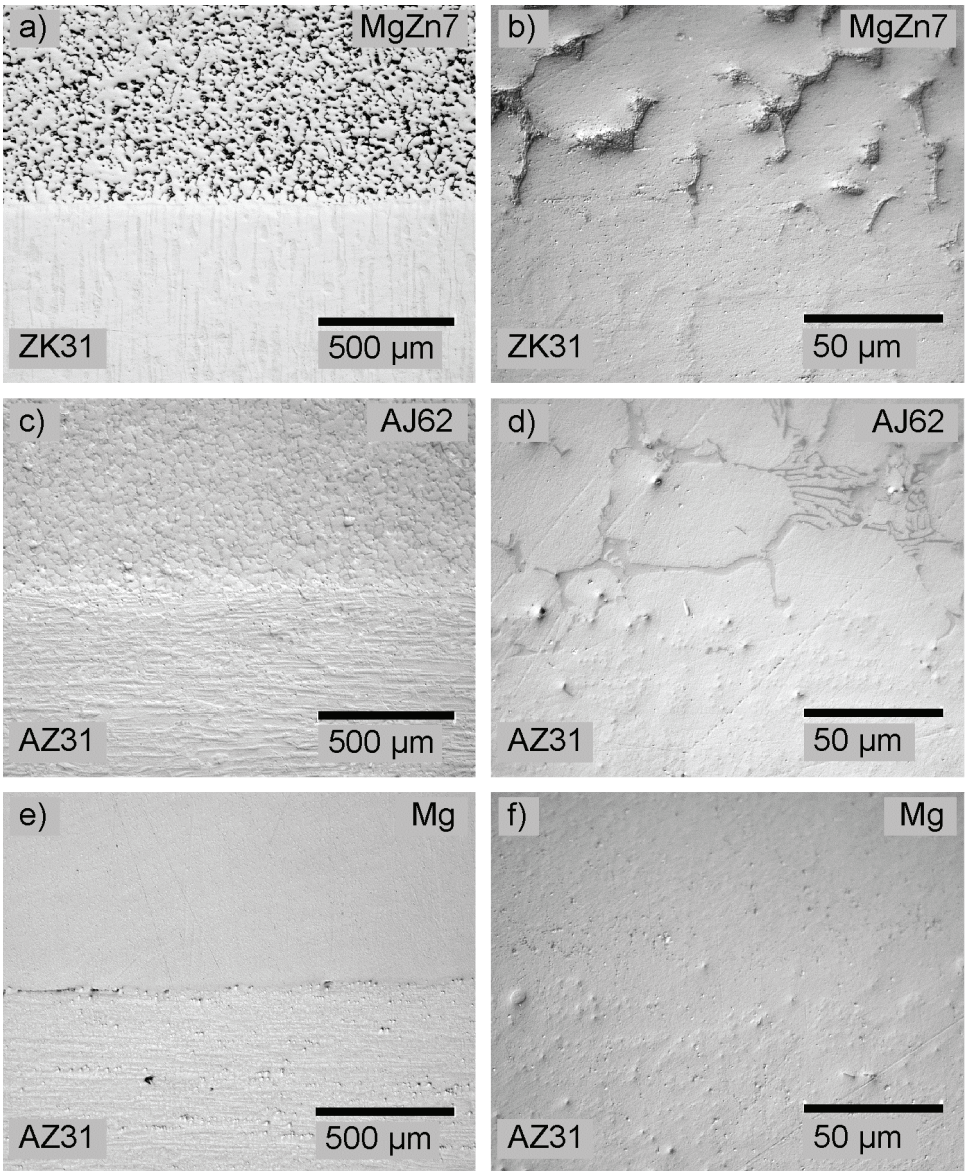

Fig. 5.1, a - f: Optical micrographs of the interfacial areas of Mg–Mg compound cast couples. ZK31 substrate with MgZn7 droplet (a, b), AZ31 substrate with AJ62 (c, d) and pure Mg (e, f). The images of higher magnification on the right give a detailed view of the various interfaces.

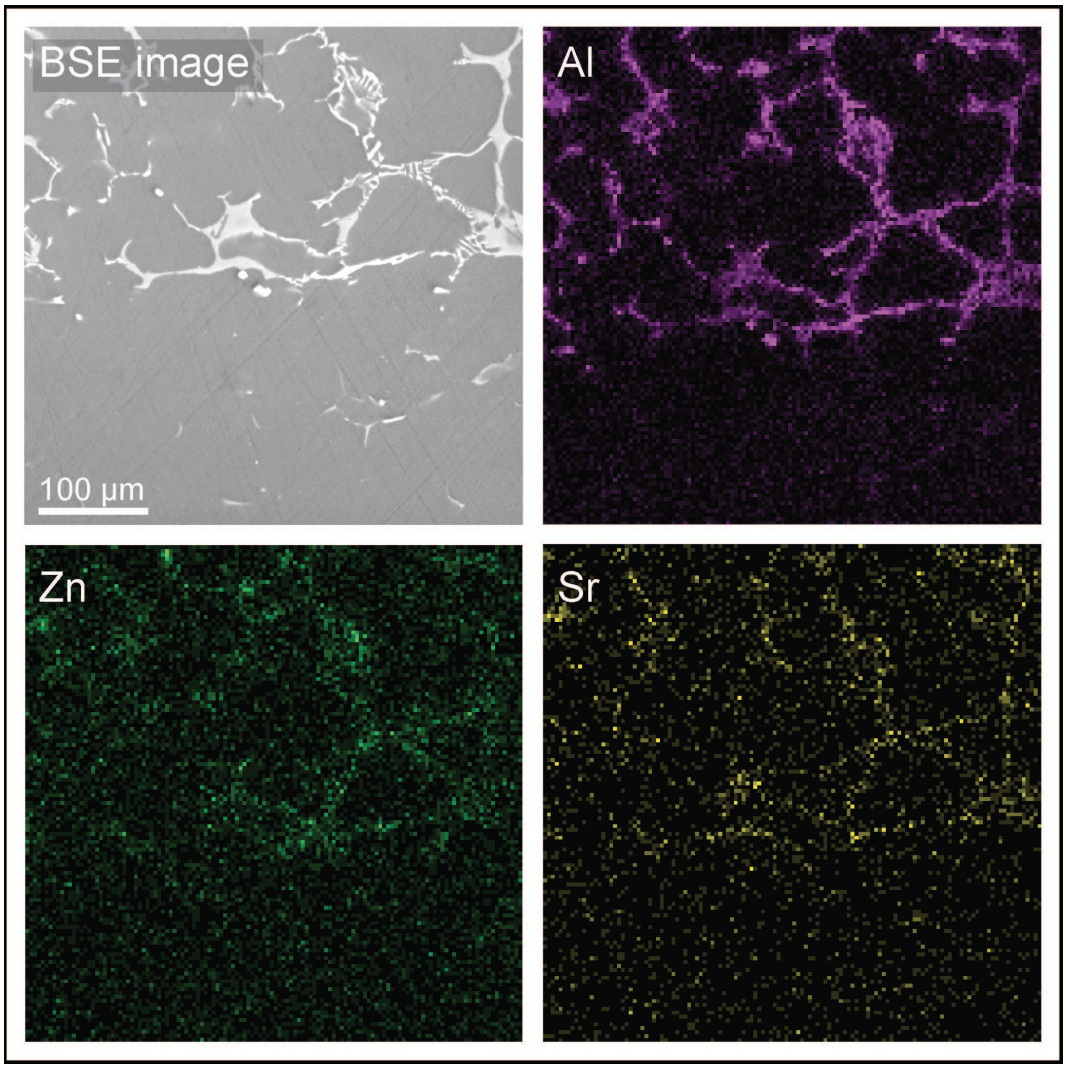

Fig. 5.2: EDX mappings of an AZ31/AJ62 sample at the interface. Zn is detected in the eutectic phases mainly.

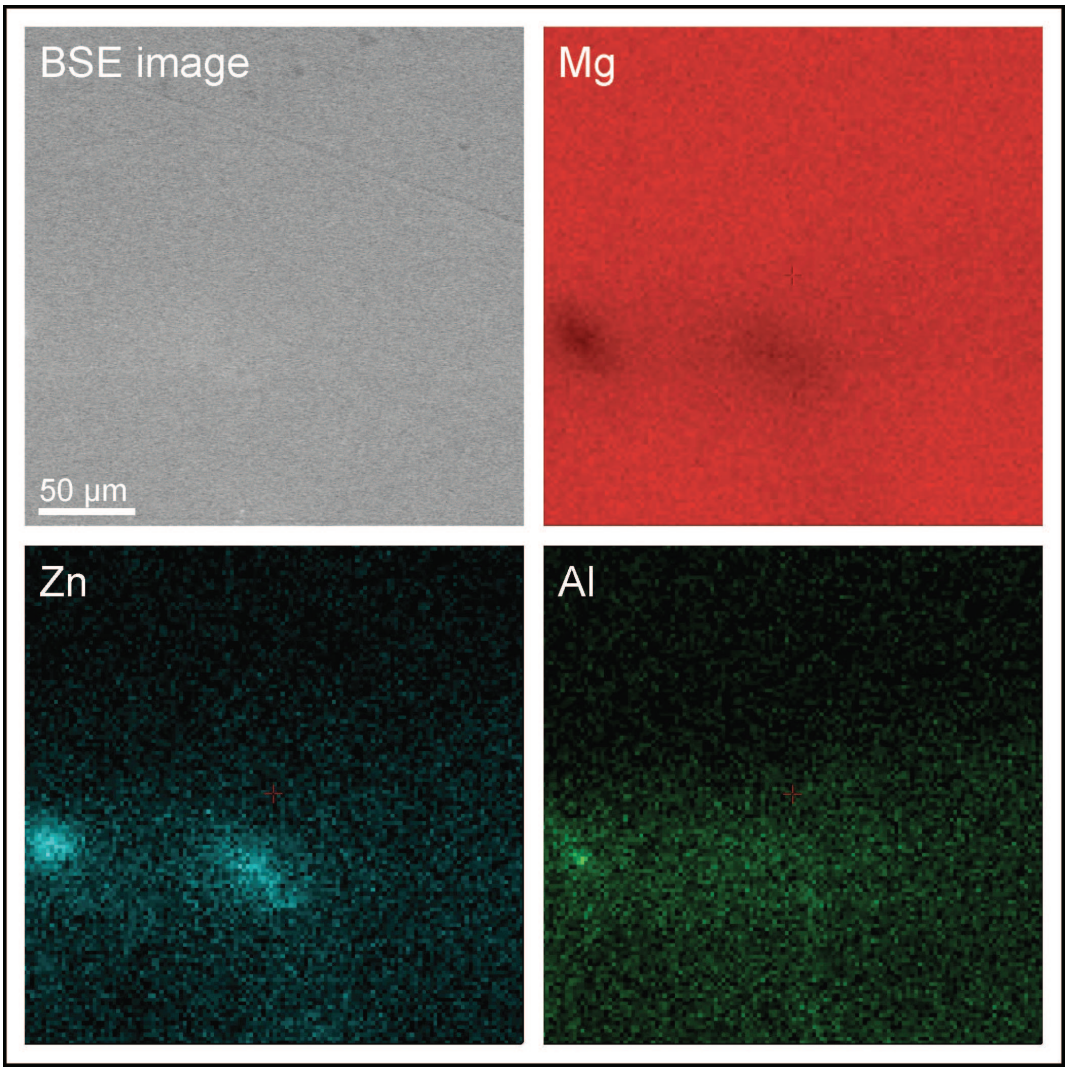

Fig. 5.3: EDX mappings of an AZ31/‘Mg’ sample. In BSE mode, no interface is seen. The substrate’s Al content reveals the location of the interface. Zn is detected in the substrate mainly.

EDX measurements reveal the location of Zn in the eutectic phase at the AJ62 droplet's side with no enrichment at the 'fuse line', which indicates complete dissolution of the coating into the melt prior to solidification. Obviously, this reaction leads to the exceptional wetting properties of the coated substrate, as wettability is a strong function of interfacial metallurgical reactions.

The AZ31/'Mg' samples showed an equally favourable transition; the EDX mappings (Fig. 5.3) reveal the location of the interface, which cannot be identified in SEM (backscattered electron (BSE) or secondary electron (SE)) images – there is simply no detectable contrast between the substrate and the droplet. Only the Al signal indicates the area of the substrate material (AZ31). Also here no undesired phases or shrinkage cavities were detected. However, a different location of the dissolved Zn coating can be revealed. In contrast to the AZ31/AJ62 couples Zn is slightly concentrated in the surface region of the AZ31 substrate, but does not form an undesired eutectic phase.

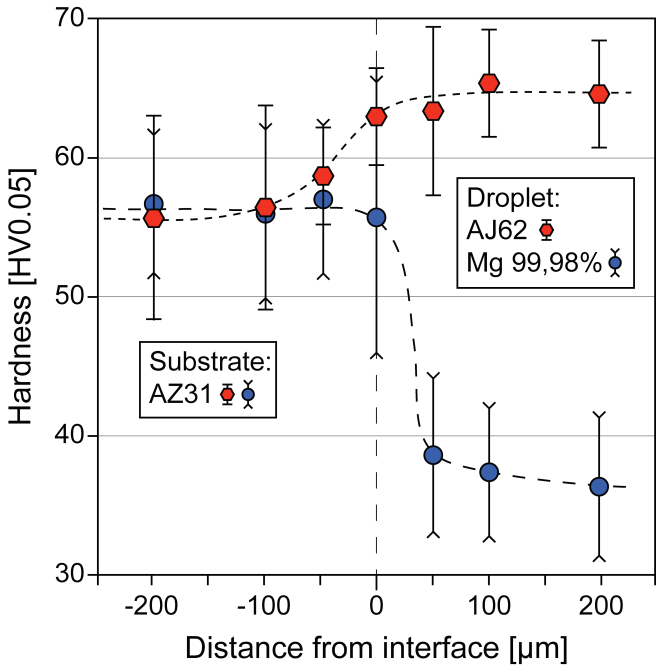

Fig. 5.4: Microhardness versus distance from interface (AZ31/AJ62: hexagon. AZ31/'Mg': circle).

5.2 Microhardness around the interfacial area

Microhardness measurements (HV0.05) in Figure 5.4 show a zone of continuous hardness alteration between the bulk of the substrate and the former liquid phase. Coming from the substrate's side, the HV values are initially constant, then continuously increase (AZ31/AJ62) or abruptly decrease (AZ31/'Mg') at the interface (indicating a change in microstructure), and finally, within a few tens of micrometers, change to the hardness of the bulk droplets. This gradient indicates the "fuse zone", which is about 100 - 200 µm wide for both couples.

5.3 Pandat calculations on the enthalpy of interfaces in Mg–Mg couples[2]

Calculations on Mg–Mg compounds focus on the solidification intervals of the various alloys and their impact on the amount of liquid phase at the interface directly after the wetting event. This is believed to affect the solidification sequence of the compound, depending on melt composition and process temperature.

Pandat (integrated computational environment for phase diagram calculation and materials property simulation of multi-component systems. CompuTherm LLC, Madison, USA) is a powerful tool to calculate phase fractions in light metal alloys, their compositions and other values, such as enthalpies of the species at varying temperatures. Investigations on phase formation strongly rely on accurately knowing the state of the material of interest, i.e. whether it is solid or (partially) liquid. The enthalpy of the compound immediately after the wetting event gives a clue on the appearance of the interface's composition and microstructure after complete solidification eventuates. Therefore, calculations on the solidification intervals were performed.

[2] K.J.M. Papis, J.F. Löffler, P.J. Uggowitzer. ‚Interface formation between liquid and solid Mg alloys – An approach to continuously metallurgic joining of magnesium parts'. Materials Science and Engineering: A, 527 (2010) 2274-2279.

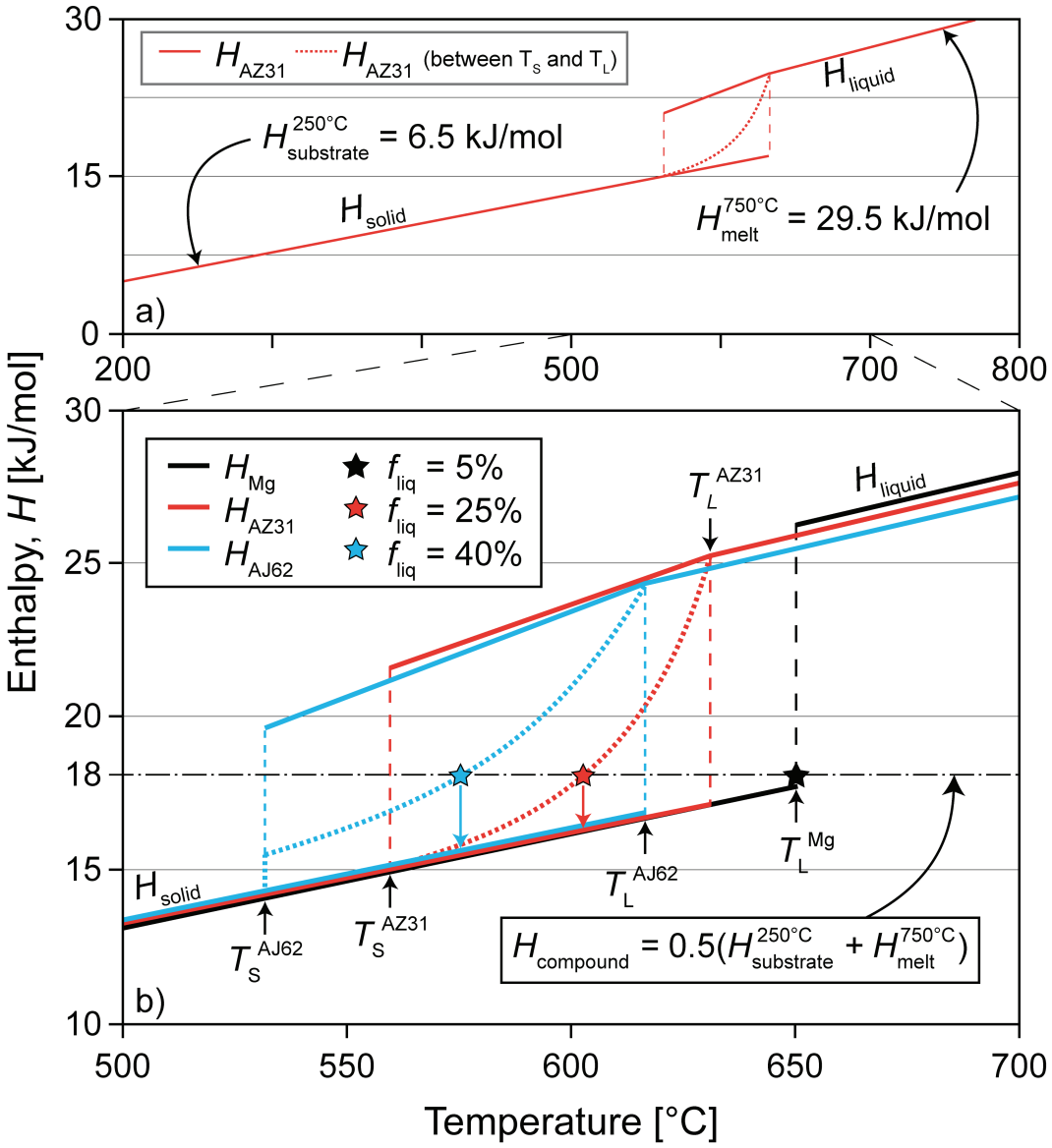

Figs. 5.5, a and b: Enthalpy of the substrate AZ31 versus temperature (a); Enthalpy of pure magnesium, AZ31 and AJ62 versus temperature (Note: AJ62 is partially eutectic) (b). Given the equal volume of substrate and melt, the liquid fraction in substrate and cast alloy can be found by the average enthalpy of the compound at the wetting incident.

With a melting temperature of 420 °C for Zn and a melting point of 590 °C for $MgZn_2$ (see Fig. 2.2 in section 2.1.2), the thin coating will not persist as such after the wetting event, but will be alloyed into the liquid phases. For the alloy AZ31 the solidus and liquidus temperatures (T_S^{AZ31}, T_L^{AZ31}) are 560 °C and 631 °C, respectively. In AJ62, solidification occurs between 614 °C (T_L^{AJ62}) and 530 °C (T_S^{AJ62}), with about 20% eutectic fraction, whereas pure Mg solidifies at 649 °C (T_L^{Mg}). The outermost micrometers of the substrate are fused partially during the initial stage of the casting process. Assuming that droplet and substrate have the same volume, one can estimate the total enthalpy *H* of the system to lie in the middle of the values for solid AZ31 at 250 °C and for the melt at 750 °C. This is illustrated in Figures 5.5, a and b.

The enthalpy of the melt is nearly independent on its composition, and the average (i.e. 0.5 × (Hmelt + Hsubstrate), assumed to be valid close to the interface) is calculated to be around 18 kJ/mol for all compounds. From the curves in Figure 5.5b, where the solidification ranges of the three alloys are shown, one can read the solid/liquid fraction after contact in the substrate and droplet areas. The substrate will be approximately 25% liquid in both cases, which is the reason why even the thin MgZn2 interlayer disappears. The AJ62 droplet will be liquid to about 40%, and the Mg droplet will be nearly completely solid.

5.4 Discussion

We observe the dissolution of the $Zn/MgZn_2$-coating into the bulk during casting. The distribution of Zn around the interface varies along with the position and width of the solidification intervals and thus with the heat, which is transferred to the substrate by the droplet alloys AJ62 and pure Mg. The substrate will fuse partially, and the melt's composition determines the mechanism of solidification and the distribution of Zn from the coating.

5.4.1 Interface composition

We will now consider the solidification sequence and the corresponding Zn distribution after the compound casting experiment. In AZ31/'Mg' couples complete solidification occurs first in the droplet (there is only very little Mg to solidify), and the interface-near region of the substrate is the last volume to solidify. Because of

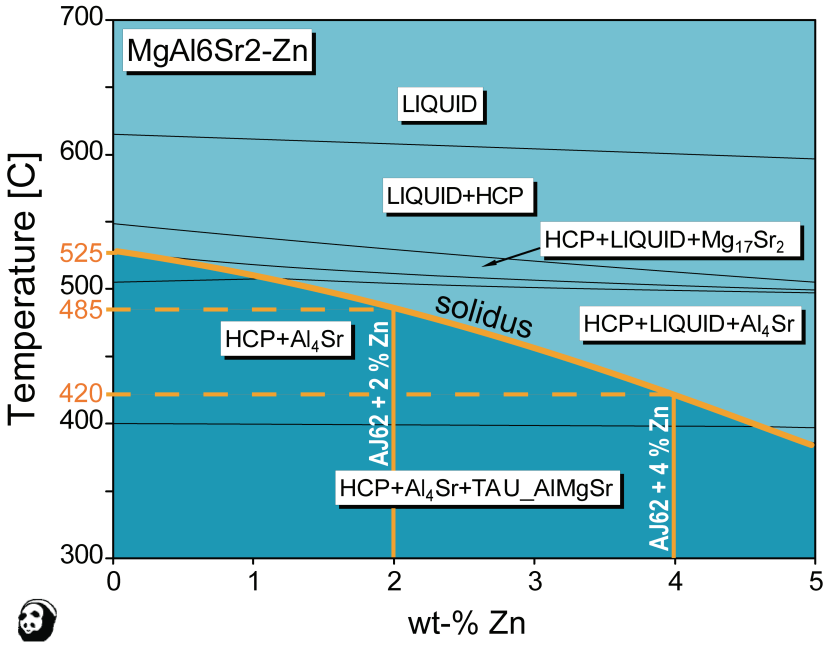

Fig. 5.6: Calculations with Pandat show, that the solidus temperature of the AJ62 alloy decreases with increasing zinc content.

element partitioning during this process, i.e. higher Zn solubility in the liquid than in the solid, Zn is detected mainly in the substrate's 'fuse zone'. The concentration level is supposed to stay well below the solubility limit (6 wt-%) as no second phase is observed.

In AZ31/AJ62 couples the solidification sequence is different. Here, after heat equalization the liquid fraction in the substrate ($f_L^{AZ31} \approx 25\%$) is lower than in the AJ62 droplet ($f_L^{AJ62} \approx 40\%$) and thus complete solidification occurs first in the substrate, and the remaining liquid will be localized in the AJ62 droplet. Accordingly, due to the element partitioning Zn will be concentrated in the residual liquid, which is the eutectic of AJ62.

So far the experimental observations are confirmed by the thermodynamic considerations. However, there is still one important question that needs to be discussed: Is the interface prone to formation of shrinkage-cavities? That might be the case if the interface region solidifies last. Such situation exists for the AZ31/'Mg' couple, or for all couples where the solidus temperature of the 'liquid partner' is higher than that of the substrate. Ever though we do not observe cavities in our experiment – maybe because of favourable conditions of heat release – the problem

has to be considered whenever a melt with high TS is used. With commercial (low-alloyed wrought or high-alloyed cast) alloys, however, this will practically never be the case. Thus the bulk 'liquid partner' will solidify last, which avoids the formation of shrinkage cavities at the interface.

In the vicinity of the interface of the AZ31/AJ62 couples some Zn was detected in the eutectic of AJ62. Thermodynamic calculations using Pandat software, shown in Figure 5.6, indicate a decrease of the solidus temperature with increasing Zn content, and thus the aforementioned cavity problem may occur. Differential Scanning Calorimetry (DSC, Seiko Instruments SSC/5200) measurements of an interface-near sample section showed that the onset of T_S is at 509 °C, i.e. slightly below the T_S of Zn-free AJ62 (520 °C measured with DSC, 525 °C calculated, Fig. 5.6). This indicates very dilute Zn-concentrations at the interface of below 1 wt-%, which can be considered to be harmless with respect to the formation of imperfections.

5.4.2 Interface microhardness

Microhardness measurements help to consolidate the observations made with SEM and EDX. The continuous change in composition in the AZ31/AJ62 couple is reflected by the gradually increasing hardness values towards the cast alloy. The hardness of 62 - 65 HV is in good accordance with available data [Meridian Inc., 2009]. Obviously the slightly increased Zn content has no hardening effect. For the AZ31/'Mg' samples the hardness values spread at the interface due to the partial fusion of interface-near regions, whereas in the 'Mg' droplet hardness reaches values of approximately 35 HV. Also here we do not observe a significant influence of the marginally segregated Zn in AZ31 close to the fuse line.

As such, the coating material has only a minor influence on the compounds' microstructure and mechanical properties. This finding is a consequence of the coating's complete dissolution into the bulk compound and of its significant influence on the substrate's wetting properties.

5.5 Conclusions

A metallurgical reaction at the modified surface of magnesium alloys leads to complete wetting of the substrate by magnesium melts. Investigations on the cross-

sections of these Mg–Mg couples reveal the continuously metallurgic transition from one bulk volume to the other, without the formation of undesired imperfections within the interfacial region. The coating's material influences the compound's composition as well as the mechanical properties only marginally, as EDX and microhardness measurements show.

The solidification sequence is of high importance for compound casting, as it determines the possibility of shrinkage cavity formation. As we did not observe such cavities in any of the samples that were produced during the presented work, we believe that this problem is not a severe threat to industrial applications. However, it is advisable to be aware of this issue whenever a melt material is used that exhibits a significantly higher solidus than the substrate. This combination of materials will not occur when using commercially available alloys, which are usually low-alloyed wrought and higher-alloyed cast products.

Calculations of the interfacial area's heat contents point at a partial fusion of the substrate material directly after the wetting event. These findings go along well with experimental observations, where a complete dissolution of even the intermetallic $MgZn_2$ interlayer (which forms during heat treatments of the plated substrate to increase the coating's adhesion, see section 2.2.2) occurs during the casting process. With this result, the potential reduction of the AJ62 alloy's solidus, as calculated with the Pandat software, remains no danger to this material's mechanical properties at elevated temperatures [Flierl, 2003; Baril, 2003; Spigarelli, 2001], because of the very dilute Zn-concentration at the interface of below 1 wt-% within the microstructure in vicinity of the interface.

Microhardness measurements reflect the continuous transition of the compounds' mechanical properties, which occurs within 50 - 100 µm of the interface. As a consequence of alloying element diffusion from one component to the other, one can think of selectively modifying the interface's strength or toughness via properly choosing the alloy compositions and heat treatment procedures after compound production, similarly to Al–Al compound casting. The scale-up experiments that were performed with those compounds could be repeated with magnesium alloys to show the feasibility of commercially implementing Mg–Mg compound casting.

References

Baril, E., Labelle, P., Pekguleryuz, M.O. Elevated temperature Mg-Al-Sr: creep resistance, mechanical properties, and microstructure. *JOM*, 11:34-39 (2003).

Flierl, R., Wolf, J., Gibisch, R. Cylinder-crankcase of a liquid cooled internal combustion engine. Patent EP20020700217, 24 (2003).

Meridian Lightweight Technologies Inc., datasheet. Available at: http://www.meridian-mag.com/magnesium/datasheet.pdf, (accessed April 16, 2009)

Spigarelli, S., Regev, M., Evangelista, E., Rosen, A. Review of creep behaviour of AZ91 magnesium alloy, produced by different technologies. *Materials Science and Technology*, 6:627-638 (2001).

Chapter 6

Aluminium-magnesium compound casting

The characterization of the interfaces in Al-Mg couples with a thin protective Mn interlayer will be discussed in this chapter. The focus of the first section 6.1 lies on investigations of interface composition and its structure. With the help of XRD measurements after various periods of heating the coated substrate, the growth (and consumption) of intermetallic compounds at the interface is documented (6.2). To round off the experimental part of this work, bending tests were performed and described in section 6.3, with the aim to determine the weak link of these Al–Mg couples. The mechanisms and kinetics, which determine the formation of the interface structure at hand, are explained theoretically in section 6.4. A discussion of the results in section 6.5 is followed by short conclusions of this topic (6.6).

6.1 Formation of interlayers in Al–Mg compounds[1,2]

6.1.1 Aims and procedures

A very different image from what we have seen so far can be drawn for compound structures of the dissimilar materials aluminium and magnesium. The AlMg1 substrate was effectively protected from getting into contact with the droplet of magnesium melt. A distinctive interlayer of manganese with virtually no composition gradient towards the droplet material prevails. This is a logical consequence of the reduced solubility of manganese in magnesium (Fig. 6.1). As wetting is observed indeed (Fig. 3.5), some sort of blending has to occur nonetheless, which has to be revealed by other means than optical microscopy.

Investigations focus on composition and mechanical properties of the Mn-Al multi-layered interface in compound cast Al–Mg couples. For localizing the 'weak link' of these structures, three-point bending tests were performed with specimens that were cut out of the samples from wetting experiments. To further assess the interface composition, coated substrate platelets were analyzed by X-ray diffraction (XRD). In order to initiate the growth of IMPs and thus simulate the heat transfer from the melt droplet to the substrate during casting, they were heat-treated at 450 °C for various periods prior to XRD measurements. These parameters are different from those applied during compound production, where they were heated during 30 s at 700 °C before the droplet was placed on the coated substrate. This was done to obtain sufficiently slow interlayer growth and thus to be able to observe changes in phase configuration.

6.1.2 Composition of the layered structure at the joint

On the other side of the manganese layer, towards the aluminium substrate, the growth of multiple phases is possible (see Figure 6.1, Al-Mn phase diagram or [McAlster, 1990]). The gradual formation of these IMP layers during a wetting experiment (heating the substrate at 700 °C for 30 s and placing the melt droplet onto

[1] K.J.M Papis, J.F. Löffler and P.J. Uggowitzer. Interface formation in Al-Mg compound cast couples. (in preparation).

[2] K.J.M Papis, J.F. Löffler and P.J. Uggowitzer. Light metal compound casting. Sci. China Ser. E Technol. Sci. 52 (2009), 46-51.

it) is illustrated in Figure 6.2. At least three different tonalities in backscattered-mode SEM images of the interface can be observed, indicating the development of a composition gradient and the subsequent formation of Al–Mn IMPs via diffusion reaction during compound casting. The Mn layer also exhibits a region with different composition than the bulk coating.

From EDX measurements with 5 kV acceleration voltage (usually 10 - 20 kV) and thus less activated volume (i.e. higher resolution), more exact (but still rather variable) compositions of these phases were determined and are listed in Table 6.1. Figure 6.3 shows an SEM micrograph with backscattered electrons detection (illustrating mass contrast), with EDX mappings of the same area. These illustrate the chemical consistency, which shows a gradient on the Al-Mn side. Each layer is labelled with the adequate composition or phase.

Table 6.1: Compositions and related phases at the Al–Mn interface.

measured composition [at-%]	Proposed phase	Theoretical composition [at-%]
Mn 86.4, Al 12.0	β-Mn	Mn 59.5 - 96.0, Al 4.0 – 40.5
Mn 30.7, Al 68.9	$Al_{11}Mn_4$	Mn 26.7, Al 73.3
Mn 25.6, Al 72.6	μ ($Al_{10}Mn_3$)	Mn 20.8, Al 79.2
Mn 1.3 - 18.3, Al 81.3 - 90.0 (rest: Zn, Mg)	Al_6Mn	Mn 14.3, Al 85.7

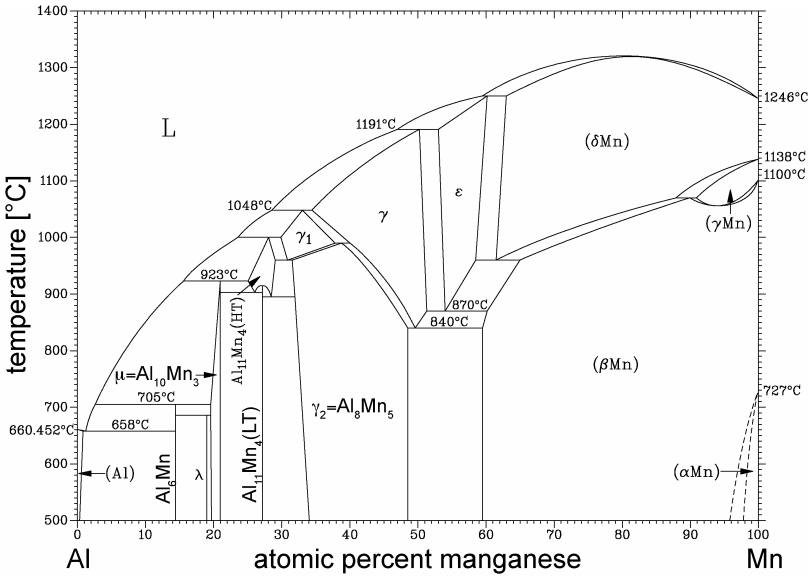

Fig. 6.1: The aluminium-manganese phase diagram. Many IMPs, mostly rich in aluminium, may form.

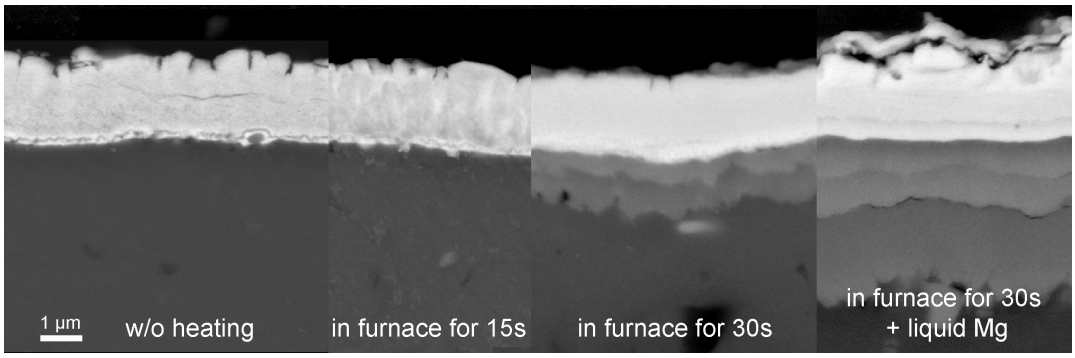

Fig. 6.2: Sequence of REM images in BSE mode, where mass contrast is seen. During a compound casting experiment (heating of the coated substrate in the furnace for 30 s, then placing the Mg droplet onto the substrate), Al–Mn IMPs grow in layers from the coating (bright = heavier Mn atoms) in direction of the Al substrate.

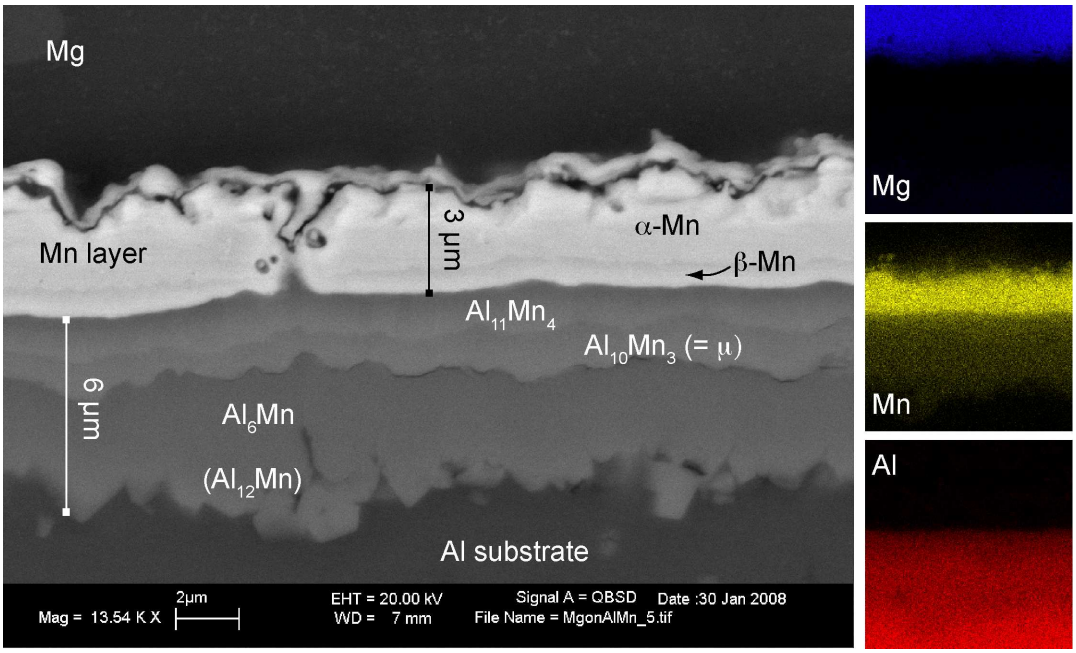

Fig. 6.3: The layered structure of Al–Mn IMPs becomes apparent after the wetting experiment. On the left, an SEM image in BSE mode is labelled with the potential phase designations. The compositions of Mg, Mn and Al are mapped via EDX and show gradients of 6 µm between Al and Mn and 1 µm between Mn and Mg (right).

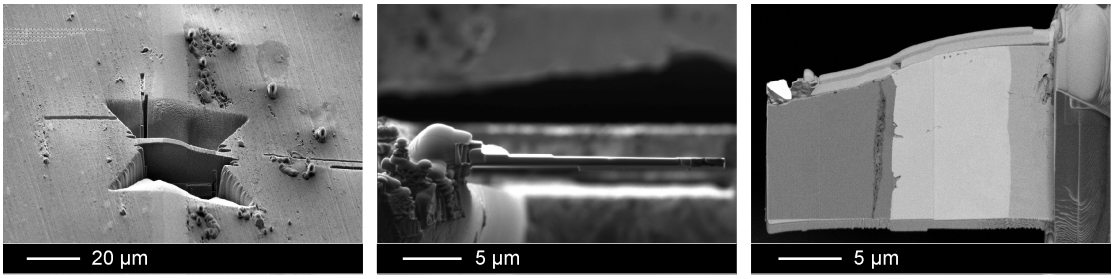

Fig. 6.4: A thin section of an Al–Mg specimen with Mn and Al–Mn IMP layer. The lamella is cut out of the bulk and thinned with a focussed beam of Ga^{3+}-ions, and subsequently analyzed via EDX and BSE-SEM.

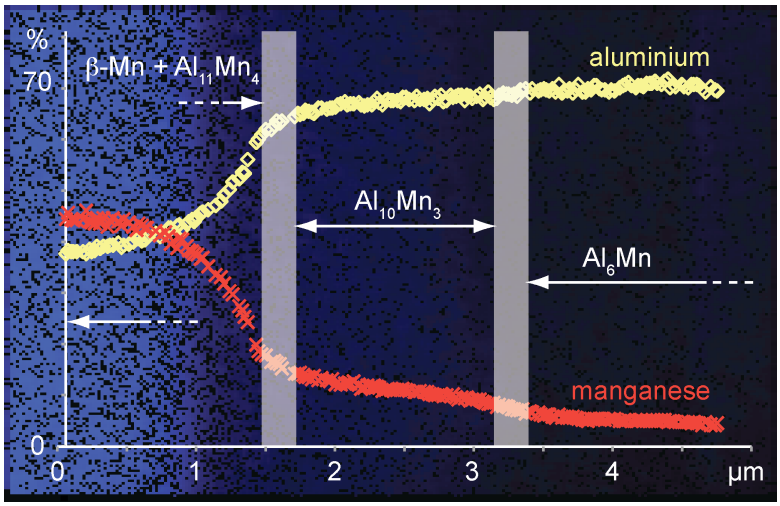

Fig. 6.5: The Mn (also illustrated in the background) and Al composition profiles across Al–Mn IMPs, measured by EDX on a thin specimen. Three distinct areas of compositions are observed.

A further improvement of resolution can only be achieved by measurements on thin samples. As the preparation of TEM samples by conventional methods (diamond thread cutting, dimpling, ion milling) is very difficult with the brittle, layered structure at hand, Focused Ion Beam (FIB) lamella cutting was applied.

The FIB is a micro-machining tool. It cuts into a specimen via bombardment of the surface with a beam of gallium ions that are accelerated by an electric field from a liquid metal ion source and focussed by electrostatic lenses on the desired spot. With this technique, a section of an Al–Mg compound's interface was prepared. Such a specimen is illustrated in Figure 6.4, and composition profiles of aluminium and manganese across the interlayer's, measured by EDX, are shown in Figure 6.5.

6.1.3 Growth of interlayers consisting of multiple IMPs

Al–Mn IMPs appear between coating and substrate after compound casting. These nominally brittle intermetallic compounds do not form from the liquid phase, which would be the case if no measures to protect the substrate had been taken, as discussed in section 2.3.2. Moreover, no cracks are observed in this layered structure, but care has to be taken not to apply too big stresses to the interface during sample preparation. It has been shown theoretically and practically [Dybkov, 1985, 1990 and 2001; Nijokep, 2001; Fragner, 2006] that the interface can be kept thin if more than one IMP is formed.

An explanation of this phenomenon from a kinetic point of view will be given in section 6.4. A brief summary will help to understand the mechanisms of simultaneous growth within a multiple-layered interface: Not all of the phases from a phase diagram need to appear, as their growth or consumption is determined by the diffusion coefficients of adjacent layers. Initially, assuming diffusion reactions to take place, linear growth of IMPs is predicted, until the layer reach a certain critical thickness after which parabolic growth takes place. The transition from linear to parabolic growth (where the diffusion rate equals the reaction rate) is specific for each phase. Therefore, one or more of them can be consumed during interface formation [Shatinsky, 1976]. As diffusivity is dependent on the parameters within the adjacent phases, multiple layers of intermetallic phases may hinder each other from growing and thus generate thin interfaces compared to single layers.

6.2 XRD analysis of intermetallic interlayer growth

Indeed, as the Mn coated AlMg1 substrate is subjected to elevated temperatures, Al–Mn IMPs start to form. It appears, that the initially appearing phases are not the same than the ones, which are present at the end of the applied heat treatments. In Figure 6.6, XRD measurements visualize this phenomenon, as the peak originating from the Al_8Mn_5 (γ_2) phase more or less disappears in favour of signals from the phases $Al_{10}Mn_3$ (μ) and Al_6Mn, which are richer in aluminium.

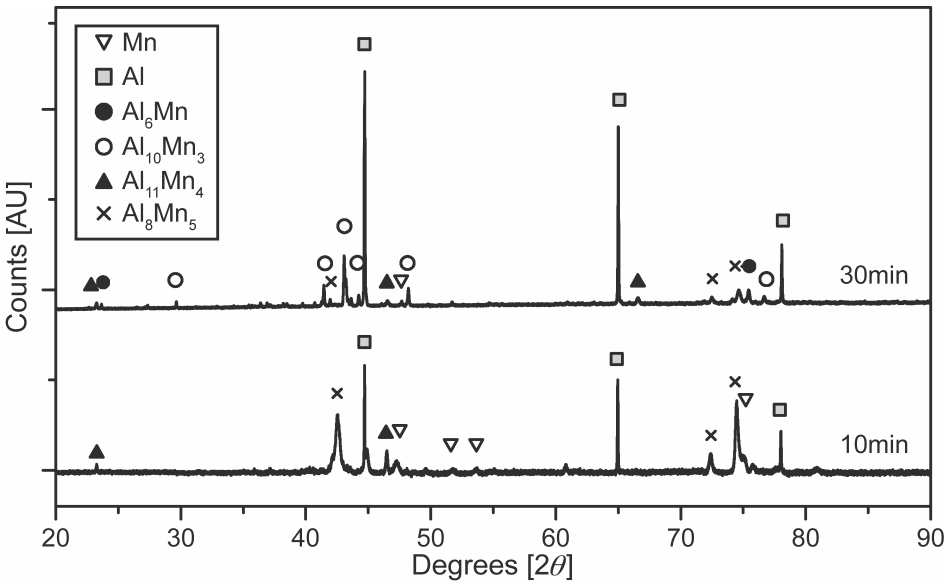

Fig. 6.6: XRD plots showing the changes in layer composition as the heat treatment of the Mn-coated Al-substrate (at 450 °C) proceeds, which simulates the supply of heat during the compound casting process.

Nevertheless, all these as well as other phases, whose thickness is below the device's limits of detection, may be present as well; EDX measurements and SEM micrographs suggest the presence of at least three intermetallic compounds between coating and substrate. Signals from the manganese coating and from the aluminium substrate are detected throughout the experiment, which means, that the interlayer composition changes, while the bordering phases remain the same.

6.3 Bending tests

6.3.1 Introduction

Al–(Mn–)Mg compound rods with variable cross-section (1 - 2 mm × 2 mm) were tested in a three-point bending equipment. The aims of these tests were to determine the 'weak link' of the compound, i.e. which location in the compound the crack chooses for initiation, and whether the failure is influenced by the interface thickness. However, due to varying specimen dimensions, measurements were not intended to determine fracture toughness values or exact mechanisms of crack propagation.

In compounds featuring thin interfaces, the overall mechanical properties are expected to change to ductile behaviour below a certain size of the brittle interface

due to a shielding effect [Wang, 1978; Suo, 1989; Hutchinson, 1991]. Cannon *et al.* describe various mechanisms of crack propagation, including fracture toughness measurements [Cannon, 1991]. They concluded, that cracks in ductile/brittle compounds under monotonic load usually propagate in the brittle material, but not directly at the interface.

6.3.2 Experimental results

The bending machine (Kammrath & Weiss Tensile/Compression Module 1000N) is illustrated in Figure 6.7. At a bending velocity of 0.2 - 0.5 µm/s, the compound was determined to be broken when the stress dropped significantly, as some slip of the clamps may be recorded as slight, more or less abrupt decrease of load. Figure 6.8 shows a typical stress-strain curve, where the load is plotted versus bending distance at constant bending rates. The initial slope of the curve gradually decreases due to the generally uniform slip of the clamps. The specimens were unloaded after sample failure at the same rate as loading occurred.

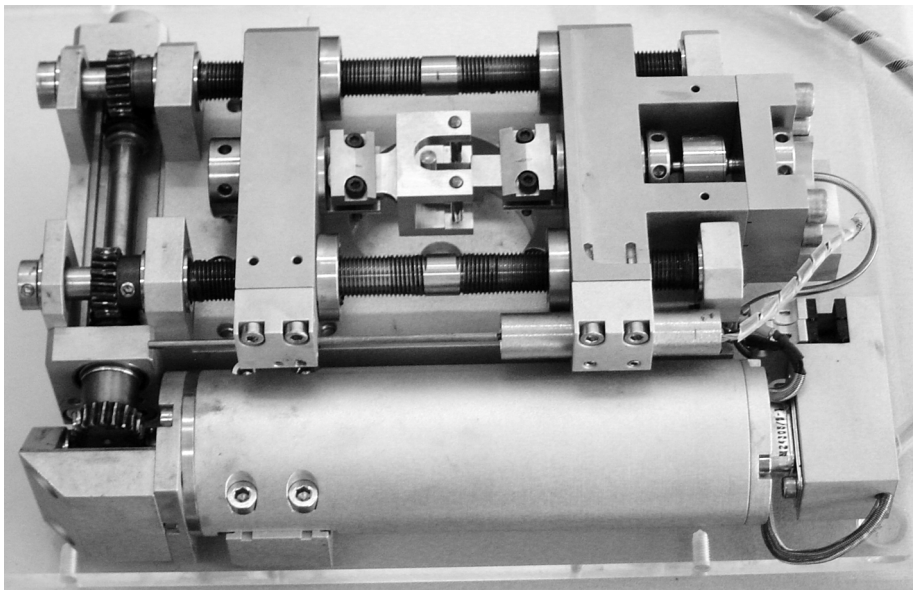

Fig. 6.7: The tensile/compression module with a 3-point bending mounting.

As shown in Figure 6.9, the predominant location for failure is the coating, including the IMPs. The crack propagates in several manners: most often, it alternates between two or more of the brittle phases (coating and IMPs). In some samples, the Mn layer stays intact, whereas the main location of failure is found to be within the intermetallic interlayer. The crack infrequently propagates along an interface, or deviates into the ductile substrate or droplet.

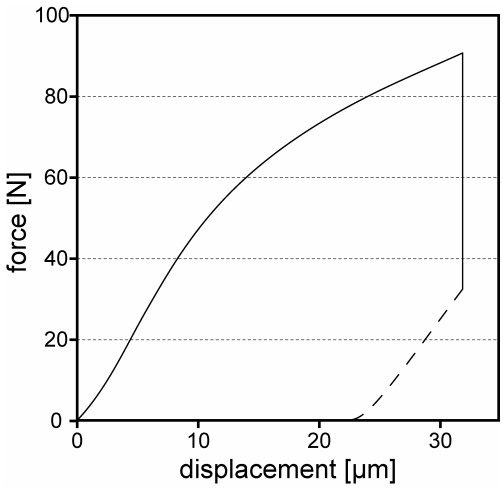

Fig. 6.8: Recorded force versus lever displacement with a bending rate of 0.2 µm/s. The dashed line illustrates the unloading behaviour, also at 0.2 µm/s.

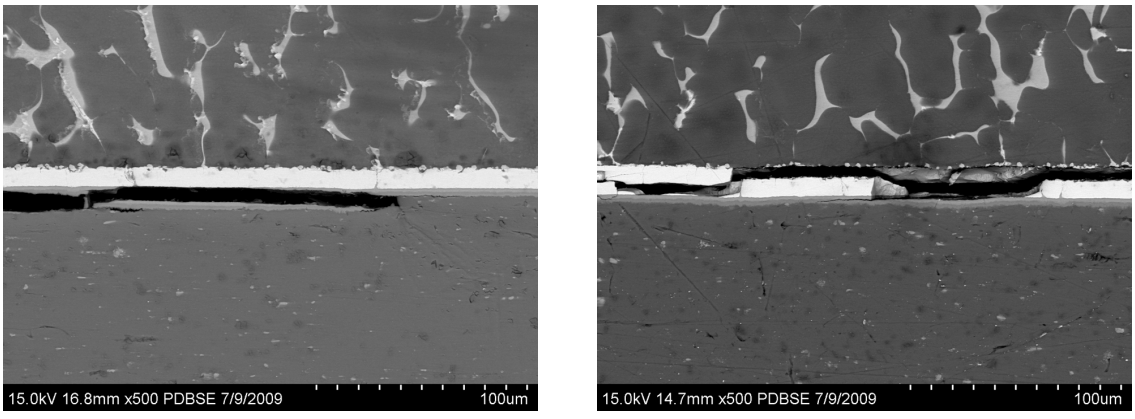

Figs. 6.9, a and b: Micrographs of a fractured AlMg1/MgZn7 compound. The crack remains within the IMPs, rarely deviating into the ductile substrate (a), or alternates from substrate to droplet within the brittle Mn and IMP layers (b).

6.4 Interface formation in systems with intermetallic phases

A metallurgic reaction between two dissimilar materials often involves the formation of one or several additional phases. These generally derogate the compound's mechanical properties, if they are on hand as a continuous layer. As this is the case in Al–Mg compounds that are produced and analyzed in this work, the theoretical characterization of the growth kinetics needs to be understood. A model for layered phase growth in a binary system with one and multiple intermetallic phases is therefore explained in this section.

In our Al–Mg system with a permanent protective coating at the interface, the possibility of multiple IMP formation via diffusion reaction exists. In theory, all possible phases that appear in an equilibrium phase diagram will form to a certain extent, but at the end of the reaction diffusion processes, only a limited number prevails. The reason for this phenomenon lies in the facts, that diffusion through a certain phase is dependent on the diffusivities in the adjacent phases, and that the common parabolic layer growth model fails to include initially occurring mechanisms, which are controlled by the reaction rate. To explain this, a simple binary system A–B with one intermetallic component and no solubility in the terminal phases is considered for a start (Fig. 6.10) according to Shatinsky *et al.* [Shatinsky, 1976].

Intermetallic phases usually exhibit a narrow composition range and nearly constant molar volume, which sustains the assumption of constant flux through the layer during growth. Conservation of matter (eq. 6.1) and the Fick's laws (eqs. 6.2 and 6.3) are given below. The first Fick's law describes a diffusion flux, which is constant in time. In contrast, the second Fick's law gives a relation between concentration differences for varying time and location, and illustrates thus instationary diffusion processes. There are a couple of analytical and numerical approaches to solve this equation, but they are all strongly dependent on particular boundary conditions.

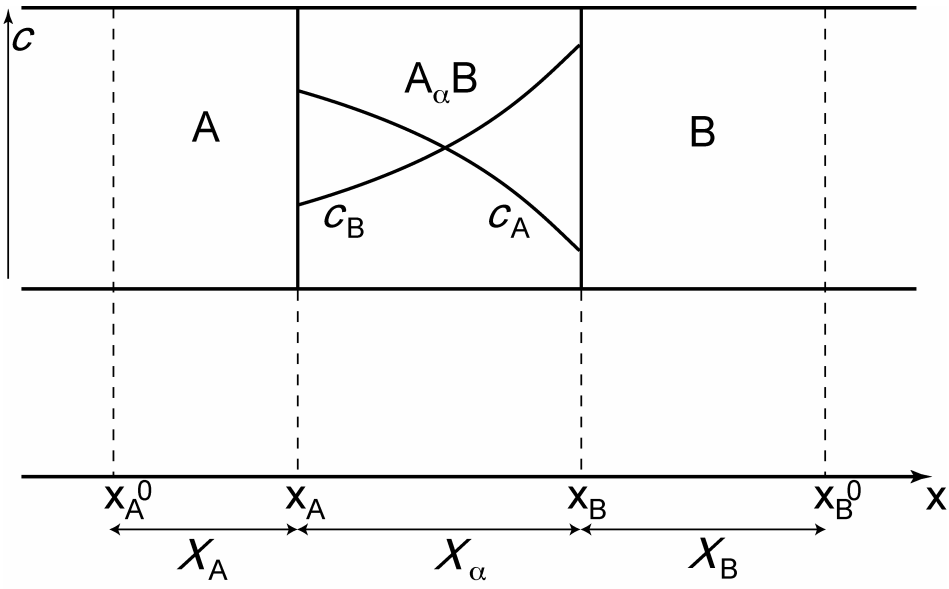

Fig. 6.10: Schematic concentration profile in a binary system with one intermetallic component and no terminal solubility. In case of a composition range in the compound $A_\alpha B$, α describes the average atomic composition.

$$\frac{\partial c}{\partial t} = -\frac{\partial J}{\partial x} \tag{6.1}$$

$$J = -D\frac{\partial c}{\partial x} \tag{6.2}$$

$$\frac{\partial c}{\partial t} = \frac{\partial}{\partial x}\left(D\frac{\partial c}{\partial x}\right) \tag{6.3}$$

From these equations, we express the motion of the interface *I* (A - $A_\alpha B$) relative to a reference x_A^0 in terms of the fluxes of both species and the pertinent stoichiometric factor.

$$\frac{dX_A}{dt} = \frac{d\left(x_A - x_A^0\right)}{dt} = -\Omega_A J_{AI}^{\alpha} + \alpha\Omega_A J_{BI}^{\alpha} = \Omega_A\left(D_A^{\alpha}\frac{\partial c_A^{\alpha}}{\partial x}\right)_I - \alpha\Omega_A\left(D_B^{\alpha}\frac{\partial c_B^{\alpha}}{\partial x}\right)_I \tag{6.4}$$

J represent the fluxes, *D* the diffusivities, *c* the concentrations and Ω the molar volumes of the particular species. A similar equation can be written for interface *II* ($A_\alpha B$ - B). The directions of the interfaces' movement determine growth or

consumption of the intermetallic layer, and by conservation of matter (eq. 6.1), the kinetics for a simple model are herewith determined. This can be written as

$$\frac{\mathrm{d}X_\alpha}{\mathrm{dt}} = -\frac{\Omega_\alpha}{\alpha} D_\mathrm{A}^\alpha \frac{\partial c_\mathrm{A}^\alpha}{\partial \mathrm{x}} + \Omega_\alpha D_\mathrm{B}^\alpha \frac{\partial c_\mathrm{B}^\alpha}{\partial \mathrm{x}}. \tag{6.5}$$

In a simplified way, this equation has the form of

$$\frac{\mathrm{d}X_\alpha}{\mathrm{dt}} = \frac{\mathrm{k}_\mathrm{p}^\alpha}{X_\alpha}, \tag{6.6}$$

where k_p^α is the parabolic growth rate constant for $A_\alpha B$, which is a function of temperature and chemical potentials, too. k_p^α can be measured from experiments, which usually result in a parabolic equation of the form

$$2\mathrm{k}_\mathrm{p}^\alpha \mathrm{t} = X_\alpha{}^2. \tag{6.7}$$

Now, if saturated terminal solubility is considered (Fig. 6.11), the equations have to be normalized to find the interface rate of growth as before. This is because the factors involving diffusion in the terminal phases don't enter the mass balance at the interfaces. Otherwise, within the terminal phases in vicinity of the interfaces, supersaturation or diffusion up a chemical potential would be caused.

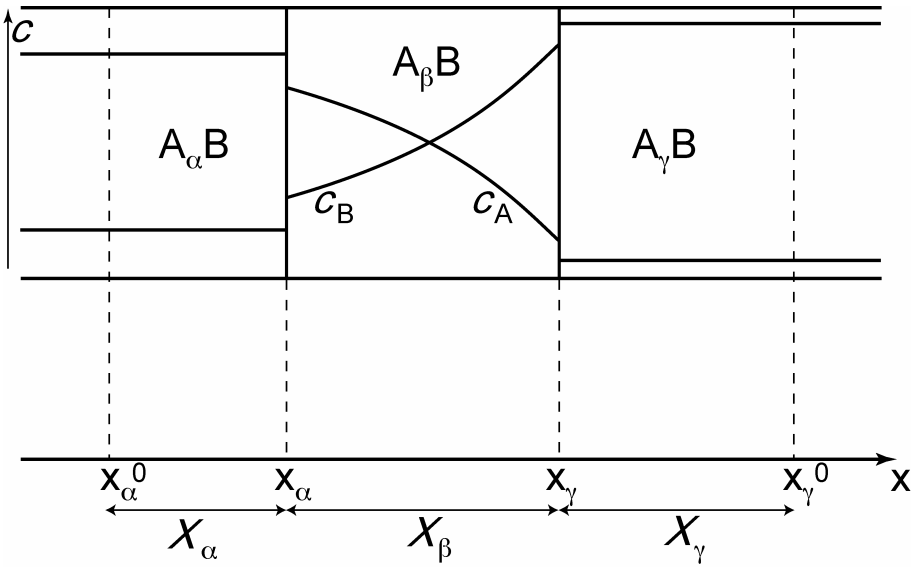

Fig. 6.11: Schematic concentration profile in a binary system with one intermetallic component and with terminal solubility.

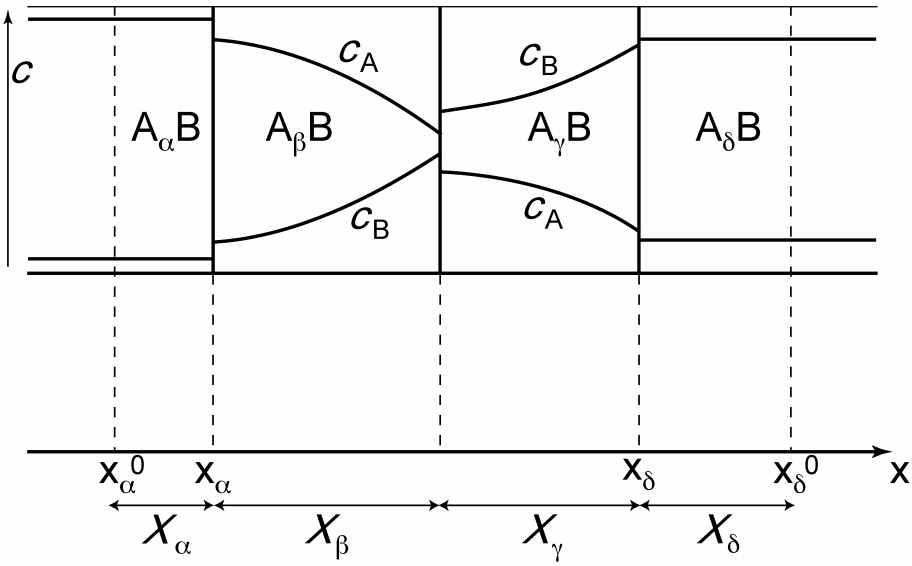

Fig. 6.12: Schematic concentration profile in a binary system with two intermetallic components and with terminal solubility.

If there are two (or more) intermetallic layers with saturated terminal solubility (Fig. 6.12), there are more partial reactions at the interfaces, and reaction constants have to be described by a system of subconstants to be able to illustrate layer growth. The parabolic growth rate constants contain terms, which involve diffusivities of the adjacent phases. Such subconstants can be determined from diffusivity measurements and the partitioning factors from the appropriate binary phase diagram.

In reality, the process of layer growth at an initial layer thickness of zero involves a chemical reaction. In the beginning, diffusion through a thin layer is much faster than this reaction, and the growth rate is limited by the reaction rate. If a critical layer thickness is reached, the diffusion rate, which decreases with increasing diffusion distance, equals the reaction rate. From there on, the intermetallic layer grows with a parabolic law, as derived above.

The same is true for the interface on the other side of the considered phase. The critical thickness will usually be different, just as the diffusivities for the distinct components. It is therefore possible, that at the beginning of interface formation, two layers start to build up first. When one of them reaches the critical thickness, it may be ‘consumed’ by the other growing layer. Therefore, not every possible IMP (read from a phase diagram) forms necessarily, but the opposite is true: Most often, in a binary couple with a multiphase system, there are some of the intermetallic phases missing! Examples of this matter of fact are described in detail by Fragner *et al.*,

investigating interface reactions between binary aluminium alloys and mild steel [Fragner, 2006].

It is obvious, that a system with multiple layers may grow at a much smaller rate than if a single phase forms. This can be used to constrain the formation of excessively thick interfaces between two components, which is our approach to improve mechanical properties of the Al–Mg compound.

6.5 Discussion

6.5.1 Microstructure and composition

As manganese shows only limited solubility in magnesium, the reactivity of the Mn coating towards Mg melts is moderate to low. It is sufficient to generate a tight bonding, but the transition from the coating to the droplet material, where there is equal concentration of these two elements, is very narrow (< 1 µm). It is assumed, that only very little of the coating is alloyed into the melt during sample production, and that at the interface, solid solutions of Mg and α-Mn, according to the phase diagram in Figure 6.1, are present.

Due to the heat transfer from melt to substrate during the casting process, solid-state diffusion of manganese into aluminium and vice versa occurs. This results in a concentration gradient and initiates the formation of a layered structure of IMPs. Depending on the amount of transferred heat, which is due to little variations in droplet size, the interface thickness varies between 3 and 6 µm. According to previous explanations about the formation of multi-phase layers, not all of the theoretically existing IMPs were found after the casting process. Instead of 5 (Al_6Mn, λ, µ (= $Al_{10}Mn_3$), $Al_{11}Mn_4$ and γ_2 (= Al_8Mn_5)), only 3 (Al_6Mn, µ and $Al_{11}Mn_4$) were revealed by EDX. This is further confirmed by XRD measurements (Fig. 6.6), where the initially appearing γ_2 phase (Al_8Mn_5) gradually vanishes during the advancing heating.

The fact that the aluminium-rich compound Al_6Mn (maybe with $Al_{12}Mn$) is much larger than the manganese-rich IMPs (Fig. 6.3) suggests an unbalanced, high diffusivity of Mn in this compound. This brings up concerns about pore generation due to volume changes and vacancy supersaturation [Weinberg, 2009] on the side of the fast diffusion species (in this case most probably Mn), as the terminal

concentration difference is much larger than 10% [Peterson, 1969]. However, the formation of these so-called Kirkendall voids was not observed, ensuring a tight connection between all interface layers.

6.5.2 Mechanical properties

Due to difficulties to obtain equal sample dimensions by the wetting experiments, the tested rods exhibited also varying and not easy to determine cross-sections. Therefore, bending curves could not be quantitatively evaluated to identify a material's characteristic, nor could they be directly compared to each other. As mentioned in the aims for the bending experiments, the focus lies on determining the fracture location in these compounds. Figures 6.9, a and b show, that the 'weak link' of the Al–Mg compound is obviously located somewhere in the brittle phases. The predominant positions where failure occurs are the Mn coating and Al–Mn intermetallic compounds, without preferred phase.

In the works of the group around R. H. Dauskardt [Cannon, 1991; Ritchie, 1993; Mroz, 1998; Dauskardt, 1998], the fracture behaviour of ductile/brittle compounds is discussed. There, the interlayer was the ductile phase. However, similar cracking modes are observed, such as the periodic switching of the crack from one side of the interlayer to the other, as observed in the present work in Figure 6.9b. Such complex cracking configurations are believed to be the origin of high toughness values. If a procedure can be found to promote such fracture behaviour, this could be a possibility to improve the compound's mechanical properties significantly.

As the total interlayer thickness after compound casting is between 5 and 10 µm, mechanical properties of Al–Mg compounds with a protective Mn coating could be further improved by choosing milder processing temperatures and an even thinner coating. With some optimization, the total thickness of the brittle phases could possibly be reduced to 2 - 4 µm.

6.6 Conclusions

The production of Al–Mg compounds with mechanically sound interfaces was facilitated by a combination of surface treatments, comprising a permanent replacement of the oxide layer with a metallic Zn deposition and a subsequent Mn

galvanizing procedure. This thin coating proved to protect the substrate efficiently from being affected by deep liquefaction upon contact with an Mg melt. This coating system was filed as a patent proposal with the aim to protect the intellectual property for future implementation of this process in an industrial application.

The IMP interlayer, which no longer forms from solidification of a liquid but via solid-state diffusion, is not subjected to large solidification shrinkage stresses, which would otherwise have catastrophic consequences to the mechanical integrity of the compound. Its thickness is reduced by two orders of magnitude roughly, from more than 500 µm (Al–Mg IMPs) to 5 - 10 µm (Mn coating and Al–Mn IMPs). Bending tests show a considerable amount of deformation before failure, which in turn is mostly brittle. Nevertheless, onsets of toughness increasing fracture mechanisms are observed, which could lead to even better mechanical properties if further optimization of the interface can be achieved.

In order to obtain reliable information on the interface's composition, the resolution of EDX measurements is increased by applying low acceleration voltages and by performing analysis on a thin sample prepared by FIB lamella cutting. The observation, that only three of the six possible phases (as of the binary phase diagram) prevail, is in theory explained by initially linear and subsequently parabolic reaction diffusion layer growth. After this, theory was experimentally demonstrated via XRD measurements on Mn coated Al substrates, which are heat treated to initiate interlayer growth, and which equally show the consumption of initially appearing IMPs in favour of the prevailing layer components.

References

Cannon, R.M., Dalgleish, B.J., Dauskardt, R.H., Oh, T.S., Ritchie, I. M. Cyclic fatigue-crack propagation along ceramic/metal interfaces. *Acta Metallurgica Et Materialia*, 39:2145-2156 (1991).

Dauskardt, R.H., Lane, M., Ma, Q., Krishna, N. Adhesion and debonding of multi-layer thin film structures. *Engineering Fracture Mechanics*, 61:141-162 (1998).

Dybkov, V.I. Growth of chemical compound layers in composite materials. *Materials Letters*, 7-8:278 (1985).

Dybkov, V.I. Interaction of 18Cr-10Ni stainless steel with liquid aluminium. *Journal of Materials Science*, 3615-3633 (1990).

Dybkov, V.I. Reaction Diffusion in Binary Solid-Solid, Solid-Liquid and Solid-Gas Systems: Common and Distinctive Features. *Defect and Diffusion Forum*, 1503-1522 (2001).

Fragner, W., Zberg, B., Sonnleitner, R., Uggowitzer, P.J., Loeffler, J.F. Interface reactions of Al and binary Al-alloys on mild steel substrates in controlled atmosphere. In: Mai, Y.W., Murch, G.E., Wohlbier, F.H. (eds.), Materials Science Forum. *Trans Tech Publications Ltd.*, Zürich (CH), p. 1157-1162 (2006).

Hutchinson, J.W., Suo, Z., John, W.H. Mixed Mode Cracking in Layered Materials. Advances in Applied Mechanics. *Elsevier*, p. 63 (1991).

McAlster, A.J., Murray, J.L. Binary Alloy Phase Diagrams. In: Massalski, T.B., Subramanian, P.R., Okamoto, H., Kacprzak, L. (eds.), second ed. *ASM International*, Materials Park (USA), p.171-173 (1990).

Mroz, J., Dauskardt, R.H., Schleinkofer, U. New adhesion measurement technique for coated cutting tool materials. *International Journal of Refractory Metals & Hard Materials*, 16:395-402 (1998).

Njiokep, E.M.T. Growth of Intermetallic Phases in the Al-Mg System. *Defect and Diffusion Forum*, 1581-1586 (2001).

Peterson, N.L., Seitz, F., Turnbull, D., Ehrenreich, H. Diffusion in Metals. In: Ehrenreich, H., Spaepen, F. (eds.), Solid State Physics. *Elsevier B.V.*, St. Louis (USA), p. 409 (1969).

Ritchie, R.O., Cannon, R.M., Dalgleish, B.J., Dauskardt, R.H., McNaney, J.M. Mechanics and mechanisms of crack growth at or near ceramic–metal interfaces: interface engineering strategies for promoting toughness. *Materials Science and Engineering: A*, 166:221-235 (1993).

Shatynski, S.R., Hirth, J.P., Rapp, R.A. A theory of multiphase binary diffusion. *Acta Metallurgica*, 12:1071 (1976).

Suo, Z., Hutchinson, J.W. Sandwich test specimens for measuring interface crack toughness. *Materials Science and Engineering: A*, 107:135-143 (1989).

Wang, S.S., Mandell, J.F., McGarry, F.J. Analysis Of Crack Tip Stress-Field In Dcb Adhesive Fracture Specimens. *International Journal Of Fracture*, 1:39-58 (1978).

Weinberg, K., Böhme, T., Müller, W.H. Kirkendall voids in the intermetallic layers of solder joints in MEMS. *Computational Materials Science*, 45:827-831 (2009).

Chapter 7

General conclusions and outlook

A series of surface pre-treatments were applied to light metal substrates in order to increase the reactivity and thus the wettability towards metallic melts. Thereafter, wetting experiments were performed to investigate the influence of these coatings on wetting properties. This was done by non-isothermal sessile drop experiments, in a device designed during the present research project for this purpose, at typical process temperatures for commercially used alloys. Compound cast couples, comprising aluminium-aluminium, magnesium-magnesium and aluminium-magnesium compounds, were successfully produced with this setup. The diffusion reaction processes at the interfaces were assessed by thermodynamic calculations with DICTRA (Al-Al compound casting) and solidification characteristics of the various alloy combinations by Pandat (Mg-Mg compound casting) software programmes. The experimental results were examined by optical and electron microscopy, as well as EDX and mechanical analysis. A major point of interest lies on solidification shrinkage and the possibility of thus resulting pores at the interfacial region. Through adequate alloy selection in the case of similar material compounds, or via the application of a protective coating in the case of dissimilar compounds, this was successfully avoided.

This final chapter concludes the experimental findings and discussions, and gives a short outlook on the work to be done for further understanding of the compound formation processes.

7.1 Surface modifications of light metals

The naturally occurring and thus always present oxide layer on light metal surfaces represents the most important feature of these alloys concerning corrosion resistance and inertness towards the environment. It also describes, however, the inherent difficulty when such a material is to be joined via metallurgical reactions, occurring in brazing, welding or compound casting, where two metal alloys – one in the solid state, the other liquid – are brought into contact with each other in such a manner, that a metallic interface forms.

Via a series of wet-chemical and electrochemical surface treatments, this oxide layer was successfully and permanently removed and replaced by a 200 - 300 nm thin metallic zinc coating. The procedures comprised pickling and activation processes as well as redox (ion exchange) reactions. It was found, that upon heating thus prepared alloys prior to being brought into contact with the melt, the zinc coating disappeared from the surface due to its most distinctive solubility. This problem was overcome by increasing the coating's thickness via galvanizing.

In the case of compound casting of the dissimilar materials aluminium and magnesium, special precautions had to be taken to avoid the formation of low-melting, brittle IMPs during the casting process. The optimal element for a protective coating proved to be manganese, which could be applied via galvanizing from an aqueous solution. The main factors for choosing this material were a higher melting point than the compound casting process' temperature, no formation of IMPs with magnesium, some solid solubility in magnesium, and the possibility to easily apply this element as a coating.

With these pre-treatments, coatings were applied to light metal surfaces, which made them highly reactive and thus exhibiting outstanding wetting properties towards metallic melts, avoiding excessive IMP formation in the case of joining dissimilar metals. Their excellent adhesion to the substrate, which was partially achieved through application of a heat treatment, make the hereby coated structures easy to handle and thus widely applicable.

7.2 Aluminium-aluminium compound casting

In order to assess basic diffusion phenomena and have the possibility to visualize these by hardness measurements of precipitation hardened interfaces, binary alloys with commercially important alloying elements, comprising copper, silicon and zinc, were used as droplet materials. Excellent wettability of the zinc coated AlMg1 substrate is observed for all of these alloys, indicating strong interfacial reactions between substrate and melt.

As a result, a continuously metallurgic interface formed. Micrographs show these interfaces, which are free from oxide layer residues or other imperfections. Microhardness measurements illustrate, that the diffusion zone, where alloying elements of either compound partner blend, can be heat-treated if desired. The interfacial area shows significantly differing mechanical properties than the bulk in terms of hardness, which means, that they can be selectively tailored to comply with the requested purpose. Furthermore, the coating material dissolved completely into the compound bulk, as no trace of zinc could be detected by means of EDX analysis. By choosing an element with expanded solid solubility in aluminium, its influence on the compound's composition, microstructure and, ultimately, mechanical properties remains marginal.

The diffusion of alloying elements during the wetting experiments and subsequent heat treatments were simulated by thermodynamic computations utilizing the software package DICTRA from the company ThermoCalc. The width of the calculated diffusion zones were comparable to these measured experimentally by microhardness indentation. The compositions in the as cast, solution annealed and artificially aged states were well reproduced by this method, which can be used to significantly reduce the scale of experiments for future alloy combinations and heat treatments.

A patent application with the aim to protect the processes of substrate modifications and their employment for compound casting was submitted. A utility patent for this purpose was granted, which is a big step towards a successful implementation of the work done during this thesis.

Upscale experiments in a squeeze casting machine were performed with various aluminium alloys. The substrate's thickness, and thus heat capacity, determines the quality of the bonding. Obviously, the joint is more distinct if the substrate can be

heated efficiently by the melt, which is the case for thin inserts. Complete wetting occurs during compound casting using similar alloys as for wetting experiments. These findings prove the feasibility of a commercial implementation of Al–Al compound casting.

7.3 Magnesium-magnesium compound casting

The applied zinc coating and heat pre-treatments significantly enhanced the wetting properties of magnesium substrates. Complete wetting of AZ31 and ZK31 by various cast alloys was achieved by deposition of a 200 – 300 nm thick zinc layer via zinc sulphate immersion after several surface treatments comprising cleaning, pickling and activation procedures. Subsequently, zinc galvanizing was performed to increase this layer's thickness, analogue to aluminium substrates. Heat-treating the substrates and hereby inducing a reaction to form an Mg–Zn interlayer significantly improved the coating's adhesion. AJ62 and pure magnesium melts were used as droplet material in order to assess the mechanisms of the interfacial zone's solidification sequence, which vary along with the solidus temperatures of these alloys. Shrinkage cavities, which could result from a late consolidation at the interface, are a threat for certain alloy combinations, but were not observed in the compounds at hand. As a general rule, the substrate should exhibit a lower solidus temperature than the melt to ascertain a shrinkage cavity-free compound. As this is practically always the case when using commercial (and thus low-alloyed) wrought and (high-alloyed) foundry products, no hazard is expected to be at hand if the Mg–Mg compound casting process, which was developed during this project, was to be implemented industrially.

In combination with EDX, DSC and microhardness measurements, the structure and composition of the interfacial zones in various couples was analyzed. A continuously metallurgic transition from substrate to droplet was found, which is a consequence of the strong interfacial reactions during the wetting event and the lack of potential IMP formation in a system of similar materials. The sequence of interface solidification determines the location of the coating material's final location. In compounds with a higher solidus temperature in the melt (e.g. pure Mg), zinc can be detected close to the interface at the substrate's side, whereas in AZ31/AJ62 couples, it was found in the eutectic areas of the cast alloy.

Thermodynamic considerations on interface solidification were verified by calculating the enthalpies of the various compound's interfacial areas directly after the wetting incident. These calculations, performed with the software program Pandat, agree well with the experimentally found compositions and microstructures. They also fortify the need of shrinkage cavity awareness, as discussed previously, if the Mg–Mg compound casting process is to be implemented.

7.4 Aluminium-magnesium compound casting

The aluminium substrate was effectively protected from being liquefied upon contact with magnesium melts via application of a manganese coating after the inevitable, oxide layer replacing zincate treatment. A 3 - 5 µm thick, electroplated Mn coating proved to be enough to prevent excessive formation of low-melting Al–Mg IMPs from the liquid phase, as otherwise observed. The limited solid solubility of manganese in magnesium proved to be enough to allow for a slight reaction at the substrate-melt interface, thereby enabling wetting of the coated substrate. As no IMPs form in the binary system of Mn and Mg, the transition between these elements is narrow and free from imperfections.

On the coating's side towards the substrate, Al–Mn IMPs form via solid state diffusion upon exposure to heat. As theoretically described, the growth of intermetallic interlayers is hindered (and may even be completely oppressed) if multiple phases are potentially present. This is manifested by observations made in scanning electron micrographs, as only three of six theoretically possible phases (as of the Al–Mn phase diagram) prevail, and by the thin appearance of these layers (even below 1 µm). EDX analysis at low acceleration voltage on bulk samples and on a thin lamella prepared by FIB cutting (both aim at increasing the measurement's resolution) reveals the compositions of these layers, which were determined to consist of the aluminium-rich intermetallics from the binary phase diagram. This is an indication to the kinetics of the interlayer formation, as the rate-controlling factor appears to be the relatively slow diffusion rate of aluminium (compared to the diffusion rate of manganese) through the prevailing layer system. However, measurements on the diffusion rates of these phases were not performed, as such complex efforts are by far out of scope of this thesis.

XRD measurements on Mn coated Al substrates, which had undergone heat treatments to initiate IMP interlayer growth, resulted in similar observations: The initially forming phases, comprising those with a relatively broad range of solubility, were consumed and replaced by aluminium-rich prime phases with strictly stoichiometric compositions. If the solubility range has anything to contribute to the layers' negative (i.e. consumption) or positive growth, remains in speculative territory.

Finally, the 'weak link' in these layered structures was determined by means of bending tests. The applied loads resulted in splitting of the compound in the area of the manganese and intermetallic layers, with the IMPs being the predominant location of rupture. Methods to inhibit the growth of these phases may shift the 'weak link' to another location. Further improvement of the compound's mechanical properties could be achieved by generally decreasing the interface's size, as explained previously, due to the possibility of shielding the brittle fracture behaviour of the coating and IMPs by ductile deformation of the bulk if the interface's thickness can be kept below a critical thickness.

7.5 Outlook

The light metal compound casting project was started with this thesis. The intention was to develop a process for lightweight construction, employing a multi-material mix. With the application of a combination of surface pre-treatments, the naturally occurring oxide/hydroxide layers on aluminium and magnesium alloys were permanently replaced by a metallic coating, which significantly enhanced the wetting properties. Al–Al, Mg–Mg and Al–Mg compound casting was thus successfully put into practice at a laboratory scale.

The mechanisms of wetting, interfacial diffusion and resulting reactions, as well as the transformation of composition and structure at the joint are well understood. To ameliorate the mechanical properties of such compounds, more work has to be done in terms of tensile tests on larger samples and thorough characterization of deformation mechanisms. These topics were excluded from the present work, as a different means to produce compound couples would be necessary. Furthermore, a mechanical assessment of the interfacial zone is not trivial: any mechanical

measurements on composite materials have to consider the multiaxial stress condition, which will occur at the interfaces due to unequal deformation properties of the varying compound partners. At best, semi-quantitative and comparative analysis could be performed on such compound systems.

To gain more knowledge on the various compound cast systems' properties, some possible future work should include the following experiments and investigations, detailed with respect to the materials used:

Al–Al

In general, the aluminium-aluminium system is the best understood of the three assessed material combinations, which are presented in this thesis. Further work should be done on mechanical properties mainly. In this thesis it was shown, that upscaling of the Al–Al compound casting process is possible without major adaptations of the surface treatments or the process' temperature parameters. By varying the tempered state of the interface, investigations of the heat treatments' effect on tensile or bending properties and on the location of eventual fracture (and thus determination of the 'weak link' of such compound systems) would be highly interesting.

These future efforts are only partially of scientific nature, they rather require engineering knowledge and standardized testing in order to evaluate the potential areas of application. Therefore, no follow-up project is planned to date on the subject of compound casting in our group. The utility patent, which was filed during this thesis, provides a basis to develop this process towards an industrial application for lightweight construction.

Mg–Mg

Similarly to Al–Al, the interface formation of Mg–Mg compounds, which are produced in non-isothermal wetting experiments at laboratory scale, is specified in detail with the presented work. The good understanding of the bonding and interface formation, which was elaborated during this thesis, is essential to upscale the process, which is the logical step to be done for investigations on the compounds' mechanical properties, analogue to all-aluminium compounds.

As for further investigations on possible heat-treatments, more specific alloy combinations need to be produced for exclusively this purpose. As blending of alloying elements occurs at a up to 500 µm around the interfacial area, its hardness and thus strength can be intentionally tailored in a controlled manner to optimize the compound's mechanical properties for a certain future application.

Al–Mg

The main achievement in processing these two metals is the reduction of the intermetallic interface's thickness of more than two orders of magnitude, as well as the prevention of IMP formation from the liquid phase. The mechanical properties of the joint were assessed in order to determine the 'weak link' of the compound. With these results and the granted utility patent for Al–Mg compound casting, an industrial application of a product, which employs form closure, could be possible.

Investigations on these compounds focus on interface formation phenomena with a system comprising intermetallic phases. It was observed, that the theoretically delineated kinetic mechanisms of layered structure formation prevail in the Al–Mn system at hand. An exact description of the emerging phases in terms of composition and mechanical properties would imply more exact measurements via high-resolution investigations on very thin specimens, prepared by conventional TEM sample preparation or, more likely to succeed, FIB lamella cutting. The latter method proved to ensure sound interfaces, whereas the former most often causes severe damage to the brittle interface by working at too large stress levels. However, only one FIB lamella could be prepared during this thesis due to time constraints.

Corrosion issues, which obviously are a big concern in metallurgically joining dissimilar metallic materials, were not in scope of this thesis. The most straightforward approach to avoid corrosive attacks on such composites is to protect the whole assembly from contact with corrosive media.

Future projects on Al–Mg compound casting should concentrate on thorough investigations on layer compositions, including analysis of TEM diffraction patterns and EDX transmission measurements. Furthermore, assessments of the compounds' mechanical properties could be better understood if larger specimens were tested. This would imply a new production method, rather than a sessile droplet experiment as developed during this project. Also, the production parameters are not optimized yet

for interlayer thickness, which is believed to have a major impact on the fracture and crack propagation mechanisms.

Appendix

List of symbols and variables used in this thesis

symbol/variable	*significance*
A	interfacial area
A	aluminium in designations for magnesium alloys
c	concentration
D	diffusion coefficient
f_{sol}, f_{liq}	fraction of solid or liquid phase
G	Gibb's free energy
H	enthalpy
J	flux
J	strontium in designations for magnesium alloys
K	zirconium in designations for magnesium alloys
k_p	parabolic growth rate constant
S	current density
S	phase designation
T	temperature
t	time
X	mole fraction
x	distance, position
Z	zinc in designations for magnesium alloys
α, β, γ	phase designations
γ_{sl}, γ_{sv}, γ_{lv}	surface energy between solid, liquid and gas phases
∂	partial derivation
η, μ	phase designations
θ	wetting angle
θ	phase designation
ρ	specific gravity or density
Ω	molar volume

Publications, patents, posters and presentations

Publications

K.J.M. Papis, J.F. Löffler, P.J. Uggowitzer. ‚Interface formation in aluminium-magnesium compound cast couples'. (in preparation).

K.J.M. Papis, J.F. Löffler, P.J. Uggowitzer. ‚Interface formation between liquid and solid Mg alloys – An approach to continuously metallurgic joining of magnesium parts'. Materials Science and Engineering: A, 527 (2010) 2274-2279.

K.J.M. Papis, J.F. Löffler, P.J. Uggowitzer. ‚Light metal compound casting'. Science in China Series E - Technological Sciences, 52 (2009) 46-51.

K.J.M. Papis, B. Hallstedt, J.F. Löffler, P.J. Uggowitzer. ‚Interface formation in aluminium-aluminium compound casting'. Acta Materialia, 56 (2008) 3036-3043.

W. Fragner, K.J.M. Papis, P.J. Uggowitzer, J. Wosik. ‚Herausforderungen und Lösungsmöglichkeiten bei der Herstellung von Verbundgussbauteilen'. Giesserei-Praxis, 1-2 (2008) 243-248.

Patents and patent applications

H. Kaufmann, K.J.M. Papis, J.F. Löffler, P.J. Uggowitzer, W. Fragner. ‚Verbundgussteil'. Utility patent, AT010478 (published 15.04.2009).

K.J.M. Papis, J.F. Loeffler, P.J. Uggowitzer, W. Fragner, H. Kaufmann. ‚Production of composite casting part for motor vehicles, comprises removing aluminium oxide from joining zone of solid body, treating the zone with zinc solution, depositing metallic layer on the layer, and contacting the body with melt'. Patent application, AT504923 (published 15.09.2008).

Conference contributions

MRC Graduate Symposium 2009, Zurich, Switzerland (poster presentation)
Materials Day 2009, Zurich, Switzerland (poster presentation)
ICAA11 2008, Aachen, Germany (paper presentation)
MRS China 2008, Chongqing, China (paper presentation)
DPG Frühjahrstagung, 2007, Regensburg, Germany (paper presentation)
Aluminium2000, 2007, Florence, Italy (paper presentation, session chair)
TMS annual meeting, 2007, Orlando, USA (2 paper presentations, session chair)